CERN–TH/96–52

# Heavy-Quark Production in the Target Fragmentation Region [‡]

**Dirk Graudenz** [*] [¶] [§]

*Theoretical Physics Division, CERN*
*CH–1211 Geneva 23*

**Abstract**

Fixed-target experiments permit the study of hadron production in the target fragmentation region. It is expected that the tagging of specific particles in the target fragments can be employed to introduce a bias in the hard scattering process towards a specific flavour content. The case of hadrons containing a heavy quark is particularly attractive because of the clear experimental signatures and the applicability of perturbative QCD. The standard approach to one-particle inclusive processes based on fragmentation functions is valid in the current fragmentation region and for large transverse momenta $p_T$ in the target fragmentation region, but it fails for particle production at small $p_T$ in the target fragmentation region. A collinear singularity, which cannot be absorbed in the standard way into the phenomenological distribution functions, prohibits the application of this procedure. This situation is remedied by the introduction of a new set of distribution functions, the target fragmentation functions. They describe particle production in the target fragmentation region, and can be viewed as correlated distribution functions in the momentum fractions of the observed particle and of the parton initiating the hard scattering process. It is shown in a next-to-leading-order calculation for the case of deeply inelastic lepton–nucleon scattering that the additional singularity can be consistently absorbed into the renormalized target fragmentation functions on the one-loop level. The formalism is derived in detail and is applied to the production of heavy quarks. The renormalization group equation of the target fragmentation functions for the perturbative contribution is solved numerically, and the results of a case study for deeply inelastic lepton–nucleon scattering at DESY (H1 and ZEUS at HERA), at CERN (NA47) and at Fermilab (E665) are discussed. We also comment briefly on the case of an intrinsic heavy-quark content of the proton.

CERN–TH/96–52
December 1996

[‡] *Habilitationsschrift, Universität Hamburg, 1996 (submitted in April 1996).*

[*] *Electronic mail address: Dirk.Graudenz@cern.ch*

[¶] *WWW URL: http://wwwcn.cern.ch/∼graudenz/index.html*

[§] *Address after February 1, 1997: Paul Scherrer Institute, Department of Nuclear and Particle Physics, Theory Group, CH-5232 Villigen PSI, Switzerland.*

# Heavy-Quark Production in the Target Fragmentation Region

**Dirk Graudenz**
*Theoretical Physics Division, CERN*
*Geneva, Switzerland*

December 1996

**Abstract**

Fixed-target experiments permit the study of hadron production in the target fragmentation region. It is expected that the tagging of specific particles in the target fragments can be employed to introduce a bias in the hard scattering process towards a specific flavour content. The case of hadrons containing a heavy quark is particularly attractive because of the clear experimental signatures and the applicability of perturbative QCD. The standard approach to one-particle inclusive processes based on fragmentation functions is valid in the current fragmentation region and for large transverse momenta $p_T$ in the target fragmentation region, but it fails for particle production at small $p_T$ in the target fragmentation region. A collinear singularity, which cannot be absorbed in the standard way into the phenomenological distribution functions, prohibits the application of this procedure. This situation is remedied by the introduction of a new set of distribution functions, the target fragmentation functions. They describe particle production in the target fragmentation region, and can be viewed as correlated distribution functions in the momentum fractions of the observed particle and of the parton initiating the hard scattering process. It is shown in a next-to-leading-order calculation for the case of deeply inelastic lepton–nucleon scattering that the additional singularity can be consistently absorbed into the renormalized target fragmentation functions on the one-loop level. The formalism is derived in detail and is applied to the production of heavy quarks. The renormalization group equation of the target fragmentation functions for the perturbative contribution is solved numerically, and the results of a case study for deeply inelastic lepton–nucleon scattering at DESY (H1 and ZEUS at HERA), at CERN (NA47) and at Fermilab (E665) are discussed. We also comment briefly on the case of an intrinsic heavy-quark content of the proton.

*Mailing address: Theoretical Physics Division, CERN, CH-1211 Geneva 23, Switzerland.*

*Address after February 1, 1997: Paul Scherrer Institute, Department of Nuclear and Particle Physics, Theory Group, CH-5232 Villigen PSI, Switzerland.*

*Electronic mail address: Dirk.Graudenz@cern.ch*

*WWW URL: http://wwwcn.cern.ch/∼graudenz/index.html*

# Contents

# 1 Introduction

Fixed-target experiments permit the study of hadron production in the target fragmentation region[1]. Indeed, to mention only a few, results have been obtained in deeply inelastic lepton–nucleon scattering for the production of $K$ mesons and $\Lambda$ hyperons [1–4], and in hadron–hadron scattering[2] for the production of $D$ mesons [6–10]. A future experiment [11, 12] with excellent particle identification capabilities will make it possible to investigate the case of polarized deeply inelastic muon–nucleon scattering. One might be interested in a study of particle production in the target fragmentation region for at least three reasons. First of all, the fragmentation of a nucleon after being hit by a highly energetic probe is interesting *per se*. Apart from phenomenological models [13–18], little is known of the dynamics involved in the fragmentation of a composite object, except for special cases, for instance diffractive scattering, where the target system is either untouched or merely excited. In non-diffractive scattering, the colour flux between the current system and the remnant of the target nucleon makes a theoretical description a complicated problem. Experimental results and a description in the framework of Quantum Chromodynamics (QCD) could shed light on the mechanisms involved. Secondly, one might hope to learn something about the nucleon state itself by tagging specific hadrons in the remnant. The analysis of, for example, $\Lambda$ production in the target fragmentation region in polarized lepton–nucleon scattering is expected to reveal information about the spin carried by the strange-quark sea [19]. Thirdly, the tagging of particles in the target fragments provides additional information on the hard scattering process. An event sample with for instance a proton in the proton remnant in electron–proton scattering is expected to be enhanced with gluon-initiated processes. This kind of mechanism therefore permits a bias in the hard scattering process towards a specific flavour content. These points illustrate that it is worth while to study particle production in the target fragmentation region in some detail.

In this paper we consider the production of heavy quarks[3] in deeply inelastic lepton–nucleon scattering with an emphasis on the target fragmentation region. Heavy quarks are well suited for two reasons. From an experimental point of view, mesons containing a heavy quark, e.g. $D$ and $D^*$ mesons, are easily tagged. On the theoretical side, the large masses of heavy quarks allow for the application of perturbative QCD, and thus predictions of experimental quantities that do not rely completely on measured fragmentation functions are possible, contrary to the case, for example, of mesons built of only light valence quarks.

The production of heavy quarks in the current fragmentation region or at finite transverse momentum $p_T$ in the target fragmentation region is accessible by means of perturbation theory. In contrast, heavy-quark production at small $p_T$ in the target fragmentation region is commonly described by non-perturbative mechanisms or by phenomenological models. It is the purpose of this paper to develop a framework that allows a unified and coherent description of heavy-quark production, in the current and target fragmentation regions, in terms of convolutions of perturbatively calculable hard scattering cross sections with phenomenological distribution functions. To this end, a new set of distribution functions, the target fragmentation functions, are employed. In this introduction, we first give a short review of two theoretical approaches to heavy-quark production. We then comment briefly on the problem of factorization in the case of semi-inclusive processes in the framework of QCD. Throughout the paper, the basic process under consideration will be deeply inelastic lepton–nucleon scattering. The developed formalism

[1] The terms "current fragmentation region" and "target fragmentation region" will be defined in Section 1.2.

[2] For a review, see also Ref. [5].

[3] For our purposes, heavy quarks are the bottom quark and the charm quark, collectively denoted by $Q$. We will also denote the photon virtuality in deeply inelastic scattering by $Q$; the meaning will be clear from the context.

is, however, more general, and applies to photoproduction in lepton–nucleon scattering and to hadron–hadron collisions as well.

### 1.1 Heavy-Quark Production

Heavy-quark production in lepton–nucleon scattering has recently been studied in great detail for the cases of both photoproduction [20–25] and deeply inelastic scattering [26–33]. The systematics of heavy-quark production in lepton–nucleon scattering, including the target fragmentation region, has been developed in Ref. [34], with some emphasis on the Fock state picture of the nucleon wave function. In principle, there are two different approaches to determine heavy-quark production cross sections: (a) by directly calculating Feynman diagrams with heavy quarks as final-state particles, as has been done for instance in Refs. [26, 27, 32], and (b) by applying the approach of perturbative heavy-quark fragmentation functions[4], where the amplitudes that are calculated have only massless partons as final-state particles, but are convoluted with heavy-quark fragmentation functions, as used, for instance, in Ref. [23]. Both approaches have their merits and drawbacks. A direct calculation to fixed order (a) allows for the determination of expectation values of arbitrary infrared-safe observables involving all momenta of outgoing partons. It requires, however, a very careful treatment of scales and the matching of various kinematical regimes [28, 29, 31] in order to obtain reliable results for differential cross sections close to, as well as far above, threshold. In particular, if the heavy quark is assumed to contribute via a non-vanishing heavy-quark density of the incident nucleon [36], and if the parton densities are evolved under the assumption of massless quarks, a subtraction procedure has to be applied to match the parton densities with hard scattering cross sections based on massive quarks. The fragmentation function approach (b) allows the resummation of terms of the form $\left[\alpha_s \ln(\mu^2/m^2)\right]^n$ by means of the renormalization group equation for fragmentation functions and is thus expected to be valid for a large range of scales $\mu$. Here $\mu$ is the factorization scale, typically set to $p_T$ in photoproduction, and $m$ is the heavy-quark mass. However, the fragmentation function picture is restricted to more inclusive observables. The heavy-quark fragmentation functions $D_{Q/i}(x, \mu^2)$ themselves are calculated in perturbation theory for $\mu \approx m$, and then evolved by means of the renormalization group equation to arbitrary scales $\mu$ [37].

The approaches mentioned so far are applicable only in the current fragmentation region or at finite $p_T$ in the target fragmentation region; the produced heavy quarks are always part of the hard scattering process, either directly as external lines of Feynman diagrams, or indirectly in the case of heavy-quark fragmentation functions. The hard scattering process being calculated in perturbative QCD, it is clear that possible non-perturbative mechanisms of heavy-quark production in the target fragmentation region cannot be taken into account in this way.

The goal of the present paper is to develop a unified picture for heavy-quark production in both the current and target fragmentation regions, based on the fragmentation function approach, for scattering processes with a hard subprocess accessible in perturbative QCD. The inclusion of the target fragmentation region in the analysis makes it necessary to introduce a new type of distribution function, the heavy-quark target fragmentation function. This function is a means to parametrize non-perturbative effects of heavy-quark production in the target fragmentation region in a way similar to that in which parton densities parametrize the non-perturbative bound-state dynamics of the proton. Therefore, the new approach relies on a possible *measurement* of these distribution functions. The advantage is that the developed

[4] We use the terminology "heavy-quark fragmentation function" for fragmentation functions of partons into heavy quarks, contrary to for example Ref. [35], where this term refers to the fragmentation function of heavy quarks into hadrons.

formalism is a natural extension of the standard one in QCD involving fragmentation functions and parton densities. Because of the lack of an experimental parametrization of heavy-quark target fragmentation functions, we restrict our numerical study to the perturbative contributions that arise from the perturbative radiation of heavy quarks in the backward direction[5], and to parametrizations based on the hypothesis of intrinsic heavy quarks in the proton [38, 39].

In the approach based on heavy quarks as external lines in the matrix elements, soft and collinear singularities are regulated by the non-vanishing heavy-quark mass $m$ in the heavy-quark propagators. The inclusive cross sections are thus finite even at small transverse momenta, but they contain terms of the form $\ln(m^2/Q^2)$, thus making the perturbative result unreliable for masses $m$ very different from $Q$. As already mentioned, this problem is taken care of in the fragmentation function approach, where these possibly large logarithmic terms are resummed. There, the parton level hard scattering matrix element itself is calculated for massless quarks. The outgoing partons, quarks and gluons, are then assumed to fragment into the observed heavy quark. Because of the vanishing parton masses, the matrix elements suffer from severe soft and collinear singularities. Soft and final-state collinear singularities related to parton lines not attached to distribution functions of the real corrections and corresponding singularities of the virtual corrections cancel [40–43], whereas the remaining collinear singularities have to be removed in a different way. In the current fragmentation region, they are taken care of by means of a suitable redefinition of the renormalized parton densities and fragmentation functions in terms of the bare ones [44–46]. It will turn out that a similar mechanism is at work in the target fragmentation region, where in this case the renormalized quantity is the target fragmentation function.

## 1.2 Factorization in Deeply Inelastic Scattering

Because of the property of asymptotic freedom [47–50], hard scattering cross sections on the parton level for large scales can be reliably calculated in perturbative QCD. However, typical hadronic mass scales are too small for perturbation theory to be valid. The confinement of partons within hadrons and the process of hadronization in scattering processes are long distance phenomena and cannot yet be calculated within the theory from first principles. Non-perturbative phenomena, such as the dynamics of bound states of hadrons in the initial state and the subsequent formation of final-state hadrons in the fragmentation process, therefore have to be incorporated into the theory in a way that makes them compatible with perturbatively calculable short-distance processes.

In the case of inclusive deeply inelastic lepton–nucleon scattering, the technical tool is the operator product expansion [50–56], which permits to separate the non-perturbative regime, expressed in terms of expectation values of local operators, from the perturbative regime, represented by calculable coefficient functions, by the observation that the processes are light-cone dominated in the leading twist approximation. In the parton picture[6], the expectation values are certain Mellin moments of parton densities. Essential in this approach is that a sum over all possible hadronic final states is performed. The local operators then arise in the operator product expansion of a commutator of two local currents. The operator product expansion is

[5] The backward direction ($x_F < 0$) is the direction of the target fragments. Please note that the conventions at HERA are such that the forward direction of the HERA machine corresponds to the backward direction in our notation. In the case of colliders, the target fragmentation region has a certain overlap with the beam pipe, and therefore measurements are difficult, so that special-purpose detectors would certainly be necessary to tag heavy flavours in the remnant jet. Fixed-target experiments are different: the strong boost in the direction of the incoming projectile makes it possible for detectors to cover effectively $4\pi$ of solid angle.

[6] See for example the comprehensive reviews by Buras, Reya and Altarelli [57–59].

not applicable in cases where the final state is not totally inclusive, as for instance in the case of one-particle inclusive processes, where more general operators than a commutator of two local currents have to be considered.

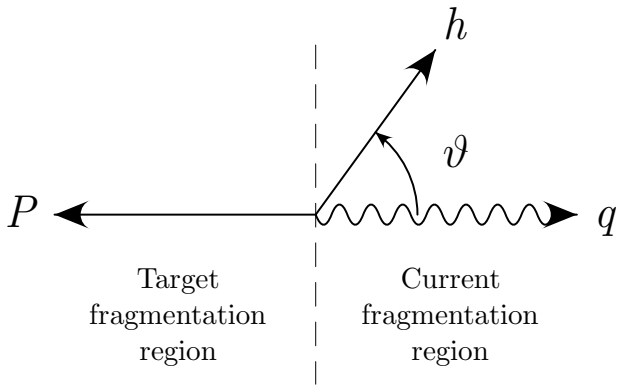


Figure 1: *The current and target fragmentation regions in deeply inelastic scattering.*

There are two kinematical regions where a hadron $h$ may be produced [60]: the current fragmentation region and the target fragmentation region, see Fig. 1. Usually, the phase space of the hadronic final state is divided up into three regions: the current region, the target region and the plateau region. Particle production in the parton model picture is then assumed to be due to the fragmentation of the current jet, of the target jet, and of wee partons emitted from the current quark, respectively. In the QCD-improved parton model, the current quark may emit a hard parton, e.g. a gluon, and thus the clear assignment of the quark to the current jet is no longer possible. We therefore use the convenient terminology that the current and target fragmentation regions simply correspond to the two hemispheres containing the virtual photon and the incident nucleon, respectively, in the hadronic centre-of-mass frame. Thus the production cross section can be written as

$$\sigma \;=\; \sigma_{\text{current}} \,+ \sigma_{\text{target}}. \tag{1}$$

If the hadron $h$ is produced in the current fragmentation region or at finite $p_T$ in the target fragmentation region, then the factorization theorems of perturbative QCD apply and allow the statement that collinear singularities are always of a form that makes it possible to define universal, process-independent parton densities and fragmentation functions [61–69]. As a consequence, the one-particle inclusive cross section in the case of deeply inelastic scattering[7] can eventually be cast into the form

$$\sigma = \int \frac{\mathrm{d}\xi}{\xi} \int \frac{\mathrm{d}\eta}{\eta} f^r(\xi,\mu_f^2)\, D^r(\eta,\mu_D^2)\, \sigma_{\text{hard}}(\xi,\eta,\mu_f^2,\mu_D^2), \tag{2}$$

where $f^r$ and $D^r$ are the renormalized, physical parton density and fragmentation function, respectively, $\mu_f$ and $\mu_D$ are factorization scales and $\sigma_{\text{hard}}$ is the mass-factorized parton-level scattering cross section.

We write $\sigma_{\text{current}}$ formally as

$$\sigma_{\text{current}} = \sigma_{fD}, \tag{3}$$

where the phase space in $\sigma_{fD}$ is suitably restricted to the current fragmentation region, with

$$\sigma_{fD} = \sigma_{fD}^{\text{hard}} \otimes f \otimes D, \tag{4}$$

[7] For two incident hadrons and the observation of more than one particle, similar formulae hold.

see Fig. 2a. The next-to-leading-order analysis has been performed in Ref. [70][8], and from an experimental point of view, this kind of process has been studied in great detail.

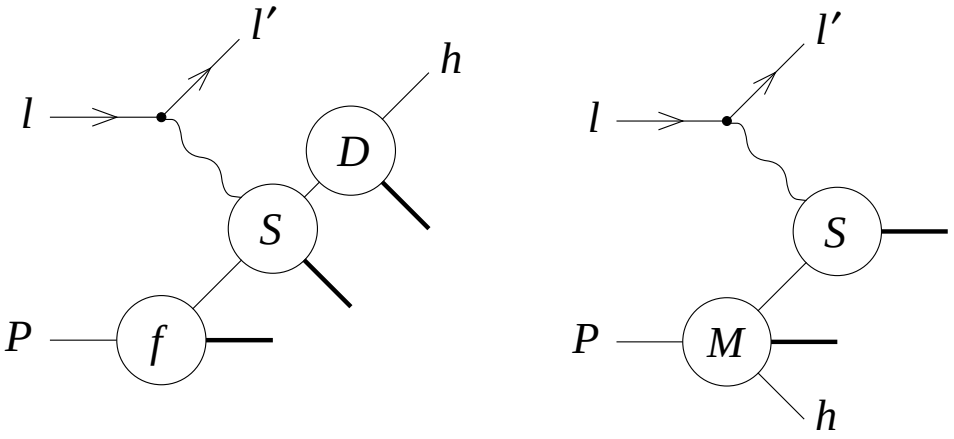


Figure 2: *Diagrams corresponding to the production of particles in the current fragmentation region (a) and in the target fragmentation region (b) in deeply inelastic lepton–nucleon scattering. Here $l$ and $l'$ are the incoming and outgoing lepton, respectively, $P$ is the incoming nucleon, $h$ stands for the observed hadron and the solid lines for the other particles in the hadronic final state; $S$ is the parton-level scattering cross section, and $f$, $D$ and $M$ are a parton density, a fragmentation function and a target fragmentation function, respectively.*

The case of particle production in the target fragmentation region has received some interest from the theoretical side [73–75]. In Refs. [73, 74], the problem is considered under the explicit assumption, going back to Ref. [76], of light-cone dominance of the commutator of time-ordered and anti-time-ordered products of the electromagnetic current and interpolating fields for the produced hadron. As a consequence, a scaling relation in $x_B$ and in the longitudinal momentum fraction of the observed hadron can be derived. It would be interesting to formulate this kind of process in the framework of perturbative QCD in the spirit of the factorization theorems, which unfortunately do not extend to this situation. Recently, a new class of distribution functions, called "fracture functions", and denoted by $M_{i,h/P}(\xi, \zeta, \mu^2)$, has been introduced [77]. Fracture functions are target fragmentation functions since they describe the production of hadrons in the target fragmentation region of, for example, a nucleon $P$ in terms of the correlated probability density for finding, at a specified scale $\mu$, a parton $i$ scattered in the hard process and a hadron $h$ in the nucleon remnant with given momentum fractions $\xi$ and $\zeta$, respectively, relative to the momentum of the incoming nucleon[9]. They fulfil a renormalization group equation which, in contrast to the one for parton densities and fragmentation functions, contains also an inhomogeneous term. The additional source term is given by a convolution of a parton density and a fragmentation function with an unsubtracted splitting function. The contribution stemming from this term will be denoted "perturbative".

[8] See also Ref. [71], and for the polarized case Ref. [72].

[9] The word "fracture", as introduced in Ref. [77], is a combination of the words "fragmentation" and "structure", describing the hybrid status of target fragmentation functions as being related to fragmentation functions and structure functions. Because the term "structure function" refers to an object different from the one defined by "parton density", and because target fragmentation functions are best described as a hybrid of fragmentation functions and parton densities, we refrain from the use of the term "fracture function".

Within the QCD-improved parton model, the basic process has the structure of the diagram depicted in Fig. 2b, corresponding to a cross section

$$\sigma_M = \sigma_M^{\rm hard} \otimes M. \tag{5}$$

The total cross section in the target fragmentation region is thus

$$\sigma_{\rm target} = \sigma_M + \sigma_{fD}, \tag{6}$$

where the phase space in $\sigma_{fD}$ is restricted to the target fragmentation region. QCD corrections to the leading-order processes in the target fragmentation region have been calculated, and it has been shown that in next-to-leading order, by a suitable definition of renormalized target fragmentation functions in terms of the bare ones, all collinear singularities can be consistently absorbed into renormalized distribution functions $f^r$, $D^r$ and $M^r$ [78]. Recently, the case of polarized deeply inelastic lepton–nucleon scattering has been treated as well [79], with similar conclusions regarding the consistent redefinition of distribution functions.

The splitting of the cross section $\sigma$ into $\sigma_{fD}$ and $\sigma_M$ in Eq. (6) for particles produced in the target fragmentation region depends on the chosen factorization scheme, because the contribution from certain finite terms may be hidden in any of the renormalized distribution functions. In the processes under consideration here, beyond the leading order, $\sigma_{fD}$ contributes to particle production in the target fragmentation region, in kinematical regimes where a parton attached to a fragmentation function is collinear to the incident parton of the hard scattering process. Only the sum of the two contributions from Eqs. (4) and (5) is physical and gives, in a fixed order of QCD perturbation theory, a consistent description. Related to this is the fact that the evolution equation for the target fragmentation functions $M^r$ is inhomogeneous and receives contributions in the form of a source term from $f^r$ and $D^r$. As a consequence, a finite renormalization of $f^r$ and $D^r$ modifies the scale evolution of $M^r$, and thus gives rise to a change in the contribution $\sigma_M$. This effect is, however, present only beyond the next-to-leading order. We finally wish to note that the introduction of target fragmentation functions of the form $f_{i,h/P}(\xi, \zeta, k_T^2, \mu^2)$, giving the probability density to find, at a scale $\mu$, a parton of momentum fraction $\xi$ and a hadron of momentum fraction $\zeta$ and transverse momentum smaller than $k_T$, is not possible in a universal, process-independent way, because the contribution of the hard matrix element at finite transverse momenta $p_T < k_T$ is process-dependent.

The picture for hadron production in deeply inelastic scattering that suggests itself based on these formal developments is the following (see also Fig. 3). Particles produced at large rapidities, i.e. in the *current fragmentation region* and at negative, but small rapidities in the *perturbative target fragmentation region* can be described by means of fragmentation functions. Particle production at large negative rapidities, in a region that we call the *non-perturbative target fragmentation region*, is due to an entirely non-perturbative mechanism, parametrized in terms of the non-perturbative piece of the newly introduced target fragmentation functions. The intermediate region of negative rapidity is called the *evolution region*. It is described by the perturbative piece of the target fragmentation functions, obtained from the inhomogeneous term in the renormalization group equation. We note that these regions do overlap; for instance, non-perturbative effects will lead to a certain spread in transverse momentum and hence in rapidity of the target fragments. The various regions are defined in the theoretical formalism by the choice of a particular factorization scheme.

### 1.3 Organization of the Paper

The paper is organized as follows. In the next section, we consider the general formalism for one-particle inclusive processes. We review some properties of fragmentation functions and calculate the one-particle inclusive cross section in deeply inelastic lepton–nucleon scattering in

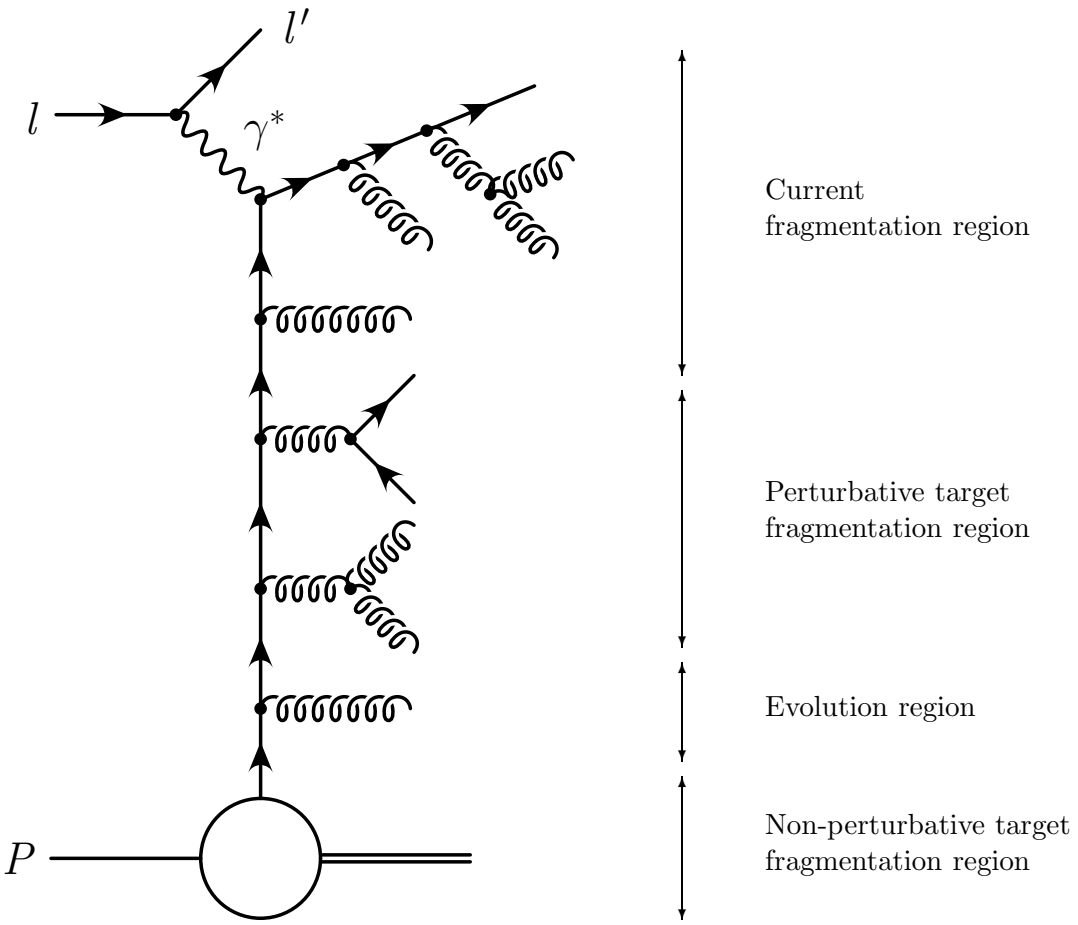


Figure 3: *Perturbative and non-perturbative fragmentation regions. The rapidity is increasing from the bottom to the top of the figure.*

next-to-leading order, paying special attention to the region of small transverse momenta of the produced hadron. This allows us to isolate the problem in the target fragmentation region and leads naturally to the introduction of the target fragmentation functions. The QCD corrections for particle production in the target fragmentation region are calculated, and it is demonstrated that a finite cross section can be obtained if the renormalization of the phenomenological distribution functions $f$, $D$ and $M$ is done properly. In Section 3 we describe the concept of target fragmentation functions in more detail and study some of the properties of their renormalization group equation. In Section 4 we review the formalism of heavy-quark fragmentation functions. We describe how they originate in perturbative QCD and solve their renormalization group equation numerically. The subject of Section 5 is heavy-quark target fragmentation functions. We define a piece that we call "perturbative", and obtain explicit numerical results from the solution of the renormalization group equation. We also briefly study the case of an intrinsic heavy-quark component of the proton. Section 6 presents a case study for heavy-quark production in the target fragmentation region in deeply inelastic lepton–nucleon scattering at HERA[10], E665 and NA47. We consider perturbative contributions and the case of an intrinsic

[10] Although HERA is a collider, and the target fragmentation region is generally not accessible for measurements because of the obstruction from the beam pipe, it is instructive to have a comparison to fixed-target experiments

heavy-quark component of the proton. Here the word "perturbative" indicates that we include only those contributions that arise from the radiation of heavy quarks in the backward direction represented by the inhomogeneous term in the evolution equation and by the perturbatively calculable contributions from the fragmentation of partons scattered in the backward direction. A typical experimental result is a differential cross section $\mathrm{d}\sigma/\mathrm{d}p_T\,\mathrm{d}x_F$; we therefore focus our attention on distributions in the corresponding variables. The paper closes with a summary, some conclusions and an outlook. Here some restrictions of the approach and open problems are discussed. Technical details are relegated to the appendices, where the explicit analytical results for the cross sections are given. Moreover, we discuss singular functions, convolution formulae for distributions, and the Laguerre method for the solution of integro-differential equations.

operating at lower energies. We do not include the HERMES experiment [80] in our study, because its particle identification capabilities do not seem to allow for the tagging of hadrons containing heavy quarks.

# 2 One-Particle Inclusive Processes

*In this section we introduce the formalism of fragmentation functions and discuss one-particle inclusive processes. The material is here developed in some detail, because similar concepts apply to the target fragmentation functions, and in order to have a concise discussion in that case we already dwell on the technical details here. As an explicit application, we consider in detail the case of the next-to-leading-order QCD corrections in deeply inelastic lepton–nucleon scattering. In the current fragmentation region and for large transverse momenta of the observed particle in the target fragmentation region, fragmentation functions and parton densities are sufficient to give a satisfactory description. For small transverse momenta in the target fragmentation region a new collinear singularity appears which cannot be taken care of by a process-independent redefinition of fragmentation functions and parton densities. The solution to the problem is the introduction of a new class of phenomenological distribution functions, the target fragmentation functions [77]. It is shown in the explicit example that all additional singularities can be absorbed into renormalized distribution functions, leading to a well-defined cross section in next-to-leading order.*

## 2.1 Fragmentation Functions

The description of one-particle inclusive processes in the framework of perturbative QCD is based on the factorization theorems[11]. For large scales, the running coupling constant $\alpha_s(\mu_r^2)$ is small, and thus hard scattering cross sections can be calculated reliably in perturbative QCD. The fragmentation process, however, involves mass scales of the order of $\Lambda_{\rm QCD}$; therefore the coupling constant is large and the perturbative picture, except for special cases involving for example heavy quarks [81], breaks down. The fragmentation of partons into hadrons is described phenomenologically by means of fragmentation functions $D_{h/i}(x,\mu^2)$, which are, by definition, probability distributions for a particle $h$ with a momentum fraction $x$ at a scale $\mu$ within a parton of type $i \in \{q, \overline{q}, g\}$, see Fig. 4.

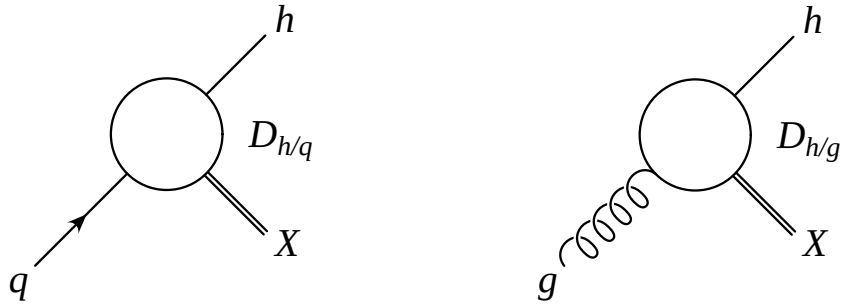


(a) (b)

Figure 4: *Fragmentation functions: $D_{h/q}(x,\mu^2)$ (a) and $D_{h/g}(x,\mu^2)$ (b). Here q stands for any quark or antiquark.*

The one-particle-inclusive cross section[12], differential in the three-momentum $\vec{h}$ of the observed hadron $h$ with four-momentum $h = (h^0, \vec{h})$ in the process

$$I \to h + X, \tag{7}$$

[11] For a review, see Ref. [69].

[12] For a brief survey, see Ref. [82].

where $I$ is the initial state, is given by[13]

$$2h^0 \frac{\mathrm{d}\sigma^{I\to hX}}{\mathrm{d}\vec{h}} = \sum_F \int \mathrm{dPS}^{(n_F)}(\underline{p}) \frac{\mathrm{d}\sigma^{I\to F}(\underline{p})}{\mathrm{dPS}^{(n_F)}(\underline{p})} \cdot \sum_{\alpha=1}^{n_F} D_{h/F_\alpha}\left(\frac{h^0}{p_\alpha^0}\right) \frac{2}{p_\alpha^0}\, \delta^S\left(\Omega_\alpha, \Omega_h\right) \frac{1}{(h^0)^{(d-3)}}. \quad (8)$$

The sum in $F$ runs over all possible partonic final states with $n_F$ partons $F_\alpha \in \{q, \overline{q}, g\}$, $\alpha = 1, \ldots, n_F$, $\underline{p}$ denotes the set of the $n_F$ parton momenta $p_\alpha$, $d = 4 - 2\epsilon$ is the space-time dimension[14], and $\sigma^{I\to F}$ is the cross section on the parton level for the process $I \to F$. The delta function $\delta^S$ is defined on the space of test functions on the $(d-2)$-dimensional sphere of solid angles by

$$\varphi(\Omega_0) = \int \mathrm{d}\Omega\, \delta^S\left(\Omega, \Omega_0\right)\, \varphi(\Omega). \quad (9)$$

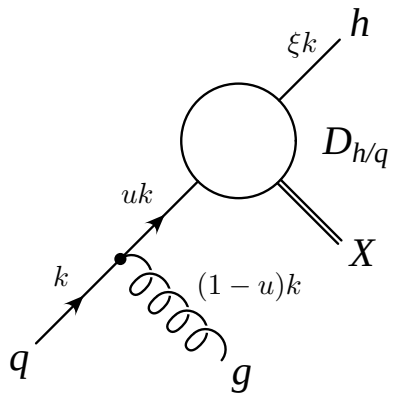


Figure 5: *An example of how a QCD correction gives rise to the scale evolution of a fragmentation function.*

Beyond the leading order of perturbation theory, the parton-level cross section $\sigma^{I\to F}$ contains collinear singularities[15] arising from processes where partons are emitted collinearly from the parent parton of the hadron; for an example, see Fig. 5. The factorization theorems guarantee that the structure of these singularities is of a universal form, and so they can be consistently absorbed into the renormalized fragmentation functions $D^r$ by a redefinition [46]

$$D_{h/i}(\xi) = \int_\xi^1 \frac{\mathrm{d}u}{u} \left[\delta_{ij}\, \delta(1-u) + \frac{1}{\epsilon} \frac{\alpha_s(\mu_r^2)}{2\pi} \frac{\Gamma(1-\epsilon)}{\Gamma(1-2\epsilon)} \left(\frac{4\pi\mu_r^2}{\mu^2}\right)^\epsilon P_{j\leftarrow i}(u)\right] D^r_{h/j}\left(\frac{\xi}{u}, \mu^2\right). \quad (10)$$

[13] By defining the variable $x = h^0/p_\alpha$, this expression can be cast into the more familiar form $\int (\mathrm{d}x/x^2)\, \sigma(h^0/x)\, D(x)$, where the angular integration of $\int \mathrm{d}p_\alpha\, \delta(p_\alpha^2)$ has been performed by means of the delta function of solid angles $\delta^S$.

[14] The regularization of ultraviolet and infrared divergences is performed in the framework of dimensional regularization (for a review, see Refs. [83, 84]), where all calculations are done in $d$ space-time dimensions. Cross sections are finite in the ultraviolet if $d < 4$ [85], and in the infrared if $d > 4$ [86–88]. The two regions may be connected by an analytical continuation. Ultraviolet and infrared singularities can be identified as poles in $\epsilon$ in the regularized expressions.

[15] In QCD, analogous to the Bloch–Nordsieck mechanism in QED [40, 41], soft singularities of the real and virtual corrections cancel owing to the Kinoshita–Lee–Nauenberg theorem [42, 43, 89]. Ultraviolet divergences are taken care of by means of a redefinition of the wave functions, the coupling constants and the masses in the process of renormalization.

This expression is valid in leading order for the $\overline{\rm MS}$ factorization scheme [45, 66]. Here $D_{h/i}(x)$ is the bare fragmentation function occurring in Eq. (8), $D^r_{h/j}\,(x,\mu^2)$ is the renormalized (i.e. physical, measurable and finite) fragmentation function[16], $\mu_r$ is the renormalization scale, and $\mu$ is the factorization scale. The singular terms are those proportional to $1/\epsilon$. Because of the process of redefinition, which has to be done at a specified scale, the renormalized fragmentation function is scale-dependent. The scale evolution of the $D_{h/j}\,(x,\mu^2)$ is governed by an Altarelli–Parisi type of evolution equation[17]

$$\frac{\partial D_{h/i}(x,\mu^2)}{\partial \ln \mu^2} = \frac{\alpha_s(\mu^2)}{2\pi} \int_x^1 \frac{{\rm d}u}{u}\, \overline{P}_{j\leftarrow i}(u)\, D_{h/j}\left(\frac{x}{u},\mu^2\right); \tag{11}$$

it can, in leading order, be derived from Eq. (10) by taking the derivative with respect to $\mu^2$ on both sides and by observing that the bare distribution function is scale-independent. In the case of the leading-order evolution equation, the evolution kernels $\overline{P}_{j\leftarrow i}(u)$ for fragmentation functions coincide with the standard Altarelli–Parisi splitting functions $P_{j\leftarrow i}(u)$, cf. Eq. (128); this is, however, no longer true beyond the leading order [91].

The momentum sum rule fulfilled by fragmentation functions is

$$\sum_h \int_0^1 {\rm d}x\, x\, D_{h/i}(x,\mu^2) = 1. \tag{12}$$

This equation expresses the fact that the momentum of every parton finally ends up as the momentum of one of the outgoing hadrons. If the equation is fulfilled for one factorization scale $\mu_0$, then the renormalization group equation ensures that it is true for all scales $\mu$. We will see in Section 3.3 that a corresponding relation for target fragmentation functions holds as well.

## 2.2 Deeply Inelastic Lepton–Nucleon Scattering: The Current Fragmentation Region

We now consider the case of one-particle inclusive cross sections in deeply inelastic lepton–nucleon scattering. After setting up the formalism, we discuss QCD corrections. In this and in the next section we focus our attention on particle production in the current fragmentation region. For the produced hadrons being strictly in the current fragmentation region or having non-vanishing transverse momentum in the target fragmentation region, the matrix elements can be found in Ref. [70]. The set-up of the present calculation is such that the limit of small transverse momenta in the target fragmentation region can be discussed. Moreover, it will be possible to identify the reason why the standard formulation fails.

Let us consider the scattering process

$$l + P \to l' + h + X, \tag{13}$$

where $l$ and $P$ are the incoming charged lepton and nucleon, respectively, $l'$ is the scattered charged lepton, $h$ is the identified hadron, and $X$ denotes anything else in the hadronic final state[18]. The integration over the angles that determine the relative orientation of the leptonic

[16] We will drop the superscript "$r$" in the following. If there is a scale argument attached to a distribution function, it is assumed that it represents a renormalized, physical quantity.

[17] In higher orders, the distribution functions depend on, in general different, factorization and renormalization scales (see for example Ref. [90]). Here we follow the common practice to identify these scales.

[18] Where possible, we identify the momenta of particles with their genuine names.

and hadronic final states can be performed. The remaining lepton phase-space variables are the Bjorken variables

$$x_B = \frac{Q^2}{2Pq}, \quad y = \frac{Pq}{Pl}. \tag{14}$$

Here $q = l - l'$ is the momentum transfer and $Q^2 = -q^2 > 0$ is the virtuality of the exchanged virtual photon. We work in the limit of vanishing lepton mass. The cross section for the production of an $n$-parton final state, differential in $x_B$, $y$ and in the phase-space variables of the final-state partons, is

$$\begin{aligned} \frac{\mathrm{d}\sigma}{\mathrm{d}x_B \mathrm{d}y \,\mathrm{dPS}^{(n)}} &= \sum_i \int \frac{\mathrm{d}\xi}{\xi} P_{i/P}(\xi)\ \alpha^2 \frac{1}{2S_H x_B} \frac{1}{e^2 (2\pi)^{2d}} \\ &\quad \cdot \left( Y^M\ (-g^{\mu\nu}) + Y^L \frac{4{x_B}^2}{Q^2} P^\mu P^\nu \right) H_{\mu\nu}. \end{aligned} \tag{15}$$

This formula is valid for the case of one-photon exchange, the exchange of weak vector bosons is neglected for simplicity; $S_H = (P + l)^2$ is the square of the total centre-of-mass energy of the lepton–nucleon scattering process, $\xi$ is the momentum fraction of the initial parton of the QCD subprocess, and $P_{i/P}(\xi)$ is the probability distribution function for the parton $i$ in the nucleon $P$; $P_{i/P}(\xi)$ can be either a parton density $f_{i/P}(\xi)$ or, as will be introduced later, a target fragmentation function $M_{i,h/P}(\xi, \zeta)$, and $\alpha = e^2/4\pi$ is the fine structure constant. The value of $Q^2$ is given by $S_H x_B y$, and the total hadronic energy is $W = \sqrt{S_H(1 - x_B)y}$, if the nucleon mass is neglected. A factor of $1/4$ for the average over the spin degrees of freedom of the incoming particles is already included. The last factor, $H_{\mu\nu}$, is the hadron tensor defined by

$$H_{\mu\nu} = \sum_{\text{spins}} \overline{\mathcal{M}_\mu}\, \mathcal{M}_\nu, \tag{16}$$

where $\epsilon^\mu(\lambda)\mathcal{M}_\mu$ is the matrix element for the process

$$\gamma^* + \text{parton} \to n \text{ partons}, \tag{17}$$

with $\epsilon^\mu(\lambda)$ the polarization vector of a virtual photon with polarization $\lambda$. The ratios

$$Y^M = \frac{1 + (1 - y)^2 - \epsilon y^2}{2(1 - \epsilon)y^2} \quad \text{and} \quad Y^L = \frac{4(1 - \epsilon)(1 - y) + 1 + (1 - y)^2 - \epsilon y^2}{2(1 - \epsilon)y^2} \tag{18}$$

specify the $y$-dependence of the contributions from the two photon polarizations under consideration. The projections operating on $H_{\mu\nu}$ are the result of the integration of the lepton tensor (see for example Ref. [92]) over the angles that describe the orientation of the momentum of the outgoing lepton with respect to the momenta of the outgoing hadrons. The cross section consists of two parts, proportional to $Y^M$, the "metric" contribution, and proportional to $Y^L$, the longitudinal contribution[19].

Let us consider the production process in the centre-of-mass frame of the incoming nucleon and the incoming virtual photon, so $\vec{P} + \vec{q} = \vec{0}$. The positive $z$-axis is defined by the $q$-direction. The hadron $h$ has polar angle $\vartheta$ relative to the virtual photon and energy $h_0$, see Fig. 1. In this frame, the energy of the incoming nucleon is

$$P_0 = \frac{Q}{2} \frac{1}{\sqrt{x_B(1 - x_B)}}. \tag{19}$$

[19] The metric and longitudinal contributions are obtained by a contraction of the hadron tensor $H_{\mu\nu}$ with the projection tensors given in Eq. (25).

Two new variables $v$ and $z$ can be defined by

$$v = \frac{1}{2}(1 - \cos\vartheta), \quad z = \frac{h_0}{P_0(1 - x_B)}, \tag{20}$$

whose range is $v,\, z \in [0, 1]$ if the masses of all particles are neglected. For $v = 1$ the angle between the observed hadron and the nucleon remnant is zero, and the hadron is produced in the target remnant direction. The value $v = 0$ corresponds to particle production in the current direction. The variables $v$ and $z$ are convenient for the discussion of the soft and collinear regions and for the explicit calculation. From an experimental point of view, however, variables such as $x_F$ and $p_T$ are more appropriate. They will be defined in Section 6.3.

We are going to calculate in the following the differential cross section

$$\frac{\mathrm{d}\sigma(l + P \to l' + h + X)}{\mathrm{d}x_B\,\mathrm{d}y\,\mathrm{d}z\,\mathrm{d}v}. \tag{21}$$

It turns out that QCD corrections to the lowest-order process for small transverse momenta require subtractions in the collinear regions $v = 0$ and $v = 1$ that make this differential cross section a distribution instead of a function of the variable $v$. Anticipating this problem, we therefore consider an observable $A(v)$ and integrate over $v$:

$$\langle A \rangle = \int_0^1 \mathrm{d}v\, \frac{\mathrm{d}\sigma}{\mathrm{d}v}\, A(v), \tag{22}$$

and correspondingly define the expectation value

$$\mathcal{A} = \frac{\mathrm{d}\langle A \rangle}{\mathrm{d}x_B\,\mathrm{d}y\,\mathrm{d}z}. \tag{23}$$

Explicitly, it is given by

$$\begin{aligned} \mathcal{A} \;=\; & \sum_j \int_{x_B}^1 \frac{\mathrm{d}u}{u} \sum_F \int \mathrm{dPS}^{(n_F)}(\underline{p})\, \frac{\alpha^2}{2S_H x_B}\, \frac{1}{e^2(2\pi)^d} \left[ Y^M\, P_M^{\mu\nu} + Y^L\, P_L^{\mu\nu} \right] H_{\mu\nu} \\ & \cdot f_{j/P}\left(\frac{x_B}{u}\right) \sum_{\alpha=1}^{N} D_{h/F_\alpha}\left(\frac{h_0}{p_\alpha^0}\right)\, \frac{P_0}{E_\alpha}\,(1 - x_B)\, A(v_\alpha), \end{aligned} \tag{24}$$

as can be inferred from Eqs. (8) and (15). The energy $p_\alpha^0$ of the $\alpha^{\text{th}}$ parton $F_\alpha$ is assumed to be defined in the hadronic centre-of-mass frame. We have defined $v_\alpha = (1 - \cos\vartheta_\alpha)/2$, where $\vartheta_\alpha$ is the polar angle of the $\alpha^{\text{th}}$ parton in the same frame; $f_{j/P}$ and $D_{h/F_\alpha}$ are the parton densities and the fragmentation functions, respectively, and we have used the following projection operators:

$$P_M^{\mu\nu} = (-g^{\mu\nu})\,, \quad P_L^{\mu\nu} = \frac{4{x_B}^2}{Q^2} P^\mu P^\nu. \tag{25}$$

From Eq. (24) we infer that the leading order given by the process of the naive parton model depicted in Fig. 6 is[21]

$$\mathcal{A}_{\mathrm{LO},\, fD} = Y^M \sum_{i=q,\overline{q}} c_i \int_{x_B}^1 \frac{\mathrm{d}u}{u} \int \frac{\mathrm{d}\rho}{\rho}\, f_{i/P}\left(\frac{x_B}{u}\right)\, D_{h/i}\left(\frac{z}{\rho}\right)\, \delta(1 - u)\, \delta(1 - \rho)\, A(0), \tag{26}$$

[20] Please note the remark in footnote 53.

[21] "LO" stands for leading order, and "NLO" for next-to-leading order, respectively.

where

$$c_i \;=\; \frac{\alpha^2}{2S_H x_B}\cdot 2\pi\cdot 4(1-\epsilon)\,Q_i^2, \tag{27}$$

$eQ_i$ being the electric charge of the quark of flavour $i$. The trivial integration variable $\rho$ is introduced already here, because later on the factorization terms will depend on the same variable. The integration in $u$ is kept for the same reason. To this order, there are no longitudinal contributions. They arise in the QCD-improved parton model in $\mathcal{O}(\alpha_s)$.

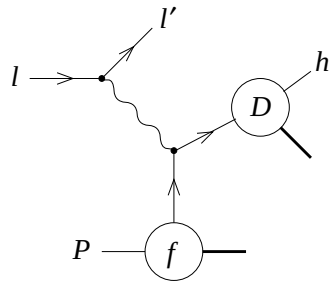


Figure 6: *Feynman diagram corresponding to the leading-order contribution in the current fragmentation region.*

## 2.3 QCD Corrections in the Current Fragmentation Region

This section gives the details of the calculation of the $\mathcal{O}(\alpha_s)$ corrections to the parton-model process. The virtual one-loop corrections to the leading-order QCD subprocess are shown in Fig. 7, and the real corrections in Figs. 8a to f.

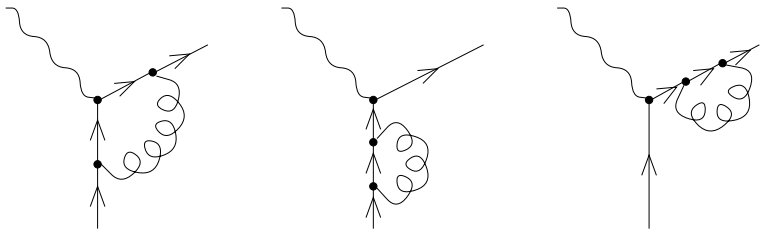

Figure 7: *Feynman diagrams of virtual QCD corrections.*

The overall effect of the virtual corrections is to multiply the leading-order cross section by a constant [45]:

$$\begin{aligned}\mathcal{A}_{\mathrm{LO+virt.},\,fD} \;=\;& Y^M \sum_{i=q,\overline{q}} c_i \\ &\cdot\int_{x_B}^1 \frac{\mathrm{d}u}{u}\int\frac{\mathrm{d}\rho}{\rho}\,f_{i/P}\left(\frac{x_B}{u}\right)\,D_{h/i}\left(\frac{z}{\rho}\right)\,\delta(1-u)\,\delta(1-\rho)\,A(0) \\ &\cdot\left\{1+\frac{\alpha_s}{2\pi}\left(\frac{4\pi\mu_r^2}{Q^2}\right)^{\epsilon}\frac{\Gamma(1-\epsilon)}{\Gamma(1-2\epsilon)}C_F\left(-2\frac{1}{\epsilon^2}-3\frac{1}{\epsilon}-8-\frac{\pi^2}{3}\right)\right\},\end{aligned} \tag{28}$$

where $\mu_r$ is the renormalization scale, $\alpha_s = \alpha_s(\mu_r^2)$, and $C_F$ is one of the Casimir invariants of the colour gauge group SU($N_C$), $N_C = 3$. The double and single poles in $\epsilon$ represent an infrared divergence, which is cancelled by a contribution from the real corrections similar to the virtual correction, but of opposite sign. To this order of perturbation theory, the strong coupling constant is not renormalized, because the loop corrections are the lowest-order QCD corrections of a QED vertex.

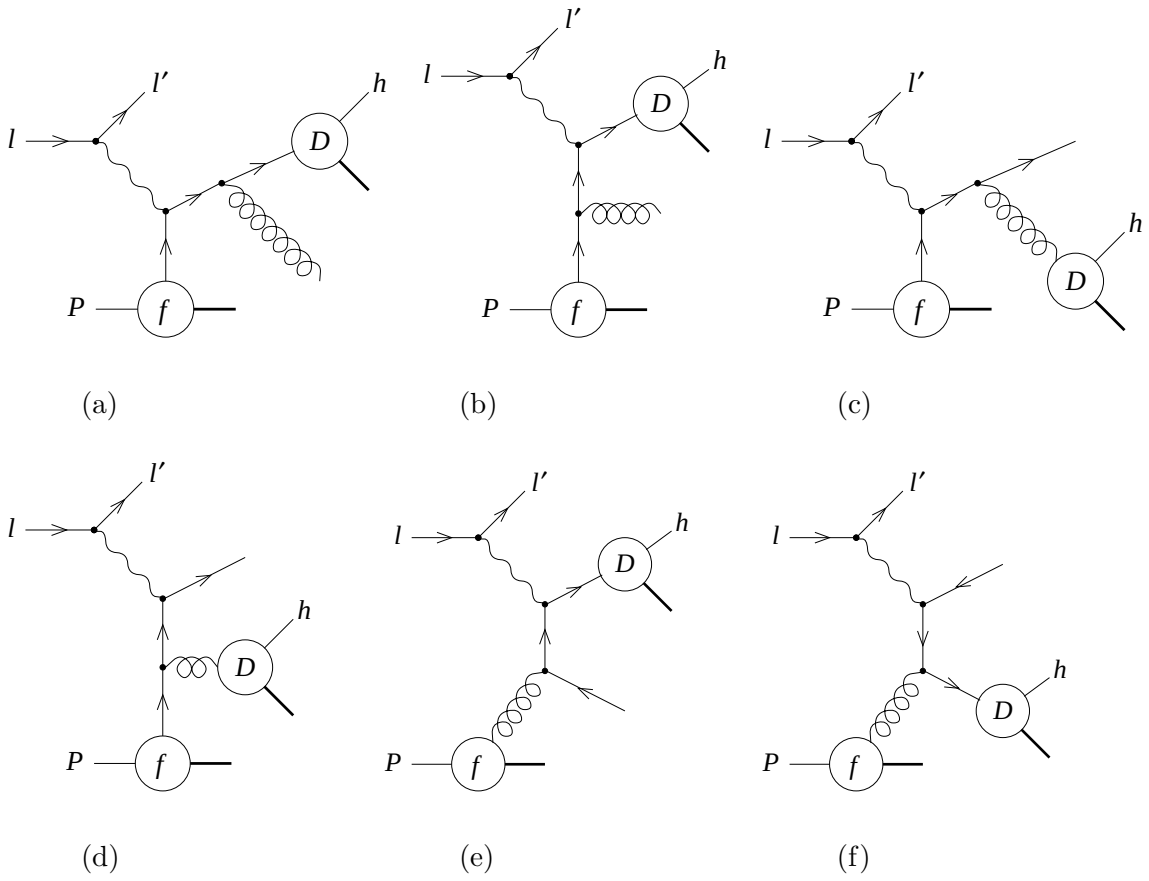


Figure 8: *Feynman diagrams of real QCD corrections for particle production in the current fragmentation region.*

The metric and longitudinal projections of the hadron tensor for the real corrections are[22] (see for example Refs. [92–95])

$$\begin{aligned}
&\frac{1}{e^2(2\pi)^{2d}} P_M^{\mu\nu} H_{\mu\nu}(\gamma^* q \to qg) \\
&\quad = 8\pi \, \frac{\alpha_s}{2\pi} \, \mu_r^{2\epsilon} \, 2\pi \, C_F \, Q_q^2 \cdot 4(1-\epsilon) \left[ (1-\epsilon) \left( \frac{s_{ig}}{s_{qg}} + \frac{s_{qg}}{s_{ig}} \right) + \frac{2Q^2 s_{iq}}{s_{ig} s_{qg}} + 2\epsilon \right], \\
&\frac{1}{e^2(2\pi)^{2d}} P_L^{\mu\nu} H_{\mu\nu}(\gamma^* q \to qg) \\
&\quad = 8\pi \, \frac{\alpha_s}{2\pi} \, \mu_r^{2\epsilon} \, 2\pi \, C_F \, Q_q^2 \cdot 4(1-\epsilon) \left[ 4 \, \frac{u^2}{Q^2} \, \frac{1}{2} s_{iq} \right],
\end{aligned}$$

[22] $C_A$ and $C_F$ are Casimir invariants of the colour gauge group. For SU($N_C$), they are given by $C_A = N_C$ and $C_F = (N_C^2 - 1)/2N_C$. For $N_f$ flavours of quarks, we define $T_R \doteq N_f/2$ and set $T_f \doteq T_R/N_f = 1/2$.

$$\frac{1}{e^2(2\pi)^{2d}} P_M^{\mu\nu} H_{\mu\nu}(\gamma^* g \to q\overline{q})$$
$$= 8\pi \frac{\alpha_s}{2\pi} \mu_r^{2\epsilon} 2\pi T_f Q_q^2 \cdot 4(1-\epsilon) \left[ \frac{s_{iq}}{s_{i\overline{q}}} + \frac{s_{i\overline{q}}}{s_{iq}} - \frac{1}{1-\epsilon} \frac{2Q^2 s_{q\overline{q}}}{s_{iq} s_{i\overline{q}}} - 2\frac{\epsilon}{1-\epsilon} \right],$$
$$\frac{1}{e^2(2\pi)^{2d}} P_L^{\mu\nu} H_{\mu\nu}(\gamma^* g \to q\overline{q})$$
$$= 8\pi \frac{\alpha_s}{2\pi} \mu_r^{2\epsilon} 2\pi T_f Q_q^2 \cdot 4(1-\epsilon) \left[ 4 \frac{u^2}{Q^2} s_{q\overline{q}} \right]. \tag{29}$$

The invariants are defined by $s_{AB} = 2p_A p_B$, and the variable $u$ is given by $u = Q^2/(Q^2 + \hat{s})$, where $\hat{s}$ is the invariant mass squared of the two outgoing partons. The momenta $p_i$, $p_q$, $p_{\overline{q}}$, $p_g$ correspond to the incident parton (quark or gluon), an outgoing quark, an outgoing antiquark and an outgoing gluon, respectively. The formulae already contain the appropriate factors for the average over the colour degrees of freedom of the incoming partons. An additional factor of $1/(1-\epsilon)$ has been provided for the terms with an incoming gluon, because gluons have $2(1-\epsilon)$ helicity states in $(4-2\epsilon)$ space-time dimensions compared with only two in the case of quarks. In order to perform the phase-space integrations, suitable parametrizations of the two-particle phase space $\mathrm{dPS}^{(2)}$, depending on two independent variables, are needed. After integration over the azimuthal angle relative to the lepton plane one variable is left over. The latter can be chosen such that it is the one that is actually used in the factorization of the collinear singularities. Three parametrizations suitable for the consideration of various collinear limits are given explicitly in Appendix B.

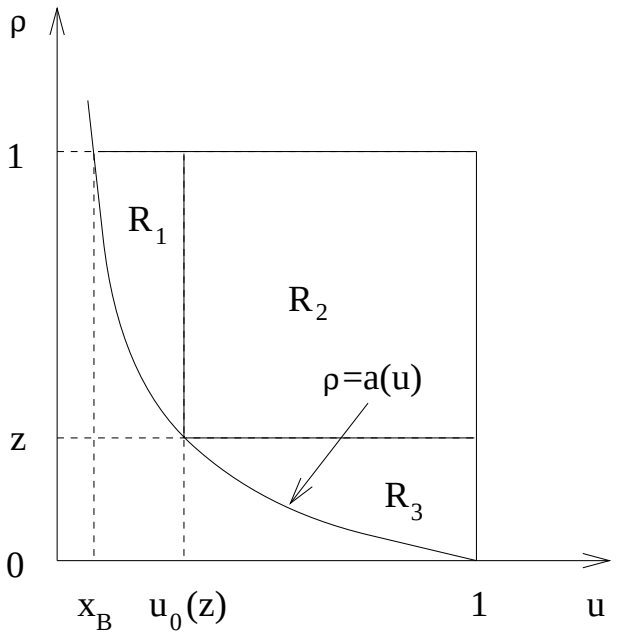


Figure 9: *Phase space for the real corrections (see text). The two regions corresponding to $\alpha = 1$ and $\alpha = 2$ are marked by $R_1$ and $R_2$, respectively. Region $R_3$ is excluded because the parent parton of the observed hadron must have an energy larger than that of the hadron itself. The curve $\rho = a(u)$ corresponds to particle production in the direction of the target remnant.*

The singularity structure of the matrix elements for the real corrections may be discussed

in terms of the variables $\rho$ and $u$ of parametrization A from Appendix B.1. The phase space is shown in Fig. 9. Let $p_1$ be the momentum of the parent parton of the observed hadron, $p_2$ the momentum of the other outgoing parton, and $p_i$ the momentum of the incident parton. Then $\rho$ is the energy corresponding to $p_1$ in the hadronic centre-of-mass frame, scaled such that $\rho \in [0,1]$. The singularities of the matrix elements are located in the phase-space regions collected in Table 1. In the case of the singularities $p_2 \parallel p_i$ and $p_1 \parallel p_2$, the hadron is produced in the current direction; $p_1 \to 0$ is excluded because the parent parton of the observed hadron must have a non-vanishing energy, and if $p_1 \parallel p_i$, then the observed hadron is part of the target fragments.

| Singularity | Condition |
|---|---|
| $p_2 \parallel p_i$ | $\rho = 1$ |
| $p_1 \parallel p_i$ | $\rho = a(u)$ |
| $p_1 \parallel p_2$ | $u = 1$ |
| $p_1 \to 0$ | $\rho = 0$ and $u = 1$ |
| $p_2 \to 0$ | $\rho = 1$ and $u = 1$ |

Table 1: *Singular phase-space regions. The variables are defined in Appendix B.1.*

By means of the given phase-space parametrizations, the infrared and collinear singularities can be factorized and the integrations can be performed. The calculation is done by expressing the product of the regulator terms from the $d$-dimensional phase space, for instance of the form of $(1-u)^{-\epsilon}$, and the singular propagators represented in this case by $1/(1-u)$, by means of a Laurent series of distributions in $\epsilon$, see Appendix A.1. In this way the singular terms can be identified, and the finite terms are directly given in a form suitable for the numerical evaluation of arbitrary observables. The intermediate steps of this straightforward but lengthy calculation are not given here. The results are presented in two steps. First we give the divergent contributions and discuss the extent to which they can be absorbed into renormalized parton densities and fragmentation functions. Then we discuss the structure of the finite contributions including the terms that compensate scale variations of the factorization scales. The contributions are denoted by $B_1^M$, $B_2^M$, $B_1^L$, $B_2^L$, where the superscript and subscript in $B_\alpha^X$ stand for

- $\alpha$: phase-space region for the integration variable $u$:
  $\alpha = 1$ (Region $\mathrm{R}_1$): $u \in \Big[x_B, x_B/(x_B + (1-x_B)z)\Big]$,
  $\alpha = 2$ (Region $\mathrm{R}_2$): $u \in \Big[x_B/(x_B + (1-x_B)z), 1\Big]$;
- $X$: polarization of the exchanged photon:
  $X = M$: metric contribution,
  $X = L$: longitudinal contribution.

The contribution of the real corrections to the expectation value $\mathcal{A}$ is given by

$$\mathcal{A}_{\text{real, } fD} = \mathcal{A}_{B_1^M} + \mathcal{A}_{B_2^M} + \mathcal{A}_{B_1^L} + \mathcal{A}_{B_2^L}. \tag{30}$$

The singular and finite contributions will be denoted by $\mathcal{A}^s_{B_\alpha^X}$ and $\mathcal{A}^f_{B_\alpha^X}$, respectively, so that $\mathcal{A}_{B_\alpha^X} = \mathcal{A}^s_{B_\alpha^X} + \mathcal{A}^f_{B_\alpha^X}$. Throughout the calculation the $\overline{\text{MS}}$ factorization scheme is used both for the parton densities and fragmentation functions. The choice of the factorization scheme defines

the finite parts unambiguously. Moreover, one has to choose three factorization scales, one ($\mu_f^2$) for the renormalized parton densities $f^r$, another one ($\mu_D^2$) for the fragmentation functions $D^r$, and a third one ($\mu_M^2$) for the target fragmentation functions $M^r$, which will soon be introduced. For the singular contributions we obtain

$$
\begin{aligned}
\mathcal{A}^s_{B_1^M} &= Y^M \sum_{i=q,\overline{q}} c_i \frac{\alpha_s}{2\pi} \\
&\cdot \Bigg\{ \int_{x_B}^{x_B/(x_B+(1-x_B)z)} \frac{\mathrm{d}u}{u} \int_{a(u)}^1 \frac{\mathrm{d}\rho}{\rho} A(v(\rho,u)) \\
&\cdot \Bigg[ f_{i/P}\left(\frac{x_B}{u}\right) D_{h/i}\left(\frac{z}{\rho}\right) \left(-\frac{1}{\epsilon}\right) \frac{\Gamma(1-\epsilon)}{\Gamma(1-2\epsilon)} \left(\frac{4\pi\mu_r^2}{\mu_f^2}\right)^{\epsilon} P_{q\leftarrow q}(u)\,\delta(1-\rho) \\
&\quad + f_{g/P}\left(\frac{x_B}{u}\right) D_{h/i}\left(\frac{z}{\rho}\right) \left(-\frac{1}{\epsilon}\right) \frac{\Gamma(1-\epsilon)}{\Gamma(1-2\epsilon)} \left(\frac{4\pi\mu_r^2}{\mu_f^2}\right)^{\epsilon} P_{q\leftarrow g}(u)\,\delta(1-\rho) \Bigg] \\
&\quad + \int_{x_B}^{x_B/(x_B+(1-x_B)z)} \frac{\mathrm{d}u}{u} (1-x_B)\, A(1) \\
&\cdot \Bigg[ f_{i/P}\left(\frac{x_B}{u}\right) D_{h/g}\left(\frac{(1-x_B)\,z\,u}{x_B(1-u)}\right) \left(-\frac{1}{\epsilon}\right) \frac{\Gamma(1-\epsilon)}{\Gamma(1-2\epsilon)} \left(\frac{4\pi\mu_r^2}{\mu_M^2}\right)^{\epsilon} \frac{1}{1-u}\frac{u}{x_B} \hat{P}_{gq\leftarrow q}(u) \\
&\quad + f_{g/P}\left(\frac{x_B}{u}\right) D_{h/i}\left(\frac{(1-x_B)\,z\,u}{x_B(1-u)}\right) \left(-\frac{1}{\epsilon}\right) \frac{\Gamma(1-\epsilon)}{\Gamma(1-2\epsilon)} \left(\frac{4\pi\mu_r^2}{\mu_M^2}\right)^{\epsilon} \frac{1}{1-u}\frac{u}{x_B} \hat{P}_{\overline{q}q\leftarrow g}(u) \Bigg] \Bigg\} \\
&\quad + \mathcal{O}(\epsilon),
\end{aligned}
$$

$$
\begin{aligned}
\mathcal{A}^s_{B_2^M} &= Y^M \sum_{i=q,\overline{q}} c_i \frac{\alpha_s}{2\pi} \int_{x_B/(x_B+(1-x_B)z)}^1 \frac{\mathrm{d}u}{u} \int_z^1 \frac{\mathrm{d}\rho}{\rho} A(v(\rho,u)) \\
&\cdot \Bigg[ f_{i/P}\left(\frac{x_B}{u}\right) D_{h/i}\left(\frac{z}{\rho}\right) \Bigg\{ \frac{\Gamma(1-\epsilon)}{\Gamma(1-2\epsilon)} \left(\frac{4\pi\mu_r^2}{Q^2}\right)^{\epsilon} C_F \left(2\frac{1}{\epsilon^2}+3\frac{1}{\epsilon}\right) \delta(1-u)\delta(1-\rho) \\
&\qquad -\frac{1}{\epsilon}\frac{\Gamma(1-\epsilon)}{\Gamma(1-2\epsilon)} \left[ \left(\frac{4\pi\mu_r^2}{\mu_f^2}\right)^{\epsilon} P_{q\leftarrow q}(u)\,\delta(1-\rho) + \left(\frac{4\pi\mu_r^2}{\mu_D^2}\right)^{\epsilon} P_{q\leftarrow q}(\rho)\,\delta(1-u) \right] \Bigg\} \\
&\quad + f_{i/P}\left(\frac{x_B}{u}\right) D_{h/g}\left(\frac{z}{\rho}\right) \left(-\frac{1}{\epsilon}\right) \frac{\Gamma(1-\epsilon)}{\Gamma(1-2\epsilon)} \left(\frac{4\pi\mu_r^2}{\mu_D^2}\right)^{\epsilon} P_{g\leftarrow q}(\rho)\,\delta(1-u) \\
&\quad + f_{g/P}\left(\frac{x_B}{u}\right) D_{h/i}\left(\frac{z}{\rho}\right) \left(-\frac{1}{\epsilon}\right) \frac{\Gamma(1-\epsilon)}{\Gamma(1-2\epsilon)} \left(\frac{4\pi\mu_r^2}{\mu_f^2}\right)^{\epsilon} P_{q\leftarrow g}(u)\,\delta(1-\rho) \Bigg] \\
&\quad + \mathcal{O}(\epsilon),
\end{aligned}
$$

$$
\begin{aligned}
\mathcal{A}^s_{B_1^L} &= 0, \\
\mathcal{A}^s_{B_2^L} &= 0.
\end{aligned}
\tag{31}
$$

Here $A(1)$ is the observable $A$ evaluated for the observed particle running in the target remnant direction. One sees immediately that the infrared singularities proportional to $2/\epsilon^2+3/\epsilon$ cancel in the sum of virtual and real corrections. Let us for the moment assume that the observable $A$ is such that $A(1)=0$, i.e. that it vanishes if the observed hadron is in the target fragmentation region. Then the only additional singular contributions are those that involve the Altarelli–Parisi splitting functions $P_{B\leftarrow A}$. They can be absorbed into renormalized fragmentation functions $D^r$ (terms $\sim\delta(1-u)$), cf. Eq. (10), and renormalized parton densities $f^r$ (terms $\sim\delta(1-\rho)$), given

by the expression [44, 45]

$$f_{i/P}(\xi) = \int_\xi^1 \frac{\mathrm{d}u}{u} \left[ \delta_{ij}\,\delta(1-u) + \frac{1}{\epsilon}\frac{\alpha_s(\mu_r^2)}{2\pi}\frac{\Gamma(1-\epsilon)}{\Gamma(1-2\epsilon)} \left(\frac{4\pi\mu_r^2}{\mu^2}\right)^\epsilon P_{i\leftarrow j}(u) \right] f^r_{j/P}\left(\frac{\xi}{u}, \mu^2\right). \quad (32)$$

The finite terms from the Born contribution, the virtual correction and the renormalization of the distribution functions are

$$\begin{aligned} \mathcal{A}^f_{\text{LO+virt., } fD} \;=\; & Y^M \sum_{i=q,\overline{q}} c_i \\ & \cdot \int_{x_B}^1 \frac{\mathrm{d}u}{u} \int \frac{\mathrm{d}\rho}{\rho}\, f_{i/P}\left(\frac{x_B}{u}, \mu_f^2\right) D_{h/i}\left(\frac{z}{\rho}, \mu_D^2\right) \delta(1-u)\,\delta(1-\rho)\,A(0) \\ & \cdot \left\{ 1 + \frac{\alpha_s}{2\pi} C_F \left(-8 - \frac{\pi^2}{3}\right) \right\}. \end{aligned} \quad (33)$$

For observables $A$ with support in the target fragmentation region, there are singular terms that cannot be taken into account by means of a redefinition of $f$ and $D$, namely those proportional to unsubtracted Altarelli–Parisi splitting functions $\hat{P}_{CB\leftarrow A}$; for explicit expressions see Appendix D.1. The redefinition of the distribution functions $f$ and $D$ is already dictated by, for example, the inclusive cross section in lepton–nucleon scattering and the one-particle-inclusive cross section in $e^+e^-$ scattering. In order for them to be universal, i.e. process-independent functions, the absorption of additional singular terms is not permitted. The kinematical configuration in the singular phase-space region $\rho = a(u)$, see Fig. 9, is such that the observed hadron is part of the target remnant, collinear to its parent parton, with the second outgoing parton in the current direction. The Feynman diagrams with singularities in this region are those from Figs. 8d and f. It can easily be seen that a term suited to absorb these singularities cannot occur in $\mathcal{O}(\alpha_s^0)$ in the standard formulation involving only parton densities and fragmentation functions. This problem is tackled in the next section, where it is shown that all singularities can be absorbed consistently if target fragmentation functions are introduced.

The finite expectation value of $A$ is given by

$$\mathcal{A}^f_{\text{total}} = \mathcal{A}^f_{\text{LO+virt., } fD} + \mathcal{A}^f_{\text{real, } fD}. \quad (34)$$

The finite terms $\mathcal{A}^f_{B^X_\alpha}$ are collected in Appendix C.1. Due to the necessary subtractions of collinear singularities, they are distributions in the variables $v$ and $\rho$. In the case of fragmentation functions $D(\sigma)$ with subtractions or delta functions at $\sigma = 1$, the cross section will be a distribution in the variable $z$, being singular at $z = 1$. All convolutions with regular observables are finite. Care must be taken, however, to choose the region of integration appropriately (for a discussion see Section 6.2). As can be seen from the explicit expressions in Eq. (118), and as is expected, the next-to-leading-order contributions provide compensating terms for the dependence on the factorization scales $\mu_f$, $\mu_D$ and $\mu_M$, the latter being introduced in Section 2.5. Formally, the factorization-scale dependence of the total cross section will therefore be of $\mathcal{O}(\alpha_s^2)$. In practice, in particular in the case of heavy-quark production, the scale dependence may still be substantial, for the reason that the photon–gluon fusion process, arising at $\mathcal{O}(\alpha_s)$, may give large contributions, and its genuine factorization-scale dependence of $\mathcal{O}(\alpha_s^2)$ is not compensated by any term included in the present calculation. Since the leading-order process is of $\mathcal{O}(\alpha_s^0)$, there is no renormalization-scale dependence in leading order. For a numerical study of the scale dependence, we refer to Section 6.7.

## 2.4 Deeply Inelastic Lepton–Nucleon Scattering: The Target Fragmentation Region

We have shown that in the standard formalism involving parton densities $f$ and fragmentation functions $D$, a collinear singularity, which cannot be absorbed into $f$ and $D$ by a renormalization, is present in the cross section for the kinematical configuration of the observed hadron collinear with the target fragments. It turns out that this problem can be resolved by the introduction of a new class of phenomenological distribution functions, the target fragmentation functions. Briefly, a target fragmentation function or "fracture function" $M_{i,h/P}(\xi,\zeta)$ is a probability density to find a parton $i$ with momentum fraction $\xi$ and a hadron $h$ with momentum fraction $\zeta$ in the nucleon $P$, where the observed hadron is collinear with the target fragments. Obviously, the kinematical restrictions on $\xi$ and $\zeta$ are $\xi \in [0,1]$, $\zeta \in [0,1]$, and $\xi + \zeta \leq 1$. For the purpose of this and the following section, we need no other properties of target fragmentation functions, and so a more detailed discussion is postponed to Section 3. Here and in the next section we calculate the cross section in next-to-leading order in deeply inelastic lepton–nucleon scattering for the observed hadron in the target fragmentation region, and show that the additional collinear singularity can be absorbed into the target fragmentation functions by a suitable renormalization, thus giving in total a finite result.

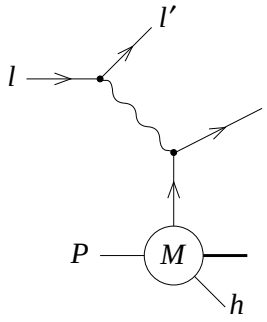


Figure 10: *Feynman diagram corresponding to the leading-order contribution in the target fragmentation region.*

The lowest-order contribution, given by the graph in Fig. 10, is

$$\mathcal{A}_{\mathrm{LO},\,M} = Y^M \sum_{i=q,\overline{q}} c_i \int_{x_B/(1-(1-x_B)z)}^1 \frac{\mathrm{d}u}{u}\, M_{i,h/P}\left(\frac{x_B}{u}, (1-x_B)z\right) \cdot \delta(1-u)\,(1-x_B)\,A(1). \tag{35}$$

This expression is similar to Eq. (26) for the current fragmentation region, with the difference that the product of a parton density and a fragmentation function is replaced by a target fragmentation function. The observable $A$ is evaluated at $v = 1$. The additional factor of $(1 - x_B)$ is explained by the fact that the momentum of the observed hadron and of the other nucleon fragments is given by $(1-x_B)P$, after the parton incident in the hard scattering process has been removed from the nucleon.

## 2.5 QCD Corrections in the Target Fragmentation Region

As in the case of the current fragmentation region, the next-to-leading-order QCD corrections consist of virtual and real corrections. The virtual corrections are given by the same graphs as

in Fig. 7, so the sum of the leading order and the virtual corrections is given by

$$\begin{aligned}\mathcal{A}_{\text{LO+virt.},\,M} &= Y^M \sum_{i=q,\overline{q}} c_i \int_{x_B/(1-(1-x_B)z)}^1 \frac{\mathrm{d}u}{u} M_{i,h/P}\left(\frac{x_B}{u}, (1-x_B)z\right) \\ &\cdot \delta(1-u)\,(1-x_B)\,A(1) \\ &\cdot \left\{1 + \frac{\alpha_s}{2\pi}\left(\frac{4\pi\mu_r^2}{Q^2}\right)^{\epsilon} \frac{\Gamma(1-\epsilon)}{\Gamma(1-2\epsilon)} C_F \left(-2\frac{1}{\epsilon^2} - 3\frac{1}{\epsilon} - 8 - \frac{\pi^2}{3}\right)\right\}. \end{aligned} \tag{36}$$

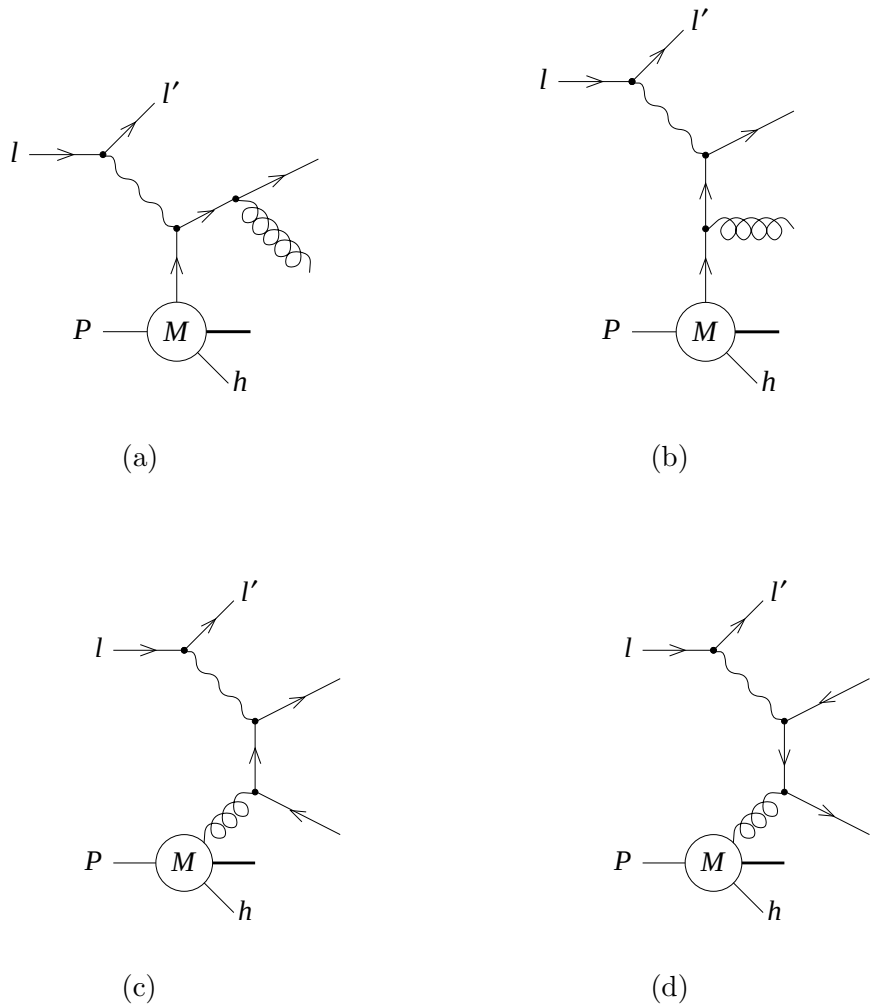


Figure 11: *Feynman diagrams of real QCD corrections for particle production in the target fragmentation region.*

The graphs for the real corrections are shown in Fig. 11. The contribution of the real corrections to the expectation value $\mathcal{A}$ is given by

$$\mathcal{A}_{\text{real},\,M} = \mathcal{A}_{C^M} + \mathcal{A}_{C^L}. \tag{37}$$

As before, we state the results for the singular and regular terms separately, $\mathcal{A}_{C^X} = \mathcal{A}^s_{C^X} + \mathcal{A}^f_{C^X}$.

The singular contributions are

$$\begin{aligned}
\mathcal{A}^s_{C^M} &= Y^M \sum_{i=q,\overline{q}} c_i \frac{\alpha_s}{2\pi} \int_{x_B/(1-(1-x_B)z)}^1 \frac{\mathrm{d}u}{u} A(1) \\
&\cdot \Bigg[ M_{i,h/P}\left(\frac{x_B}{u},(1-x_B)z\right) \Bigg\{ \frac{\Gamma(1-\epsilon)}{\Gamma(1-2\epsilon)} \left(\frac{4\pi\mu_r^2}{Q^2}\right)^{\epsilon} C_F \left(2\frac{1}{\epsilon^2}+3\frac{1}{\epsilon}\right) \delta(1-u)\,(1-x_B) \\
&\qquad -\frac{1}{\epsilon}\frac{\Gamma(1-\epsilon)}{\Gamma(1-2\epsilon)} \left(\frac{4\pi\mu_r^2}{\mu_M^2}\right)^{\epsilon} P_{q\leftarrow q}(u)\,(1-x_B) \Bigg\} \\
&\quad + M_{g,h/P}\left(\frac{x_B}{u},(1-x_B)z\right) \Bigg\{ -\frac{1}{\epsilon}\frac{\Gamma(1-\epsilon)}{\Gamma(1-2\epsilon)} \left(\frac{4\pi\mu_r^2}{\mu_M^2}\right)^{\epsilon} P_{q\leftarrow g}(u)\,(1-x_B) \Bigg\} \Bigg] \\
&\quad + \mathcal{O}(\epsilon), \\
\mathcal{A}^s_{C^L} &= 0.
\end{aligned} \tag{38}$$

Again, the singularities from the virtual corrections cancel against corresponding terms from the real corrections. The singularities proportional to $-(1/\epsilon)P_{B\leftarrow A}(u)$ have the same structure as those for the case of parton densities. It can easily be seen that, in order to take into account the additional collinear singularities proportional to $-(1/\epsilon)\hat{P}_{CB\leftarrow A}(u)$ from Section 2.3, the bare target fragmentation functions $M$ have to be defined in terms of the renormalized ones $M^r$ as [78][23]

$$\begin{aligned}
&M_{i,h/P}(\xi,\zeta) \\
&= \int_{\xi/(1-\zeta)}^1 \frac{\mathrm{d}u}{u} \left[ \delta_{ij}\,\delta(1-u) + \frac{1}{\epsilon}\frac{\alpha_s(\mu_r^2)}{2\pi}\frac{\Gamma(1-\epsilon)}{\Gamma(1-2\epsilon)} \left(\frac{4\pi\mu_r^2}{\mu^2}\right)^{\epsilon} P_{i\leftarrow j}(u) \right] M^r_{j,h/P}\left(\frac{\xi}{u},\zeta,\mu^2\right) \\
&+ \int_{\xi}^{\xi/(\xi+\zeta)} \frac{\mathrm{d}u}{u} \frac{1}{1-u} \frac{u}{\xi} \frac{1}{\epsilon} \frac{\alpha_s(\mu_r^2)}{2\pi} \frac{\Gamma(1-\epsilon)}{\Gamma(1-2\epsilon)} \left(\frac{4\pi\mu_r^2}{\mu^2}\right)^{\epsilon} \\
&\qquad \cdot \hat{P}_{ki\leftarrow j}(u)\, f_{j/P}\left(\frac{\xi}{u}\right) D_{h/k}\left(\frac{\zeta u}{\xi(1-u)}\right).
\end{aligned} \tag{39}$$

Of course, as usual, the finite terms of the convolution kernels may be chosen in a way in principle arbitrary, thereby defining a specific factorization scheme. The expression just given subtracts the poles in $\epsilon$ such that no unnatural transcendental numbers are left over in the finite terms. We define the functions $M^r$ as given in Eq. (39) to be the renormalized target fragmentation functions in the $\overline{\mathrm{MS}}$ scheme. The sum of all terms

$$\mathcal{A}_{\mathrm{total}} = \mathcal{A}_{\mathrm{LO+virt.},\,fD} + \mathcal{A}_{\mathrm{real},\,fD} + \mathcal{A}_{\mathrm{LO+virt.},\,M} + \mathcal{A}_{\mathrm{real},\,M}, \tag{40}$$

expressed in terms of renormalized quantities, is finite. Here the finite contribution from the leading order and from the virtual correction in Eq. (36) reads

$$\begin{aligned}
\mathcal{A}^f_{\mathrm{LO+virt.},\,M} &= Y^M \sum_{i=q,\overline{q}} c_i \int_{x_B/(1-(1-x_B)z)}^1 \frac{\mathrm{d}u}{u} M_{i,h/P}\left(\frac{x_B}{u},(1-x_B)z,\mu_M^2\right) \\
&\qquad \cdot \delta(1-u)\,(1-x_B)\,A(1) \left\{ 1 + \frac{\alpha_s}{2\pi} C_F \left(-8-\frac{\pi^2}{3}\right) \right\},
\end{aligned} \tag{41}$$

and the explicit expressions for the finite contributions $\mathcal{A}^f_{C^X}$ are collected in Appendix C.1.

[23] The terms involving the splitting functions $P_{g\leftarrow g}$ and $\hat{P}_{gg\leftarrow g}$ are not needed for the process under consideration.

# 3 Target Fragmentation Functions

*Target fragmentation functions are joint probability distributions for an observed particle in the target fragmentation region and a parton incident in the hard scattering process. The expression of the renormalized distribution functions in terms of the bare ones follows from the requirement that the additional collinear singularity that was calculated in Section 2.3 be absorbed. From this expression a renormalization group equation can be derived. Scale evolution is driven by two terms, a homogeneous one, reminiscent of the Altarelli–Parisi equation, and an inhomogeneous one, due to particle production by the fragmentation of partons emitted in the backward direction. The scale evolution equation can also be motivated by an intuitive argument, and rewritten in a form that allows an analogy to the Altarelli–Parisi equation to be drawn. We also briefly discuss momentum sum rules. It turns out that a momentum sum rule related to the momentum fraction of the observed particle is fulfilled, whereas the one that would naively be expected to hold in relation to the momentum fraction of the incoming parton is violated. This violation can be traced back to the inhomogeneous term in the evolution equation.*

## 3.1 Definition

Target fragmentation functions $M_{i,h/P}(\xi,\zeta)$ [77][24], see Fig. 12, are probability densities to find a parton $i$ with momentum fraction $\xi$ and a hadron $h$ with momentum fraction $\zeta$ in the nucleon $P$, where the observed hadron is collinear with the target fragments. The kinematical restrictions on $\xi$ and $\zeta$ are $\xi \in [0,1]$, $\zeta \in [0,1]$, and $\xi+\zeta \leq 1$. There is no definition of target fragmentation functions in terms of the operator product expansion, because the process under consideration is not fully inclusive. In the case of QCD corrections, target fragmentation functions, very similar to parton densities, have to be redefined in order to be finite and physical quantities. As a consequence, they become scale-dependent. The expression for the bare target fragmentation functions in terms of the renormalized ones has already been given in Eq. (39).

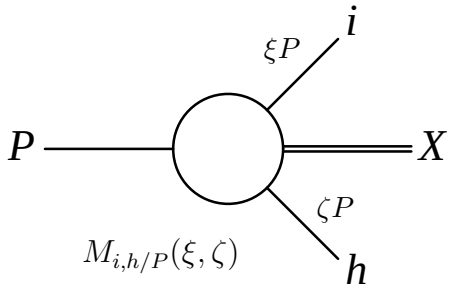


Figure 12: *A target fragmentation function: $P$ is the incoming hadron, $h$ is the observed particle, and $i$ is the parton incident in the hard scattering process.*

## 3.2 Renormalization Group Equation

The renormalization group equation for $M$, corresponding to Eq. (39), is [77]

$$\begin{aligned}\frac{\partial M_{i,h/P}(\xi,\zeta,\mu^2)}{\partial \ln \mu^2} &= \frac{\alpha_s(\mu^2)}{2\pi}\int_{\xi/(1-\zeta)}^1 \frac{\mathrm{d}u}{u}\, P_{i\leftarrow j}(u)\, M_{j,h/P}\left(\frac{\xi}{u},\zeta,\mu^2\right) \\ &+\frac{\alpha_s(\mu^2)}{2\pi}\int_\xi^{\xi/(\xi+\zeta)} \frac{\mathrm{d}u}{u}\,\frac{1}{1-u}\,\frac{u}{\xi}\,\hat{P}_{ki\leftarrow j}(u)\, f_{j/P}\left(\frac{\xi}{u},\mu^2\right)\, D_{h/k}\left(\frac{\zeta u}{\xi(1-u)},\mu^2\right), \quad (42)\end{aligned}$$

[24] See also Ref. [96].

where the sums over the parton indices $j$ and $k$ are done implicitly. There are two contributions to the scale evolution: the homogeneous term is related to the emission of partons in the initial state, as indicated in Fig. 13a; the inhomogeneous term comes from a source term that originates from the fact that a parton radiated collinearly from the incident parton in the backward direction is the parent parton of the observed hadron (see Fig. 13b).

Intuitively, this scale evolution equation can be derived as follows. The parton content of the nucleon in the interval $[\xi, \xi + \mathrm{d}\xi]$ at a scale $\mu^2 + \mathrm{d}\mu^2$ under the assumption that a hadron is observed in the target fragmentation region is given by the contribution at the scale $\mu^2$ plus the contribution (a) from the radiation of a parton (Fig. 13a) and (b) from particle production in the backward direction (Fig. 13b). Case (a) gives, up to a factor of $\alpha_s/(2\pi)$, and suppressing the particle labels and scales, a contribution $\int \mathrm{d}\rho\, M(\rho,\zeta) \int \mathrm{d}u\, P(u)\, \delta(\xi - \rho u)$, since $M(\rho,\zeta)\,\mathrm{d}\rho$ is the probability to find a parton in the interval $[\rho, \rho + \mathrm{d}\rho]$ in the nucleon, and $P(u)\,\mathrm{d}u$ is the probability of the incident parton splitting into a parton carrying only a fraction $u$ of the parent parton's momentum. Performing the $\rho$-integration by means of the $\delta$-function, we arrive at $\int \mathrm{d}u/u\, M(\xi/u,\zeta)\, P(u)$. The range of integration in $u$ has to be chosen such that the momentum fraction $\rho$ of the parton before the splitting process is in the range of $\xi$ (the parton does not split at all) and $(1-\zeta)$ (the parton carries all of the available momentum of the nucleon, after removing the momentum fraction $\zeta$ for the observed hadron). This is the first term of Eq. (42). The second term is obtained from case (b). The contribution is $\int \mathrm{d}\rho\, f(\rho) \int \mathrm{d}u\, \hat{P}(u)\, \delta(\xi - \rho u) \int \mathrm{d}z\, D(z)$: $D(z)\,\mathrm{d}z$ is the probability for a parton to turn into a hadron with momentum fraction in the interval $[z, z + \mathrm{d}z]$, and $\hat{P}(u)\,\mathrm{d}u$ is the probability for a parton to split into two partons, one of these carrying a momentum fraction $u$, under the condition that the second parton is not soft (cf. Appendix D.1). By performing the $\rho$-integration by means of the $\delta$-function and by using the fact that $\mathrm{d}z = \mathrm{d}\zeta\, u/[\xi(1-u)]$, we arrive at $\int \mathrm{d}u/u\, f(\xi/u)\, \hat{P}(u) \int \mathrm{d}\zeta\, u/[\xi(1-u)]\, D(\zeta u/[\xi(1-u)])$, which is, after "dividing" by $\mathrm{d}\zeta$ to obtain the distribution differential in the momentum fraction of the observed hadron, the second term of Eq. (42). The range of integration in $u$ has to be such that the momentum fraction of the incident parton $\rho$ is between $\xi + \zeta$ (so as to produce a parton with momentum $\xi P$ and a hadron with momentum $\zeta P$) and 1 (the maximum possible momentum fraction).

The general solution of the inhomogeneous differential equation (42) is a sum of a special solution of the inhomogeneous equation and an arbitrary solution of the homogeneous equation. Let us denote these two terms by $M^{(P)}$ and $M^{(NP)}$, respectively, such that $M = M^{(P)} + M^{(NP)}$. The equations satisfied by these functions are, in symbolic form,

$$\begin{array}{lcll} \partial_{\ln \mu^2} M & = & K \otimes M & + \quad \hat{K} \otimes f \otimes D, \\ \partial_{\ln \mu^2} M^{(P)} & = & K \otimes M^{(P)} & + \quad \hat{K} \otimes f \otimes D, \\ \partial_{\ln \mu^2} M^{(NP)} & = & K \otimes M^{(NP)}. & \end{array} \tag{43}$$

Here $K$ and $\hat{K}$ stand for the evolution kernels. We may use the boundary condition

$$M^{(P)}(\xi, \zeta, \mu_0^2) = 0 \tag{44}$$

for an arbitrary scale $\mu_0$. This definition then fixes $M^{(NP)}$ for a given $M$. The superscripts $(P)$ and $(NP)$ stand for "perturbative" and "non-perturbative", respectively. The interpretation we have in mind is that the contribution to $M$ via $M^{(P)}$ comes from the "perturbative" production of hadrons, via the radiation of partons in the backward direction and their subsequent fragmentation, corresponding to graphs such as those of Figs. 8d and f. Given the parton densities $f$ and fragmentation functions $D$, this contribution can be calculated in perturbation theory. Loosely speaking, $M^{(P)}$ contains all contributions that arise by this mechanism for scales larger than $\mu_0$. Everything below this scale is termed "non-perturbative", and has to be determined

experimentally or via explicit phenomenological models. It should be clear that there is no strict separation of the perturbative and non-perturbative contributions, due to the fact that they are defined by an arbitrary scale $\mu_0$[25].

For the solution of the renormalization group equations, it is useful to redefine the arguments of the target fragmentation functions by introducing *reduced* target fragmentation functions $N$ by

$$N_{i,h/P}(x,\zeta,\mu^2) \doteq M_{i,h/P}(x(1-\zeta),\zeta,\mu^2). \tag{45}$$

Thus $x$ is the momentum fraction carried by the parton incident in the hard subprocess with respect to the momentum $P-h$. The renormalization group equation of the functions $N$ is

$$\begin{aligned}\frac{\partial N_{i,h/P}(x,\zeta,\mu^2)}{\partial \ln \mu^2} &= \frac{\alpha_s(\mu^2)}{2\pi}\int_x^1 \frac{\mathrm{d}u}{u}\, P_{i\leftarrow j}(u)\, N_{j,h/P}\left(\frac{x}{u},\zeta,\mu^2\right) \\ &+ \frac{\alpha_s(\mu^2)}{2\pi}\int_{(1-\zeta)x}^{(1-\zeta)x/(x+(1-x)\zeta)} \frac{\mathrm{d}u}{u}\,\frac{1}{1-u}\,\frac{u}{x(1-\zeta)} \\ &\cdot \hat{P}_{ki\leftarrow j}(u)\, f_{j/P}\left(\frac{x(1-\zeta)}{u},\mu^2\right)\, D_{h/k}\left(\frac{1}{x}\frac{u}{1-u}\frac{\zeta}{1-\zeta},\mu^2\right).\end{aligned} \tag{46}$$

The first term has exactly the same form as the one in the scale evolution equation of parton densities $f$ [97]:

$$\frac{\partial f_{i/P}(x,\mu^2)}{\partial \ln \mu^2} = \frac{\alpha_s(\mu^2)}{2\pi}\int_x^1 \frac{\mathrm{d}u}{u}\, P_{i\leftarrow j}(u)\, f_{j/P}\left(\frac{x}{u},\mu^2\right). \tag{47}$$

Parton densities fulfil the sum rule

$$\sum_i \int_0^1 \mathrm{d}x\, x\, f_{i/P}(x,\mu^2) = 1; \tag{48}$$

the $\mu^2$-independence follows from the fact that

$$\sum_i \int_0^1 \mathrm{d}u\, u\, P_{i\leftarrow j}(u) = 0. \tag{49}$$

In the next section it is shown that the corresponding sum rule for target fragmentation functions is violated.

### 3.3 Momentum Sum Rules

In analogy to the sum rule for fragmentation functions in Eq. (12), target fragmentation functions fulfil a momentum sum rule [77]

$$\sum_h \int_0^{1-\xi} \mathrm{d}\zeta\, \zeta\, M_{i,h/P}\left(\xi,\zeta,\mu^2\right) = (1-\xi)\, f_{i/P}(\xi,\mu^2), \tag{50}$$

i.e. the sum over all possible tagged particles corresponds to the probability distribution of the parton incident in the hard subprocess. Under the assumption that the sum rule in Eq. (50) is valid for some scale $\mu_0$, Eq. (50) can be proved for any $\mu$ by an application of the renormalization group equations (11), (42) and (47), and by means of relations from the "jet calculus" of Refs. [98, 99].

[25] In the application to the production of heavy quarks, this scale will be set to a value of the order of the heavy-quark mass.

It is interesting to note that the momentum sum rule with respect to the variable $\xi$ for fixed $\zeta$ is violated. As in the case of parton densities, cf. Eq. (48), the homogeneous term does not give a contribution to the evolution of the sum over parton species $i$. The inhomogeneous term, however, is not zero. Because the convolution kernels $\hat{P}$ are positive, the inhomogeneous term is positive, and consequently the integral

$$\sum_i \int_0^1 \mathrm{d}x\, x\, M_{i,h/P}(x,z,\mu^2) \tag{51}$$

is increasing with increasing $\mu^2$. This can also be seen by considering[26] the double moments $M(n,m)$, defined by

$$M(n,m) \doteq \int_0^1 \frac{\mathrm{d}\xi}{\xi}\, \xi^n \int_0^{1-\xi} \frac{\mathrm{d}\zeta}{\zeta}\, \zeta^m\, M(\xi,\zeta), \tag{52}$$

suppressing the scale argument for the moment. The Mellin moments of functions $F$ of only one argument, such as $f$, $D$ and the splitting functions $P$, are defined by

$$F(n) \doteq \int_0^1 \frac{\mathrm{d}\xi}{\xi}\, \xi^n\, F(\xi), \tag{53}$$

and we define the moments $\hat{P}(n,m)$ of the unsubtracted splitting functions $\hat{P}$ by

$$\hat{P}(n,m) \doteq \int_0^1 \frac{\mathrm{d}u}{u}\, u^n\, (1-u)^m\, \hat{P}(u). \tag{54}$$

After some formal manipulations, the renormalization group equation (42) can be rewritten in terms of the $M(n,m)$, $f(n)$, $D(n)$, and $P(n,m)$, the scale derivative of $M(n,m)$ being a sum of two terms corresponding to the homogeneous and inhomogeneous terms of the renomalization group equation, respectively. The first moment in $\xi$ (i.e. $n = 2$) of the sum over all parton species $i$ of the homogeneous term, being of the same structure as the scale derivative of the sum rule for parton densities in Mellin space, is zero. The inhomogeneous term, however, turns out to be a product of positive definite factors, and thus does not generally give a zero result. As a consequence, the derivative of the first moment with respect to the factorization scale is non-vanishing. The interpretation is obvious: the fragmentation of partons emitted in the backward direction enhances the particle multiplicity of the target remnant jet. The momentum sum rule violation causes no problem with respect to unitarity, as can be seen by considering the regularized, i.e. $\epsilon$ being non-zero, expression for the cross section. The factorization terms that are ultimately absorbed into the renormalized target fragmentation functions, giving rise to the inhomogeneous evolution term, are effectively subtracted from the real corrections involving parton densities and fragmentation functions.

### 3.4 Extended Factorization

According to Eqs. (4) and (5), the complete one-particle-inclusive cross section is given by

$$\sigma = \sigma_{fD}^{\mathrm{hard}} \otimes f \otimes D + \sigma_M^{\mathrm{hard}} \otimes M. \tag{55}$$

In the current fragmentation region, only the first term contributes, whereas the target fragmentation region receives contributions from both terms. In the standard approach to particle production in the current fragmentation region, the form of the first term as a convolution of a hard scattering cross section and distribution functions is guaranteed by the factorization

[26] D. Graudenz, L. Trentadue, G. Veneziano, unpublished manuscript (1995).

theorems of perturbative QCD. For particle production in the target fragmentation region, the factorization theorems have to be generalized; we call the form of Eq. (55) the *extended factorization conjecture*. Although there is no proof of this conjecture yet, the general picture, which is to be expected, is that the soft infrared divergences cancel in the sum of virtual and real corrections, and that all remaining collinear singularities can be absorbed into the renormalized process-independent distribution functions $f^r$, $D^r$ and $M^r$. This mechanism works in the explicit next-to-leading-order calculation to one-loop as described in Section 2. We wish to point out that Eq. (55) provides a method to calculate the *total* one-particle inclusive cross section, without any restrictions to specific phase-space regions.

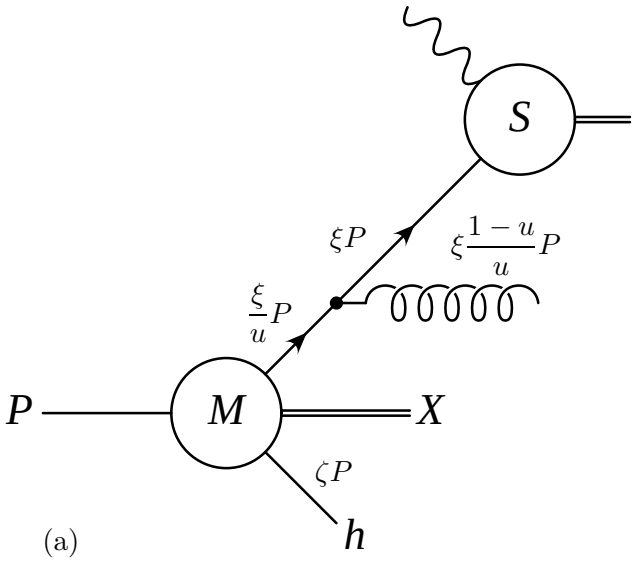


(a)

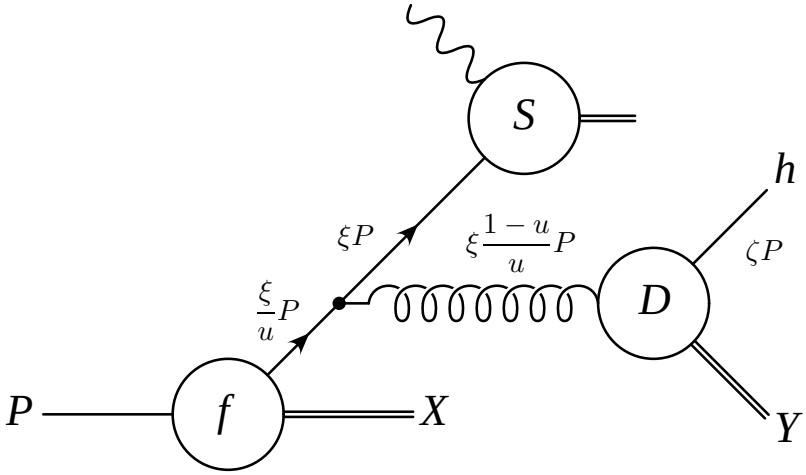


(b)

Figure 13: *Examples of contributions to the scale evolution of target fragmentation functions: emission of a parton in the initial state giving rise to the standard Altarelli–Parisi scale evolution $K \otimes M$ (a) and the additional source term $\hat{K} \otimes f \otimes D$ for particle production in the backward direction (b). The hard scattering process is denoted by $S$.*

# 4 Heavy-Quark Fragmentation Functions

*We now consider the case of heavy quarks in the final state. The heavy-quark mass*[27] *$m$ is a large scale ($m = 4.5\,GeV$ for bottom quarks and $1.5\,GeV$ for charm quarks), and it is expected that perturbative QCD is applicable to determine fragmentation functions for partons into heavy quarks, although it fails for other particles in the final state, such as mesons built of only light valence quarks. Indeed it is possible to calculate the heavy-quark fragmentation functions in QCD from first principles. A short review is given in Section 4.1. Heavy-quark fragmentation functions for arbitrary scales can be obtained by means of the renormalization group equation. Explicit numerical results are discussed in Section 4.2.*

## 4.1 Fragmentation Functions from Perturbative QCD

The heavy-quark mass $m$ is a scale parameter large enough to justify the application of perturbative QCD. This is certainly true for the bottom quark, and probably true for the charm quark[28]. The fragmentation functions $D_{Q/i}(x,\mu^2)$ for partons $i$ into a heavy quark $Q$ depend on two mass scales: the heavy quark mass $m$ and the factorization scale $\mu$. For $\mu$ of the order of $m$, possible logarithmic terms $\sim \ln(\mu^2/m^2)$ in the only available scales $\mu$ and $m$ must be small, and so $D_{Q/i}(x,\mu^2)$ has an expansion in terms of the strong coupling constant:

$$D_{Q/i}(x,\mu^2) = \sum_n \left(\frac{\alpha_s(\mu^2)}{2\pi}\right)^n D^{(n)}_{Q/i}(x,\mu^2). \tag{56}$$

The coefficients $D^{(n)}_{Q/i}(x,\mu^2)$ may be obtained by a comparison of a direct calculation of heavy-quark inclusive processes with heavy quarks represented by external lines in Feynman diagrams, with a calculation based on the fragmentation function formalism as described in Section 2.1.

The coefficients may be interpreted in terms of the diagrams in Fig. 14. To $\mathcal{O}(\alpha_s^0)$, the only diagram is the one in Fig. 14a describing the direct "propagation" of the heavy quark. Obviously,

$$\begin{aligned} D^{(0)}_{Q/Q}(x,\mu^2) &= \delta(1-x), \\ D^{(0)}_{Q/i}(x,\mu^2) &= 0 \quad \text{for } i \neq Q. \end{aligned} \tag{57}$$

In next-to-leading order, corresponding to the diagrams in Figs. 14b to d, the calculation has been done in Refs. [37, 101]. The results are collected in Appendix D.2.

## 4.2 Solving the Renormalization Group Equation

In order to obtain $D_{Q/i}(x,\mu^2)$ for scales $\mu$ very different from the heavy-quark mass $m$, the large logarithms $\sim \ln(\mu^2/m^2)$ must be summed by means of the renormalization group equation (11), with $h$ being replaced by $Q$. In this section we discuss explicit numerical results in leading order for the heavy-quark fragmentation functions. Numerical results in next-to-leading order have been obtained in Refs. [102, 103]. We restrict ourselves to the leading order, because

[27] In next-to-leading order, some care has to be taken to define the mass of a heavy quark, see for example the review in Ref. [100], p. 1433.

[28] It can be questioned whether 1.5 GeV is a sufficiently large scale to have a valid perturbative expansion. In case of doubt, it is, in principle, possible to use experimentally determined fragmentation functions for charmed mesons, or fragmentation functions of the type proposed in Ref. [35], in the applications later on.

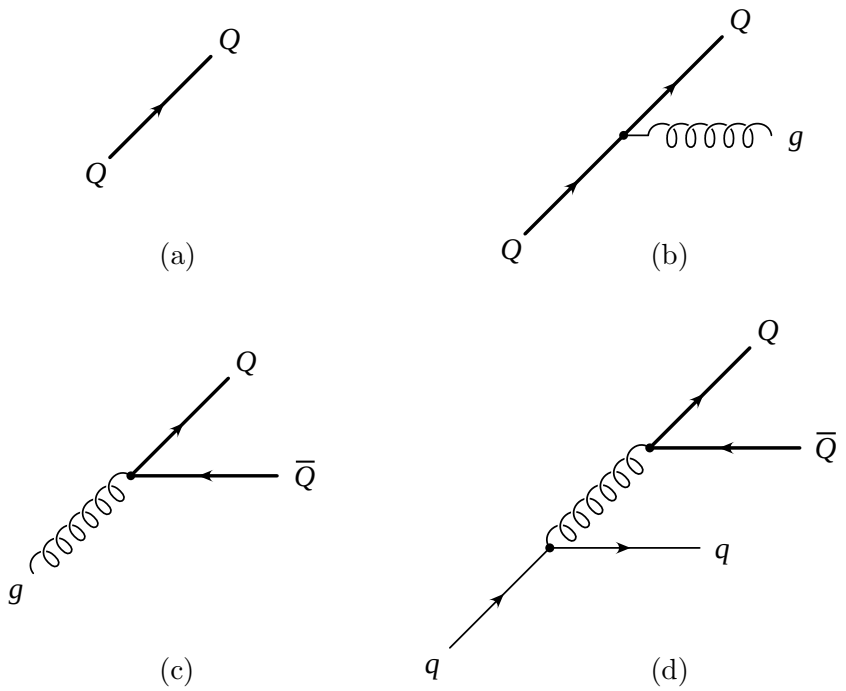


Figure 14: *Feynman diagrams corresponding to heavy-quark fragmentation functions:* $D_{Q/Q}(x)$ *in* $\mathcal{O}(\alpha_s^0)$ *(a),* $D_{Q/Q}(x)$ *in* $\mathcal{O}(\alpha_s)$ *(b),* $D_{Q/g}(x)$ *in* $\mathcal{O}(\alpha_s)$ *(c),* $D_{Q/q}(x)$ *in* $\mathcal{O}(\alpha_s^2)$ *(d). Here* $q$ *stands for any light-flavoured quark or antiquark, or for the heavy antiquark* $\overline{Q}$*.*

the main focus of the present work is the issue of target fragmentation functions, where the evolution kernels are known in leading order only. On this level a next-to-leading-order input for the heavy-quark fragmentation functions in the inhomogeneous term of Eq. (42) would be inconsistent. Of course, a full next-to-leading-order analysis would be desirable.

As can be seen, the heavy-quark fragmentation functions $D_{Q/i}(x,\mu^2)$ are singular at $x=1$. In leading order, the only singularity is $\delta(1-x)$; in next-to-leading order additional singularities of the form $(\ln(1-x)/(1-x))_{+x[0,\underline{1}]}$ come in, cf. Eq. (130). The splitting functions of the renormalization group equation (11) contain singular terms, which means that the evolved contributions will be singular as well[29].

The leading-order results[30] for the bottom- and charm-quark fragmentation functions $D_{Q/i}\left(x,\mu^2\right)$ at a scale of $\mu = 100\,\mathrm{GeV}$ are shown in Fig. 15. The fragmentation functions are set to the perturbative input $D_{Q/Q}\left(x,\mu_0^2\right) = \delta(1-x)$ from Eq. (57) at the factorization scale $\mu_0 = m$. The probability $D_{Q/Q}\left(x,\mu^2\right)$ to find the heavy quark within a heavy quark is singular, as $(1/(1-x))_{+x[0,\underline{1}]}$ for $x \to 1$, up to factors of logarithms $\ln^m(1-x)$. We have not

[29] A direct computation by means of Eq. (97) shows that actually terms $\sim \alpha_s^m \left(\ln^m(1-x)/(1-x)\right)_{+x[0,\underline{1}]}$ appear. In principle, this means that, for an accurate result, the terms $\left(\alpha_s \ln(1-x)\right)^k$ should be resummed for $x \to 1$ [37]. We apply the fragmentation functions later on to get a result for what we call the "perturbative piece" of the target fragmentation function, depending on a scale $\mu_0$. Since we work in leading order, due to the lack of compensating terms in the expansion, the results will depend considerably on $\mu_0$. Therefore, at this stage of the development of the formalism, we do not consider it necessary to go into the details of the subtle problem of $x \to 1$, whose influence is probably smaller than the dependence on the perturbative input scale. For more precise predictions, this problem should however be treated along the lines of Ref. [37], where the technical details are explained.

[30] The numerical solution of the renormalization group equation for heavy-quark fragmentation functions is described in Appendix E.1.

shown the subtraction term proportional to $\delta(1-x)$ in the figure. The contributions of gluons, light quarks and heavy antiquarks $\overline{Q}$ are rather small at large $x$, because they are of $\mathcal{O}(\alpha_s)$ and $\mathcal{O}(\alpha_s^2)$, respectively. The results at very small $x$ are not reliable, because there is an ambiguity in whether the momentum-fraction variable $x$ refers to the fraction of momenta or to the fraction of energies. In next-to-leading order, numerical studies indicate that the fragmentation functions go to $-\infty$ for $x \to 0$ [102, 103].

The scale evolution of heavy-quark fragmentation functions is shown in Fig. 16 for three different factorization scales. Again, the perturbative input is chosen at the scale $\mu_0 = m$. The increase of the distributions at small $x$ for increasing factorization scale can be seen clearly.

The dependence of heavy-quark fragmentation functions on the scale $\mu_0$ of the perturbative input is shown in Fig. 17 for the three different choices $\mu_0 = m/2$, $\mu_0 = m$ and $\mu_0 = 2m$. The factorization scale is chosen to be $\mu = 100\,\text{GeV}$. The dependence on the input scale $\mu_0$ is particularly strong for small $x$, and much smaller for large $x > 0.1$. The strong dependence for small $x$ has its origin in the fact that the contribution comes exclusively from the evolution (the input distribution at $\mu_0$ is located at $x = 1$), and a large evolution span in $\mu$ leads to a strong enhancement in this region. At large $x$, the variation from $\mu_0 = m$ to $\mu_0 = m/2$ and to $\mu_0 = 2m$ is about $\pm 25\%$. This input-scale dependence is much smaller in next-to-leading order, owing to a compensating logarithmic term in the input distribution at the scale $\mu_0$ [102, 103], cf. Appendix D.2.

(a)

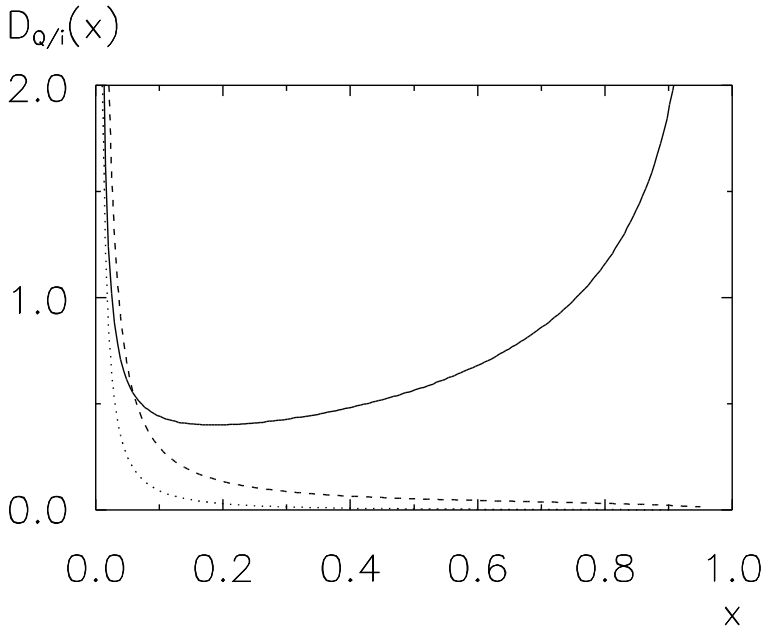


(b)

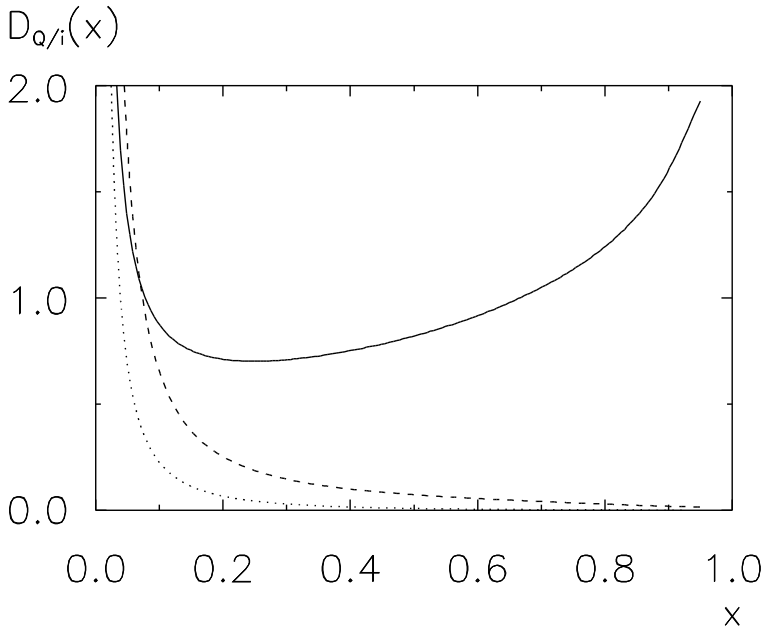


Figure 15: *Bottom (a) and charm (b) quark fragmentation functions at $\mu = 100\,GeV$. The input distribution is defined by the distribution in fixed order at $\mu_0 = m$. Heavy quark $Q$ (——), gluon (– – –), light quark flavours (· · ·).*

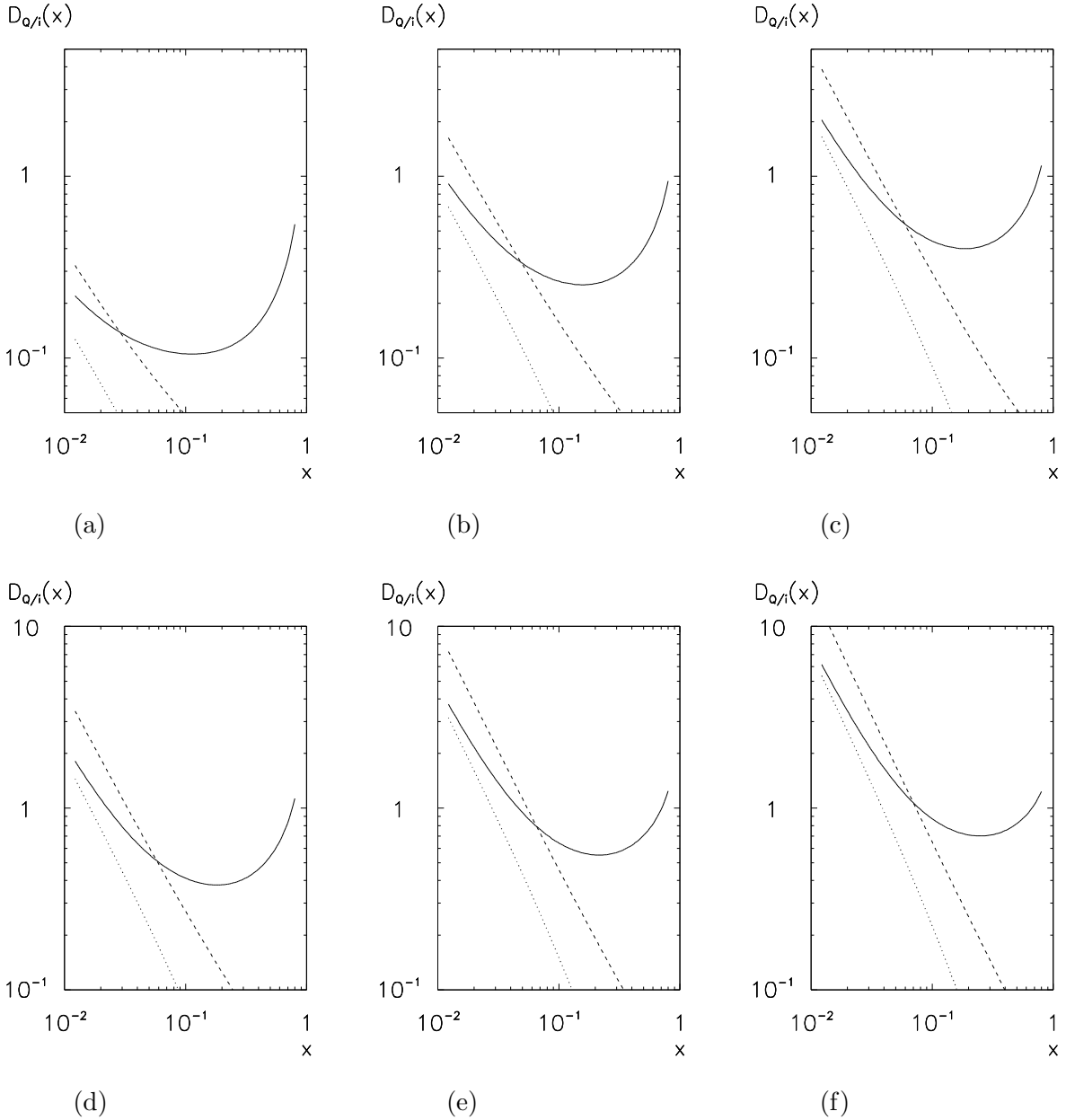


Figure 16: *Scale evolution of bottom (a)–(c) and charm (d)–(f) quark fragmentation functions. The factorization scale is $\mu = 10\ GeV$ (a), (d); $\mu = 30\ GeV$ (b), (e); $\mu = 100\ GeV$ (c), (f). The input distribution is defined by the distribution in fixed order at $\mu_0 = m$. Heavy quark $Q$ (——), gluon (– – –), light quark flavours (· · ·).*

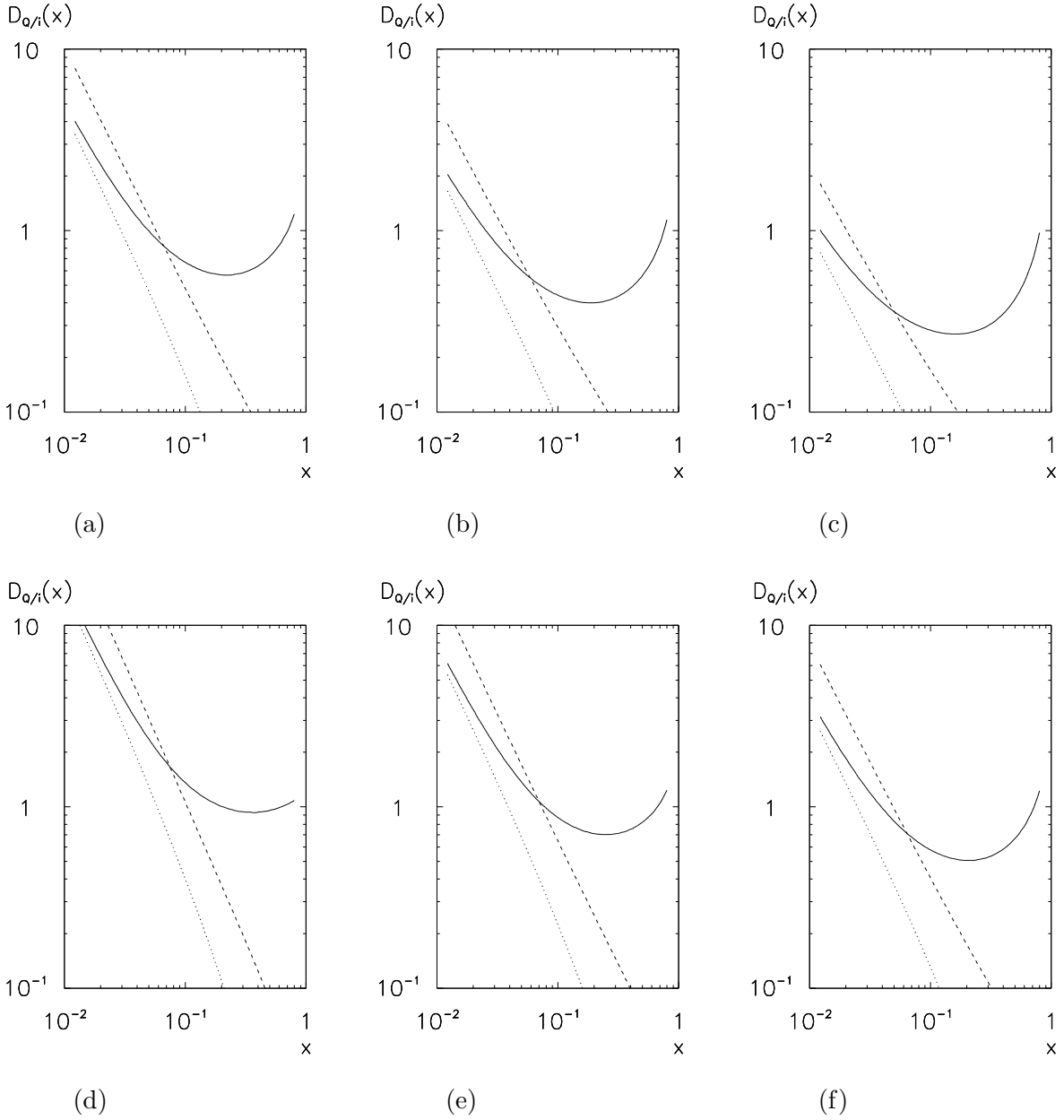


Figure 17: *Dependence on the scale $\mu_0$, where the input distribution is defined by the fixed-order calculation, for bottom (a)–(c) and charm (d)–(f) quark fragmentation functions at $\mu = 100\,GeV$. The input scale is $\mu_0 = m/2$ (a), (d); $\mu_0 = m$ (b), (e); $\mu_0 = 2m$ (c), (f). Heavy quark Q (——), gluon (– – –), light quark flavours (· · ·).*

# 5 Heavy-Quark Target Fragmentation Functions

*Having set up the necessary formalism, we now consider target fragmentation functions for heavy quarks for the case of incident protons. Perturbative heavy-quark target fragmentation functions, corresponding to the production of heavy quarks via the fragmentation of a parton emitted in the backward direction, are defined in Section 5.1. The corresponding renormalization group equation is solved numerically in Section 5.2. Due to the radiative production mechanism, the distribution in the momentum-fraction variable $z$ of the observed heavy quark falls off rapidly for $z \to 1$. To give a qualitative example for the non-perturbative piece, we consider the hypothesis of intrinsic heavy quarks in Section 5.3. Based on a simple expression for a correlated distribution function of the $|uudQ\overline{Q}\rangle$ Fock state, we obtain numerical results for the non-perturbative target fragmentation functions via the homogeneous evolution equation. As is expected, the $z$-distribution is harder for this particular non-perturbative piece.*

## 5.1 Target Fragmentation Functions from Perturbative QCD

In Section 3 it has been shown that target fragmentation functions $M$ may be written as a sum $M = M^{(P)} + M^{(NP)}$ of a "perturbative" and a "non-perturbative" contribution. The perturbative contribution is defined to be zero at an (arbitrarily chosen) factorization scale $\mu_0$. The non-perturbative piece $M^{(NP)}$, with rescaled arguments as in Eq. (45), evolves according to the homogeneous Altarelli–Parisi equation. The perturbative piece $M^{(P)}$ may be calculated, under the assumption that the fragmentation functions and parton densities are known, by solving the inhomogeneous renormalization group equation (42). The contributions from $M^{(P)}$ are therefore related to the production of heavy quarks by means of the mechanism shown in Fig. 13b. A complete set of the lowest-order contributions for heavy-quark production is shown in Fig. 14, where the "incoming parton" has to be attached to a parton density. From these graphs it is clear that a correlation of the flavour of an observed heavy quark in the target fragmentation region and of the type of parton incident in the hard scattering process is to be expected. If the heavy-quark content of the nucleon is not too large, then there is a large probability that a heavy antiquark initiates the hard scattering process, for the case of an observed heavy quark in the target fragmentation region, owing to the splitting of the gluons in Figs. 14c and d into a $Q\overline{Q}$-pair.

As long as non-perturbative methods to calculate target fragmentation functions from first principles are not available, the non-perturbative piece can only be determined by means of a measurement, much as is the case for parton densities, or from phenomenological models. The perturbative contribution to the case of heavy quarks in the remnant of a proton will be considered in the next section, and the hypothesis of intrinsic heavy quarks in Section 5.3.

## 5.2 Solving the Renormalization Group Equation

The standard method to solve renormalization group equations of phenomenological distribution functions is to transform the equation into the Mellin moment space, where the moments of the convoluted expression can be written as the products of the respective moments. The differential equations for the moments decouple, and can be solved analytically for complex values of the moment variable. An inverse Mellin transform allows the transformation back into $x$-space. This method works for the homogeneous case, and for some inhomogeneous cases as well, namely in those cases where the expression of the moments for the inhomogeneous part are known analytically, see for instance Ref. [104]. In our case, however, the inhomogeneous term of Eq. (42) contains two sets of quantities that are known only numerically, namely the parton

densities and the fragmentation functions. The complicated arguments of those functions and the unusual limits of the integral prevent an expression of the single moments in $x$ for fixed $z$ of this term in a simple way. Therefore the renormalization group equation (42) is solved numerically in the form of Eq. (46) by a discretization in the relevant variables[31].

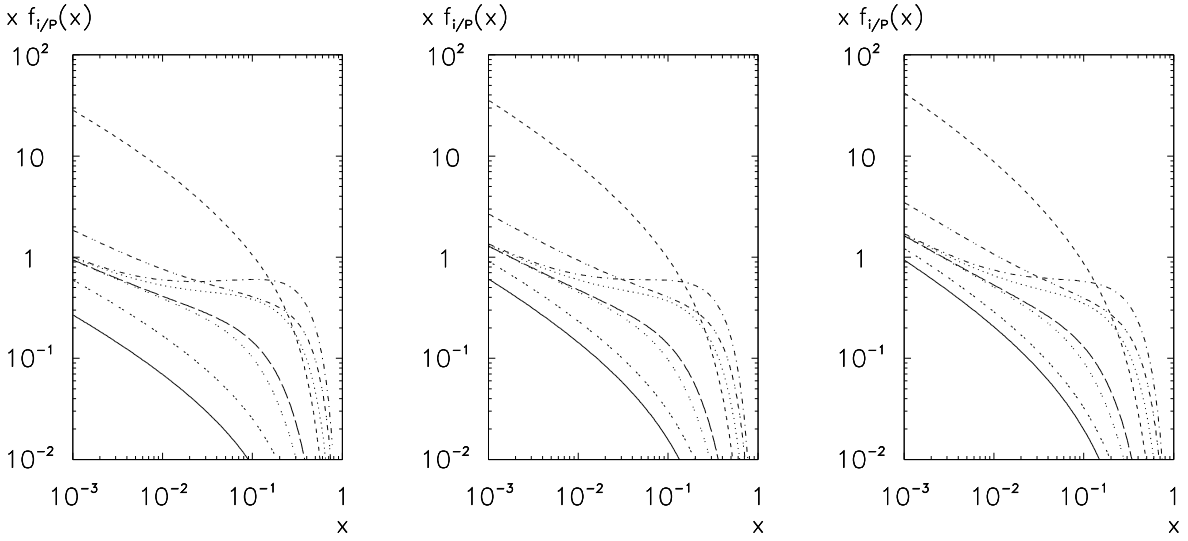


Figure 18: *Scale evolution of the leading-order GRV parton densities $x\,f_{i/P}(x,\mu^2)$. The factorization scale is $\mu = 10\,GeV$ (a); $\mu = 30\,GeV$ (b); $\mu = 100\,GeV$ (c). The flavours $i$ are given by $b$, $\overline{b}$ (——); $c$, $\overline{c}$ (-- --); $g$ (– – –); $d$ (· · ·); $\overline{d}$ (— —); $u$ (– · –); $\overline{u}$ (·· ··); $F_2$ (– – ··).*

The parton densities which we have used in the inhomogeneous term of the renormalization group equation are given by the leading-order parametrizations[32] by Glück, Reya and Vogt (GRV) [105, 106], which we show in Fig. 18 for comparison with the following distributions. The heavy-quark fragmentation functions are those described in Section 4, where the perturbative input is used at the scale of the heavy-quark mass $m$. The scale evolution of perturbative heavy-quark target fragmentation functions is shown in Fig. 19, where we have set the input distribution for the perturbative heavy-quark target fragmentation functions to zero at $\mu_0 = m$. The plotted quantity is

$$x \int_{z_0}^{1-x} \mathrm{d}z\, M^{(P)}_{i,Q/P}(x,z,\mu^2), \tag{58}$$

for $z_0 = 0.1$. The momentum fraction of the observed heavy quark is therefore between 0.1 and $1-x$. We define $F_2^M$ by

$$F_2^M(x,z,\mu^2) \doteq x \sum_{i=q,\overline{q}} Q_i^2\, M_{i,Q/P}(x,z,\mu^2), \tag{59}$$

in analogy to the leading-order expression for the structure function

$$F_2(x,\mu^2) = x \sum_{i=q,\overline{q}} Q_i^2\, f_{i/P}(x,\mu^2) \tag{60}$$

[31] The numerical solution of the renormalization group equation for heavy-quark target fragmentation functions is described in Appendix E.2.

[32] The heavy-quark contribution is zero in the parametrization from Ref. [105]. We adopt the suggestion from the authors of this parametrization to use the heavy-quark distributions from Ref. [106] and the light quark and gluon distributions from Ref. [105].

in terms of parton densities. The perturbative heavy-quark target fragmentation functions have the following main features:

- At fairly large $x$, i.e. $0.05 \lesssim x \lesssim 0.3$, the distributions are dominated by $M^{(P)}_{\overline{Q},Q/P}$, whereas at small $x$, i.e. $x \lesssim 0.01$, the distributions are dominated by $M^{(P)}_{g,Q/P}$. At small $x$, the quark distributions converge to a common limit distribution. The latter property is comparable to the case of parton densities. The large values of $M^{(P)}_{\overline{Q},Q/P}$ can be explained by the splitting of a gluon into a $Q\overline{Q}$ pair, see Fig. 14c, and the dominance of $M^{(P)}_{g,Q/P}$ at small $x$ by the $1/u$-term in the $q \to g$ splitting function.

- The distributions $M^{(P)}_{q,Q/P}$ and $M^{(P)}_{\overline{q},Q/P}$ for light quarks and $M^{(P)}_{Q,Q/P}$ are small. Among the light quark distributions, the $u$- and $d$-distributions are the largest. This is due to the fact that a $u$- or $d$-quark may radiate a gluon in the backward direction before the hard scattering process, this gluon subsequently splitting into a $Q\overline{Q}$-pair, where $Q$ is observed in the target fragmentation region.

- The perturbative charm-quark target fragmentation functions are much larger than the bottom-quark target fragmentation functions. This is because the charm-quark fragmentation functions are larger than the bottom-quark ones, and moreover the evolution span is wider in the charm-quark case, because of the choice $\mu_0 = m$.

In Fig. 20 we show the dependence on the mass scale $\mu_0$, where $M^{(P)}$ is set to zero, i.e. the dependence on the boundary condition for the evolution equation. This variation introduces an inherent uncertainty in our predictions. It is clearly unphysical, and would be compensated by a corresponding variation, proportional to $\ln \mu_0^2$, of the non-perturbative piece $M^{(NP)}$.

As mentioned in the introduction, the observation of particles in the target fragmentation region may be exploited to gain information on the hard scattering process itself. This possibility is illustrated in Fig. 21, showing the ratio of perturbative heavy-quark target fragmentation functions and parton densities. Tagging a heavy quark $Q$ in the backward direction clearly enhances those processes that have a heavy antiquark $\overline{Q}$ initiating the hard process. The scale dependence of the ratio is large for the light quark flavours and for the gluon, and nearly absent for the heavy quark, the reason being that the heavy-quark contributions are produced by similar radiation mechanisms in both cases (i.e. for the parton densities and the perturbative heavy-quark target fragmentation functions), whereas the light flavours and the gluon are already non-vanishing at some small scale in the case of the parton densities. Of course, Fig. 21 can only be taken as an indication of this fact, since the non-perturbative contribution is not included, and since there is also the production process described by the graphs in Fig. 8 that contributes in the collinear limit.

The dependence of the perturbative target fragmentation functions on the momentum fraction $z$ carried by the observed heavy quark is shown in Figs. 22 and 23. The dependence is very steep, and the production at small $z$ is clearly favoured, because of the radiative production mechanism. It is interesting to note that the distributions tend to become harder for increasing factorization scales.

Finally, we show the dependence on the input parton density in Fig. 24. Except for large differences at very large $x$, $x \gtrsim 0.2$, where the values of $M^{(P)}$ are small, the uncertainty is of the order of $20 - 40\%$.

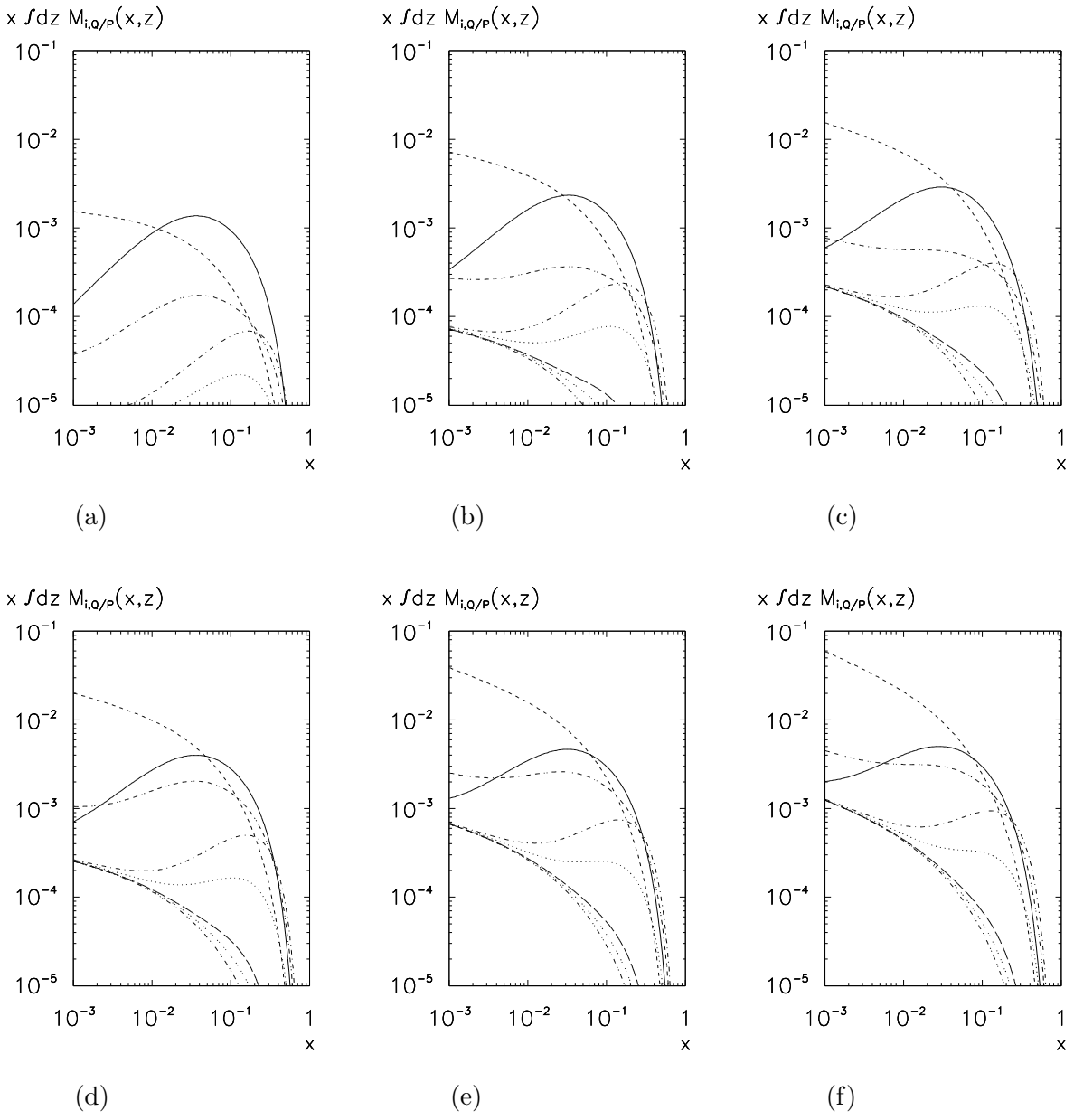


Figure 19: *Scale evolution of perturbative bottom (a)–(c) and charm (d)–(f) quark target fragmentation functions* $x \int dz\, M^{(P)}_{i,Q/P}(x,z,\mu^2)$*, where* $z$ *is integrated from* $0.1$ *to* $1-x$*. The factorization scale is* $\mu = 10\,GeV$ *(a), (d);* $\mu = 30\,GeV$ *(b), (e);* $\mu = 100\,GeV$ *(c), (f). The input distribution is zero at* $\mu_0 = m$*. The flavours* $i$ *are given by* $\overline{Q}$ *(——),* $g$ *(– – –),* $d$ *(· · ·),* $\overline{d}$ *(— —),* $u$ *(– · –),* $\overline{u}$ *(·· ··),* $Q$ *(– ··),* $F_2^M$ *(– – ··).*

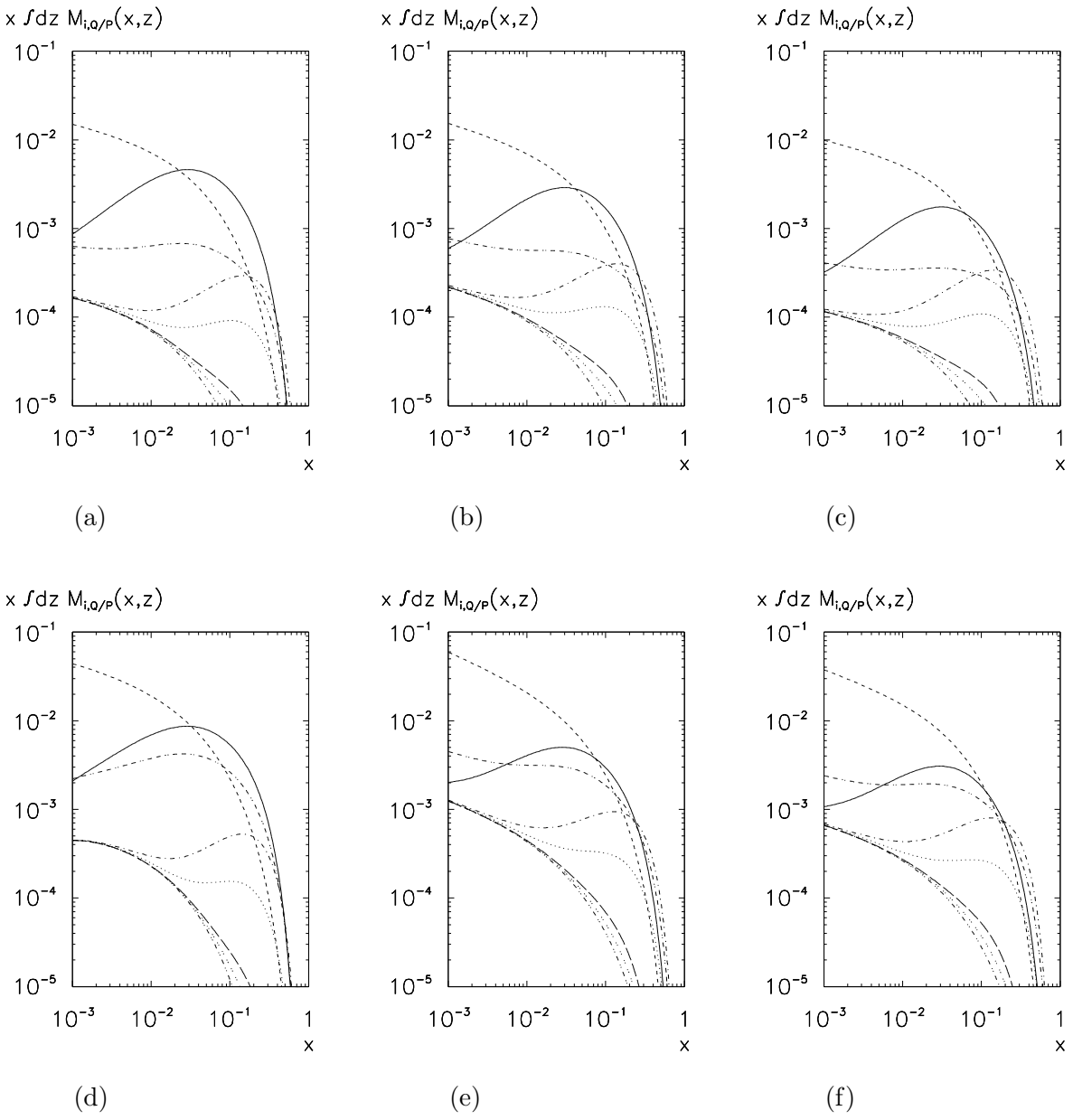


Figure 20: *The dependence on the scale $\mu_0$, where $M^{(P)}$ is set to zero, for perturbative bottom (a)–(c) and charm (d)–(f) quark target fragmentation functions $x \int dz\, M^{(P)}_{i,Q/P}(x,z,\mu^2)$ at $\mu = 100\,GeV$, where $z$ is integrated from 0.1 to $1-x$. The definition scale is $\mu_0 = m/2$ (a), (d); $\mu_0 = m$ (b), (e); $\mu_0 = 2m$ (c), (f). The flavours $i$ are given by $\overline{Q}$ (——), $g$ (– – –), $d$ (· · ·), $\overline{d}$ (— —), $u$ (– · –), $\overline{u}$ (·· ··), $Q$ (– ··), $F_2^M$ (– – ··).*

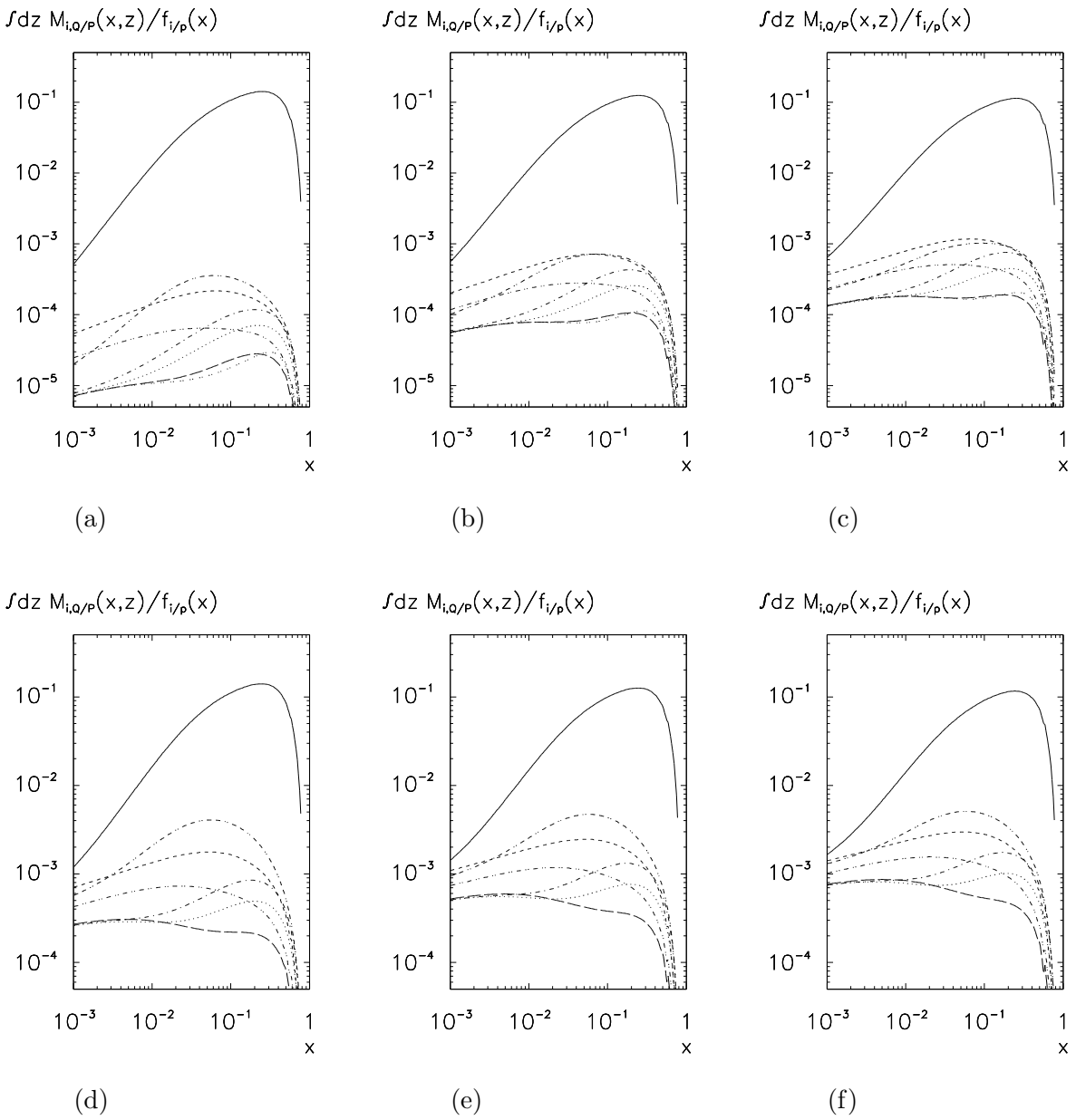


Figure 21: *Ratio of perturbative bottom (a)–(c) and charm (d)–(f) quark target fragmentation functions* $\int dz\, M^{(P)}_{i,Q/P}(x,z,\mu^2)$*, where* $z$ *is integrated from* 0.1 *to* $1-x$*, and parton densities* $f_{i/P}(x,\mu^2)$*. The factorization scale is* $\mu = 10\,GeV$ *(a), (d);* $\mu = 30\,GeV$ *(b), (e);* $\mu = 100\,GeV$ *(c), (f). The input distribution for* $M^{(P)}$ *is zero at* $\mu_0 = m$*. The flavours* $i$ *are given by* $\overline{Q}$ *(——),* $g$ *(– – –),* $d$ *(· · ·),* $\overline{d}$ *(—— ——),* $u$ *(– · – ·),* $\overline{u}$ *(·· ·· ··),* $Q$ *(– ··),* $F_2^M/F_2$ *(– – ··).*

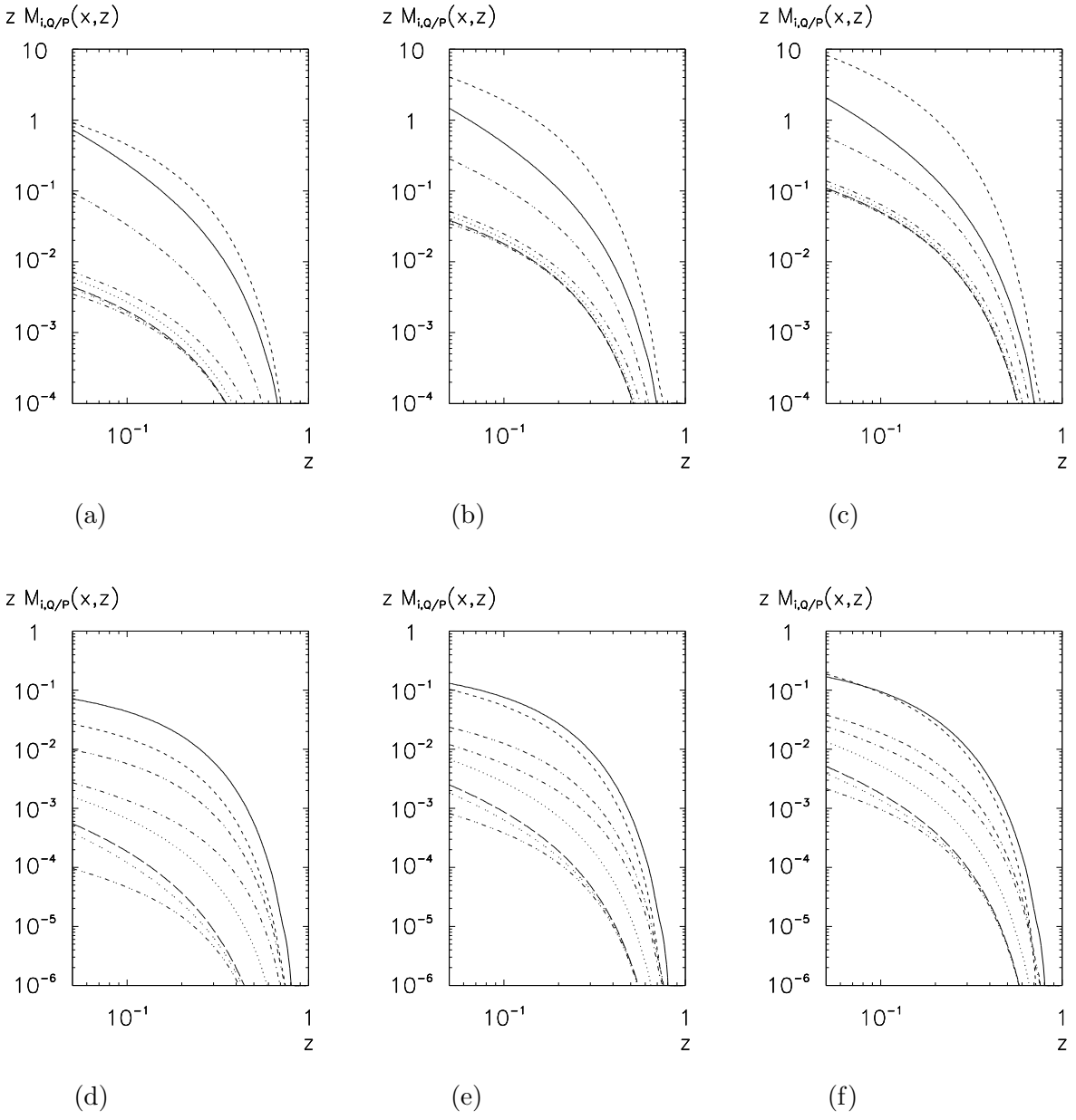


Figure 22: *Dependence of perturbative bottom-quark target fragmentation functions* $z\,M^{(P)}_{i,Q/P}(x,z,\mu^2)$ *on the momentum fraction* $z$ *of the observed heavy quark. The momentum fraction of the parton incident in the hard subprocess is* $x = 0.005$ *(a)–(c) and* $x = 0.05$ *(d)–(e), respectively. The factorization scale is* $\mu = 10\ GeV$ *(a), (d);* $\mu = 30\ GeV$ *(b), (e);* $\mu = 100\ GeV$ *(c), (f). The input distribution for* $M^{(P)}$ *is zero at* $\mu_0 = m$*. The flavours* $i$ *are given by* $\overline{b}$ *(——),* $g$ *(– – –),* $d$ *(· · ·),* $\overline{d}$ *(— —),* $u$ *(– · –),* $\overline{u}$ *(·· ··),* $b$ *(– ··),* $F_2^M$ *(– – ··).*

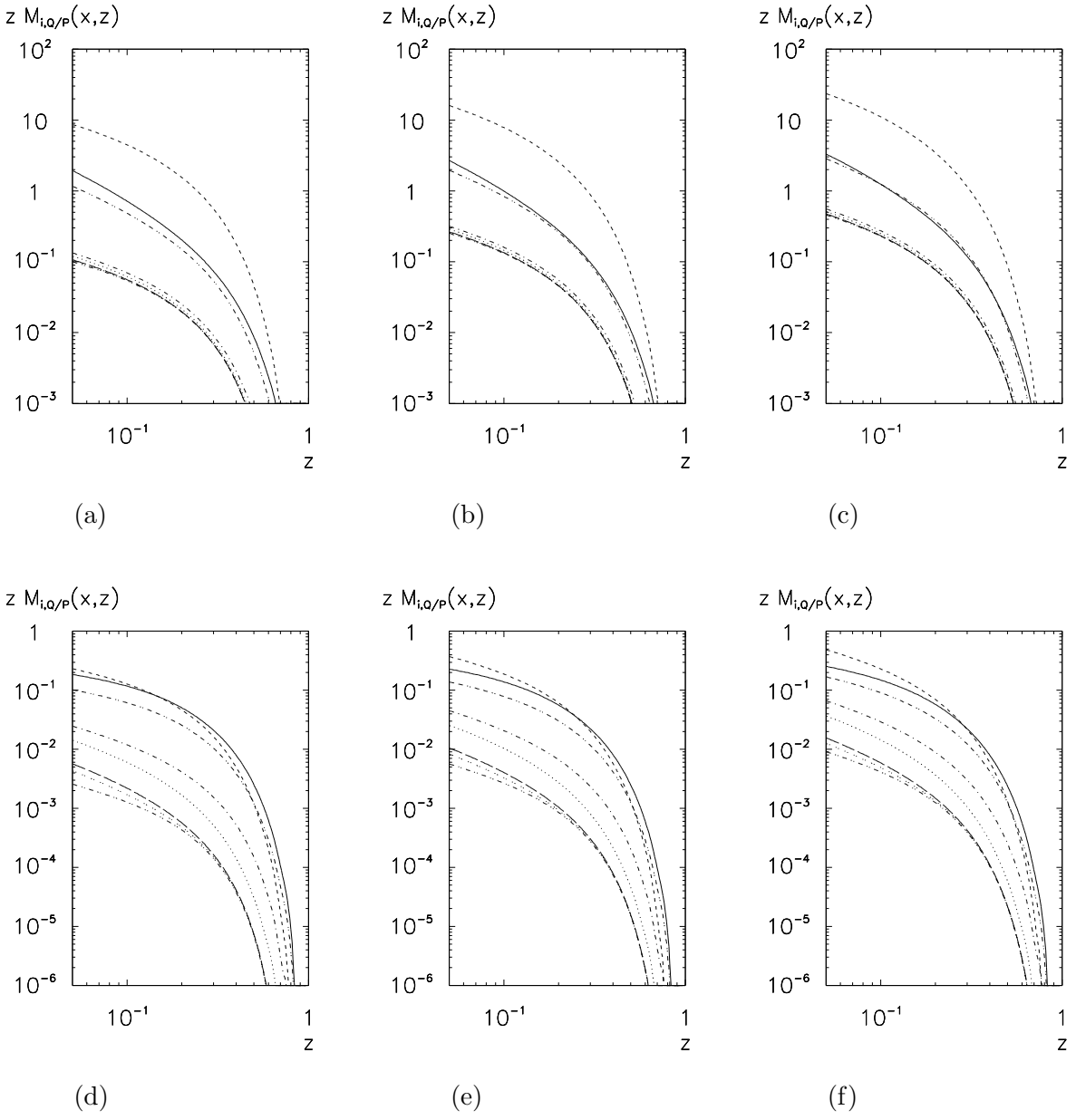


Figure 23: *Dependence of perturbative charm-quark target fragmentation functions* $z\,M^{(P)}_{i,Q/P}(x,z,\mu^2)$ *on the momentum fraction* $z$ *of the observed heavy quark. The momentum fraction of the parton incident in the hard subprocess is* $x = 0.005$ *(a)–(c) and* $x = 0.05$ *(d)–(e), respectively. The factorization scale is* $\mu = 10\ GeV$ *(a), (d);* $\mu = 30\ GeV$ *(b), (e);* $\mu = 100\ GeV$ *(c), (f). The input distribution for* $M^{(P)}$ *is zero at* $\mu_0 = m$*. The flavours* $i$ *are given by* $\overline{c}$ *(——),* $g$ *(– – –),* $d$ *(· · ·),* $\overline{d}$ *(— —),* $u$ *(– · –),* $\overline{u}$ *(·· ··),* $c$ *(– ··),* $F_2^M$ *(– – ··).*

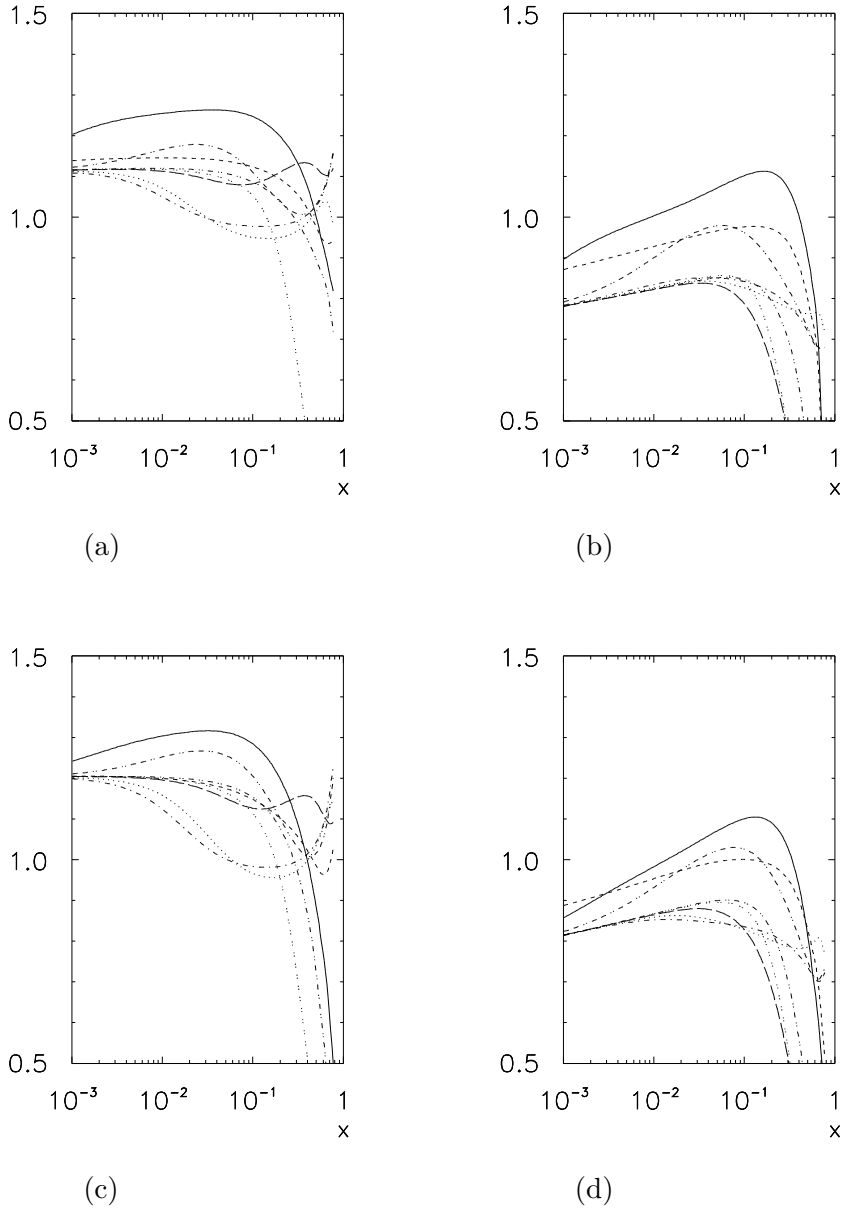


Figure 24: *Ratios of target fragmentation functions* $\int dz\, M^{(P)}_{i,Q/P}(x,z,\mu^2)$ *for different input parton densities: CTEQ, leading order (CTEQ 3L) [107] (a), (c) and MRS, next-to-leading order (MRS (G)) [108] (b), (d), divided by GRV, leading order [105, 106], for the bottom (a), (b) and charm (c), (d) quark at* $\mu = 100\,GeV$. *The input distribution* $M^{(P)}$ *is zero at* $\mu_0 = m$, *and* $z$ *is integrated from* $0.1$ *to* $1-x$. *The flavours* $i$ *are given by* $\overline{Q}$ (——), $g$ (– – –), $d$ (· · ·), $\overline{d}$ (—— ——), $u$ (– · – ·), $\overline{u}$ (·· ··), $Q$ (– ··), $F_2^M$ (– – ··).

### 5.3 Intrinsic Heavy Quarks

The hypothesis of intrinsic heavy quarks in the proton asserts that there is a non-vanishing non-perturbative component $|uudQ\overline{Q}\rangle$ in a Fock space expansion of the proton state vector [38, 39]. For charm quarks, this hypothesis is not in contradiction with experimental facts [109]. As a consequence of the large mass of the heavy quark with respect to the up and down quarks, and since all quarks must have comparable velocities to stay together in a coherent bound state, the fraction of proton momentum carried by the intrinsic heavy quarks should be comparably large, eventually giving rise to a substantial contribution to $f_{Q/P}(x)$ at large $x$. So far, analyses of an intrinsic heavy quark content, based on experimental data, are available for charmed mesons in the final state in the current fragmentation region: see for example Ref. [109] and references therein. If the charm quark in these mesons comes from the intrinsic component, then it was the quark that initiated the hard scattering process, as shown in Fig. 25a. If the intrinsic component is not negligible, then there is another region in phase space where it is reasonable to look for intrinsic heavy quarks, namely the target fragmentation region [110]. In the parton model, the scattering process at large $Q^2$ breaks up the proton, and any of the valence quarks, the heavy antiquark $\overline{Q}$, or sea partons may take part in the hard scattering process. The intrinsic heavy quark $Q$ is liberated, it fragments and is seen in the target fragmentation region, as indicated in Fig. 25b. In the case of charm-quark production, it is expected to recombine preferably with valence or sea quarks from the proton remnant into $D$ mesons and $\Lambda_c$ baryons; the latter, owing to a leading-particle effect, occur more frequently than $\overline{\Lambda_c}$ baryons because of the abundance of $u$ and $d$ valence quarks with respect to $\overline{u}$ and $\overline{d}$ sea quarks.

To study this process semi-quantitatively, we employ a simple model distribution as an example of a non-perturbative contribution to a target fragmentation function. Following Ref. [38], we write the correlated distribution function for the momentum distribution of three light valence quarks $uud$ and a pair $Q\overline{Q}$ of heavy quarks with momentum fractions $x_1$, $x_2$, $x_3$ and $x_Q$, $x_{\overline{Q}}$, respectively, as

$$\frac{\mathrm{d}P}{\mathrm{d}x_1\mathrm{d}x_2\mathrm{d}x_3\mathrm{d}x_Q\mathrm{d}x_{\overline{Q}}} = 36\,\beta\,\frac{x_Q^2 x_{\overline{Q}}^2}{(x_Q + x_{\overline{Q}})^2}\,\delta\left(1 - x_1 - x_2 - x_3 - x_Q - x_{\overline{Q}}\right), \tag{61}$$

where the momentum distribution is symmetric in the momentum fraction variables $x_1$, $x_2$ and $x_3$ of the three light quarks. The normalization factor $\beta$ is not predicted by the model. Instead, it has to be obtained from experiment. The value $\beta = 1$ is a reasonable value for intrinsic charm quarks, close to what is obtained from a fit to experimental data [109]. The distributions should scale as $1/m_Q^2$ with the heavy-quark mass. Thus, $\beta = 0.1$ is a reasonable assumption for the bottom quark.

In Refs. [38, 39], the expression in Eq. (61) is integrated over the variables $x_1$, $x_2$, $x_3$ and $x_{\overline{Q}}$ in order to obtain the single particle distribution for intrinsic heavy quarks in the proton:

$$f_{Q/P}^{(\mathrm{IHQ})}(x) = 36\,\beta\,\frac{x^2}{2}\left[\frac{1}{3}(1 + 10x + x^2)(1 - x) + 2x(1 + x)\ln x\right]. \tag{62}$$

A normalization factor of $\beta = 1$ actually corresponds to an intrinsic heavy-quark content of $\int_0^1 \mathrm{d}x\, f_{Q/P}^{(\mathrm{IHQ})}(x) = 1\%$. The resulting distributions, evolved in the factorization scale $\mu$ with the input from Eq. (62) at $\mu_0 = m$, are shown in Fig. 26. Compared with standard parton densities, cf. Fig. 18, the heavy-quark content is fairly large and peaked at large values of $x$ of about 0.3.

Here, instead, we integrate over only three of the variables $x_1$, $x_2$, $x_3$, $x_Q$, $x_{\overline{Q}}$, leaving a pair $(x, z)$ of variables in the distribution function. The result is interpreted as a correlated

distribution function for a heavy quark $Q$ and another quark (either a valence quark or the heavy antiquark $\overline{Q}$), i.e. a target fragmentation function in leading order. Here $x = x_1,\, x_2,\, x_3,\, x_{\overline{Q}}$ is the momentum fraction of the quark initiating the hard process, and $z = x_Q$ is the momentum fraction of the heavy quark detected in the proton remnant. For simplicity, we neglect all mass effects[33], and assume that the hard scattering process, possibly involving neither of the heavy quarks, breaks the coherence of the $Q\overline{Q}$ pair and allows them to propagate into the final state without recombination. For a detailed discussion, see Ref. [110]. The numerical results obtained in this section therefore cannot be more than a crude estimate for a simple model. They give, however, a good idea of the qualitative features for the case of intrinsic heavy quarks in the proton.

Performing the integrations, the final result for the target fragmentation functions is

$$\begin{aligned} M^{(\mathrm{IHQ})}_{d,Q/P}(x,z) &= 36\,\beta\,z^2\left[\frac{1}{2}(1-x)^2 + 2z(1-x) - \frac{5}{2}z^2 + (2z(1-x)+z^2)\ln\frac{z}{1-x}\right], \\ M^{(\mathrm{IHQ})}_{u,Q/P}(x,z) &= 2\,M_{d,Q/P}(x,z), \\ M^{(\mathrm{IHQ})}_{\overline{Q},Q/P}(x,z) &= 36\,\beta\,z^2\,\frac{1}{2}\frac{x^2}{(x+z)^2}(1-x-z)^2, \end{aligned} \tag{63}$$

these expressions being valid for a factorization scale of the order of the heavy-quark mass[34]. We therefore use them as input distributions for a factorization scale of $\mu_0 = m$ for the homogeneous part of the evolution equation (42), corresponding to the "non-perturbative" distributions. We wish to note that, in principle, the non-perturbative target fragmentation functions should have a dependence, proportional to $\ln\mu_0^2$, on the unphysical scale $\mu_0$, in order to cancel a corresponding term from the evolution equation of the perturbative target fragmentation functions. We assume that the exact cancellation takes place at $\mu_0 = m$.

The $x$-distributions of target fragmentation functions, for $z$ integrated from 0.1 to $1-x$, are shown for a set of factorization scales in Fig. 27. They are of the same order of magnitude as the perturbative heavy-quark target fragmentation functions, cf. Fig. 19. The $z$-distributions are shown in Fig. 28. It is obvious that the $z$-distribution is harder than in the case of the perturbative functions, cf. Figs. 22 and 23.

[33] A complete next-to-leading-order analysis of $f^{(\mathrm{IHQ})}$, including mass effects, has been done in Ref. [109]. A comparable analysis of $M^{(\mathrm{IHQ})}$ is beyond the scope of the present paper.

[34] S. Brodsky, private communication. The input distribution scales with $m$ as $1/m^2$ for factorization scales $\mu$ larger than $m$, whilst for $\mu < m$, the distribution is suppressed by a resolution factor and scales as $1/m^4$.

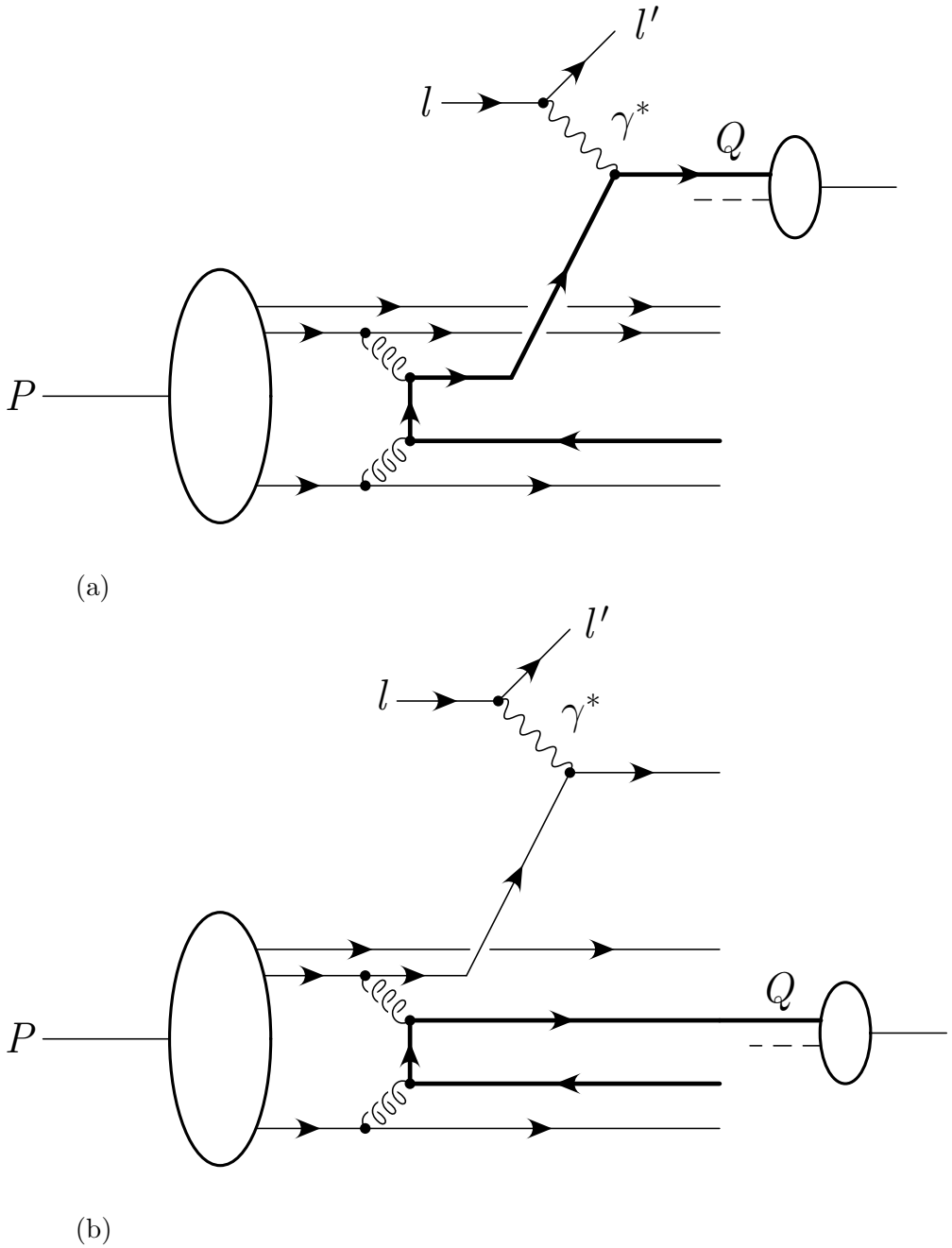


Figure 25: *Intrinsic heavy-quark production in the current (a) and target (b) fragmentation regions. The solid line stands for the heavy quark that subsequently fragments into a hadron.*

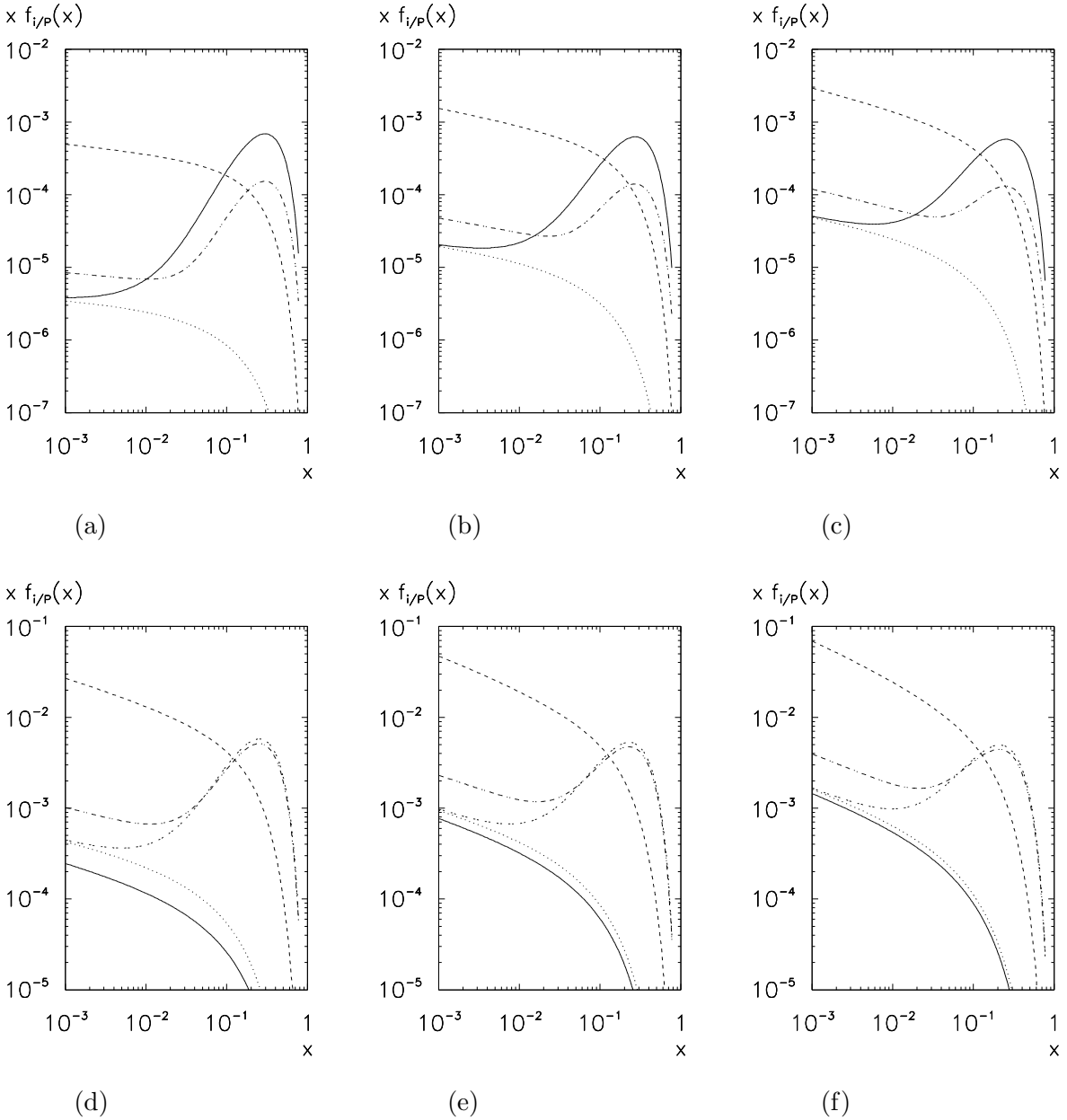


Figure 26: *Scale evolution of the parton densities* $x\, f_{i/P}^{(\mathrm{IHQ})}(x,\mu^2)$ *based on intrinsic bottom (a)–(c) and charm (d)–(f) quark distributions. The factorization scale is* $\mu = 10\,GeV$ *(a), (d);* $\mu = 30\,GeV$ *(b), (e);* $\mu = 100\,GeV$ *(c), (f). The flavours i are given by b,* $\overline{b}$ *(——); c,* $\overline{c}$ *(-- --); g (– – –); light quarks (· · ·);* $F_2$ *(– – ··).*

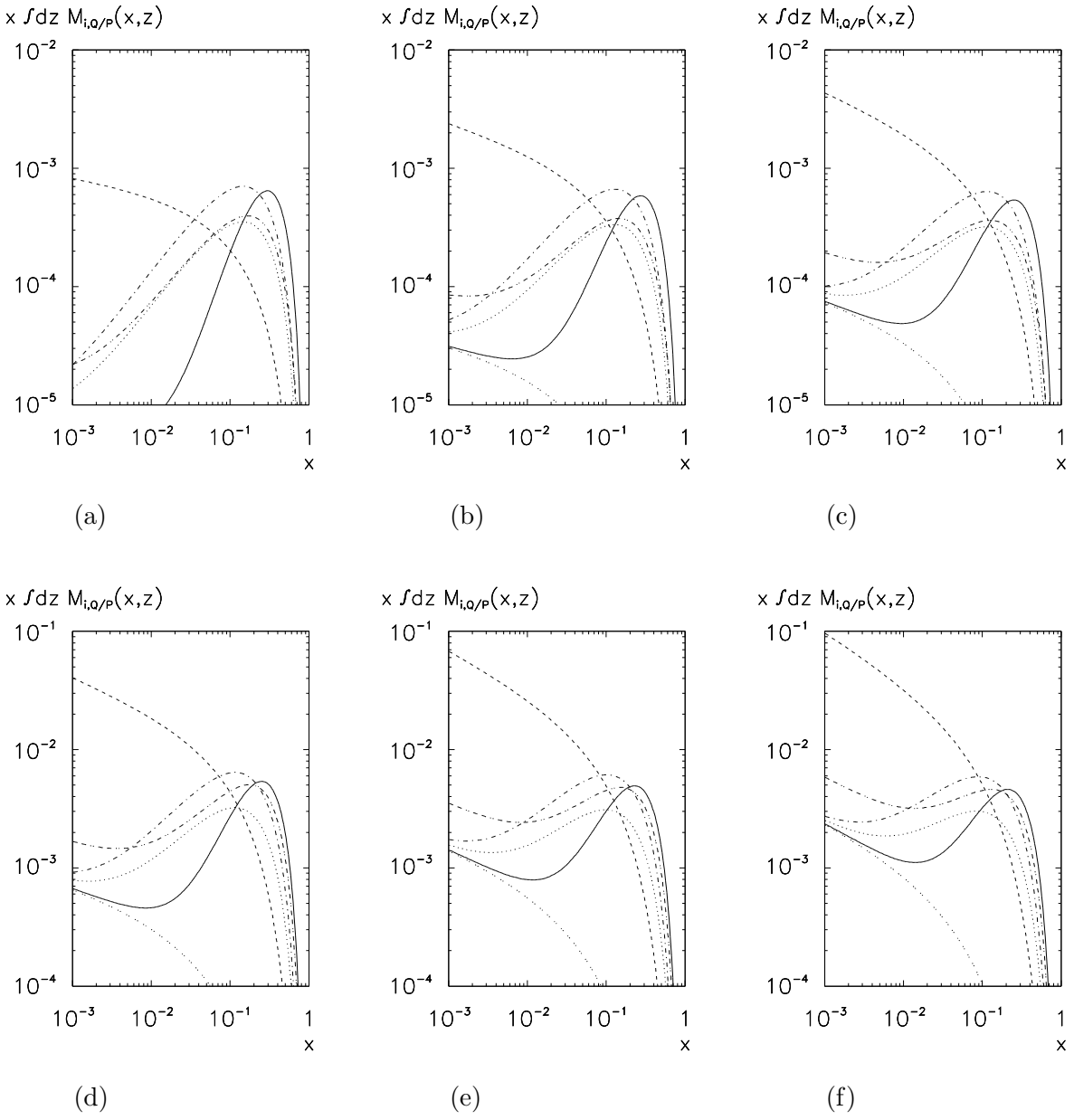


Figure 27: *Scale evolution of target fragmentation functions* $x \int dz\, M^{(\mathrm{IHQ})}_{i,Q/P}(x,z,\mu^2)$ *for intrinsic bottom (a)–(c) and charm (d)–(f) quarks, where* $z$ *is integrated from* 0.1 *to* $1-x$*. The factorization scale is* $\mu = 10\,GeV$ *(a), (d);* $\mu = 30\,GeV$ *(b), (e);* $\mu = 100\,GeV$ *(c), (f). The input distribution is defined at* $\mu_0 = m$*. The flavours* $i$ *are given by* $\overline{Q}$ *(——); g (– – –); d (· · ·); u (– · –); $\overline{u}$, $\overline{d}$ (·· ··); $F_2^M$ (– – ··).*

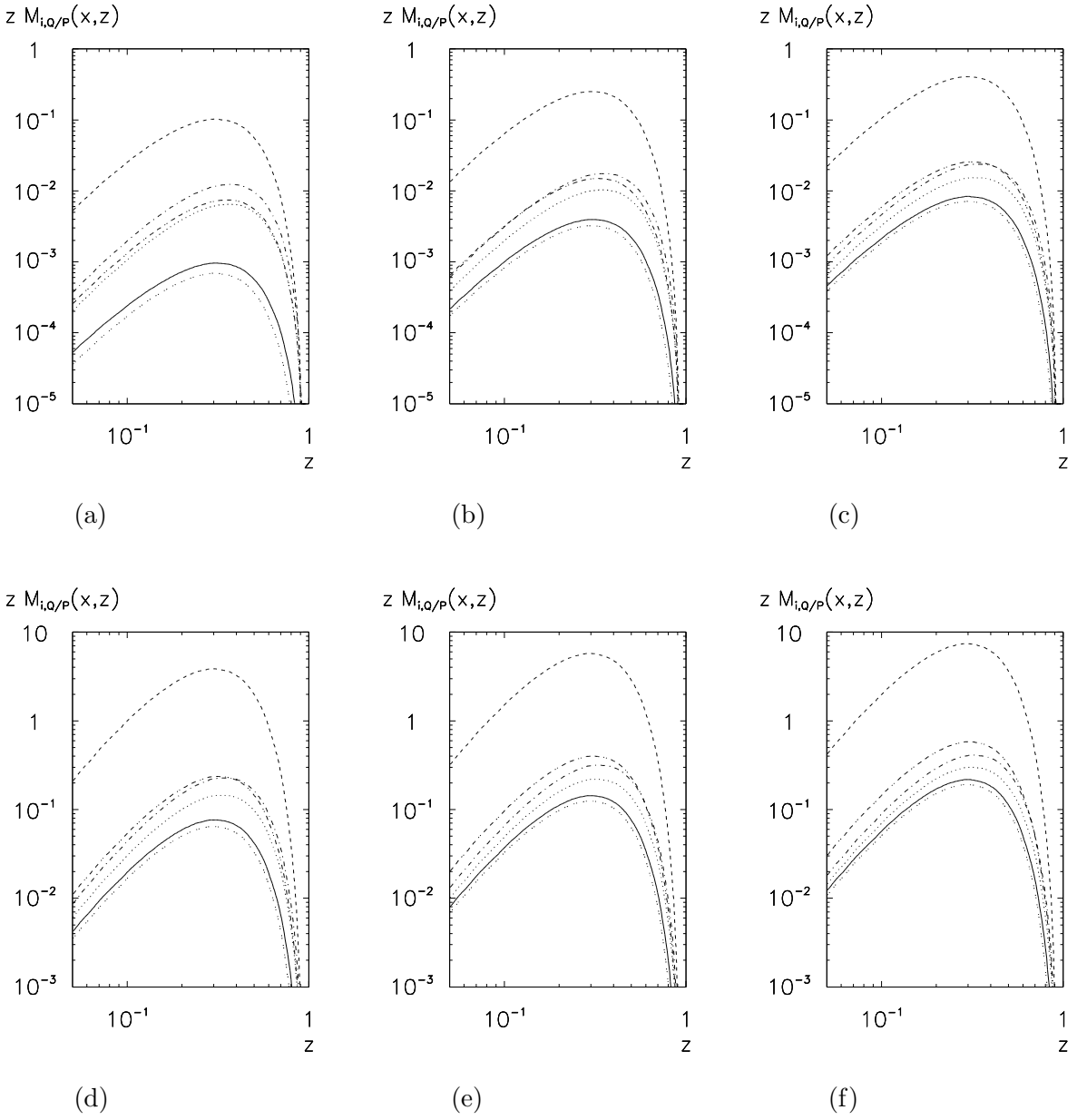


Figure 28: *Dependence of target fragmentation functions* $z\,M_{i,Q/P}^{(\mathrm{IHQ})}(x,z,\mu^2)$ *for intrinsic bottom (a)–(c) and charm (d)–(f) quarks on the momentum fraction of the observed heavy quark. The momentum fraction of the parton incident in the hard subprocess is* $x = 0.005$. *The factorization scale is* $\mu = 10\,GeV$ *(a), (d);* $\mu = 30\,GeV$ *(b), (e);* $\mu = 100\,GeV$ *(c), (f). The input distribution for* $M$ *is defined at* $\mu_0 = m$. *The flavours* $i$ *are given by* $\overline{Q}$ *(——); g (– – –); d (· · ·); u (– · –); $\overline{u}$, $\overline{d}$ (·· ··); $F_2^M$ (– – ··).*

# 6 A Phenomenological Case Study

*This section contains the results of a numerical case study for heavy-quark production in deeply inelastic lepton–nucleon scattering at HERA, E665 and NA47. The goal of this study is twofold: (a) to show that for an actual experimental situation reasonable theoretical results may be obtained for heavy-quark production in the target fragmentation region, and (b) to investigate how the mechanism that cancels singularities works in principle. Section 6.1 gives a short introduction to the fragmentation function picture of heavy-quark production as applied in this study. Section 6.2 briefly describes how the matrix elements are implemented. The parameters for the numerical evaluation are given in Section 6.3. Section 6.4 serves to give an overview of cross sections in various phase-space regions. Transverse momentum distributions and the subtraction process in the collinear phase-space regions are investigated in Section 6.5. A comparison of distributions in $x_F$ in leading and next-to-leading order, including the case of intrinsic heavy quarks, is done in Section 6.6. The scale dependence of the cross sections is investigated in Section 6.7. Our results indicate that, in deeply inelastic scattering, taking into account the fragmentation of the heavy quarks into observable mesons, the cross section is too small to allow for an experimental determination of the heavy-quark target fragmentation functions for the luminosities of the experiments under consideration. A similar analysis based on the photoproduction process, although not treated in the present paper, is expected to be a more realistic scenario.*

## 6.1 Heavy-Quark Production

Having obtained the fragmentation and target fragmentation functions of heavy quarks, we can now treat heavy-quark production in the fragmentation function picture. The cross section is written as

$$\sigma = \sum_{i,j} \sigma^{\text{hard}}_{fD,ij} \otimes f_{i/P} \otimes D_{Q/j} + \sum_{i} \sigma^{\text{hard}}_{M,i} \otimes M_{i,Q/P}, \tag{64}$$

cf. Eq. (6). The hard scattering matrix elements are those from Section 2, where all quarks are treated as massless. Depending on the available phase space, we assume $N_f = 4$ or $N_f = 5$ active flavours in the photon–gluon fusion process. The treatment of the heavy quarks as massless flavours in the hard scattering process is justified in two cases. It may be done as an approximation for the case of large transverse momenta, where the heavy-quark propagators are far off-shell, see for example Ref. [111]. It is also justified as a technical tool for the extraction of mass singularities, as in the fragmentation function approach to heavy-quark production, as developed in Refs. [37, 101], where massless partons fragment into heavy quarks. The region of small transverse momenta gives rise to terms $\sim \log m^2/Q^2$ (the mass singularities for $m \to 0$) for the integrated massive matrix element, corresponding to the $1/\epsilon$ collinear singularities in the massless approach. Absorbing the $1/\epsilon$ singularities into the renormalized target fragmentation functions corresponds to a resummation of the terms logarithmic in $m^2/Q^2$. In principle, the universality of the coefficient of the mass singularities renders the use of "massless" heavy quarks in the hard scattering matrix element a valid procedure[35].

We will compare our results to the leading-order process $\gamma^* g \to Q\overline{Q}$, shown in Fig. 29, with massive quarks in the matrix element. Since the heavy-quark mass $m$ acts as a regulator of the collinear and soft singularities, it is possible to integrate the cross section over the full phase

[35] It is certainly desirable to extend the formalism in such a way that the heavy quarks can be treated as massive, even if the limit $m \to 0$ in the matrix element is done only for the extraction of the mass singularities in the $\overline{\text{MS}}$ scheme. This would affect the renormalization group equation and the calculation of the hard scattering matrix elements. The present approach has the advantage that we can treat the fragmentation of light quarks and gluons into heavy quarks.

space without encountering divergent terms. Although this approach, as already discussed in the introduction, is probably not sufficient to fully describe the target fragmentation region, the comparison will be instructive. Since the $\gamma^* g \to Q\overline{Q}$ matrix element will be studied only in leading order, the results of the comparison should, however, be interpreted with great care.

The required projections of the hadron tensor in $d = 4$ space-time dimensions are (see for example Ref. [27]):

$$\begin{aligned}
&\frac{1}{e^2(2\pi)^8} P_M^{\mu\nu} H_{\mu\nu}(\gamma^* g \to Q\overline{Q}) \\
&\quad = 8\pi \frac{\alpha_s}{2\pi} 2\pi T_f Q_Q^2 \cdot 4 \cdot \left[ \frac{s_{iQ} + 2m^2}{s_{i\overline{Q}}} + \frac{s_{i\overline{Q}} + 2m^2}{s_{iQ}} - \frac{2(Q^2 - 2m^2) s_{Q\overline{Q}}}{s_{iQ} s_{i\overline{Q}}} \right. \\
&\qquad\qquad \left. + 2m^2 \frac{s_{i\overline{Q}} - s_{Q\overline{Q}} - 4m^2}{s_{iQ}^2} + 2m^2 \frac{s_{iQ} - s_{Q\overline{Q}} - 4m^2}{s_{i\overline{Q}}^2} \right], \\
&\frac{1}{e^2(2\pi)^8} P_L^{\mu\nu} H_{\mu\nu}(\gamma^* g \to Q\overline{Q}) \\
&\quad = 8\pi \frac{\alpha_s}{2\pi} 2\pi T_f Q_Q^2 \cdot 4 \cdot \left[ 4 \frac{u^2}{Q^2} \left( s_{Q\overline{Q}} - m^2 \left[ \frac{s_{iQ}}{s_{i\overline{Q}}} + \frac{s_{i\overline{Q}}}{s_{iQ}} \right] \right) \right];
\end{aligned} \tag{65}$$

for the conventions see Sections 2.2 and 2.3. A suitable phase-space parametrization is listed in Appendix B.2.

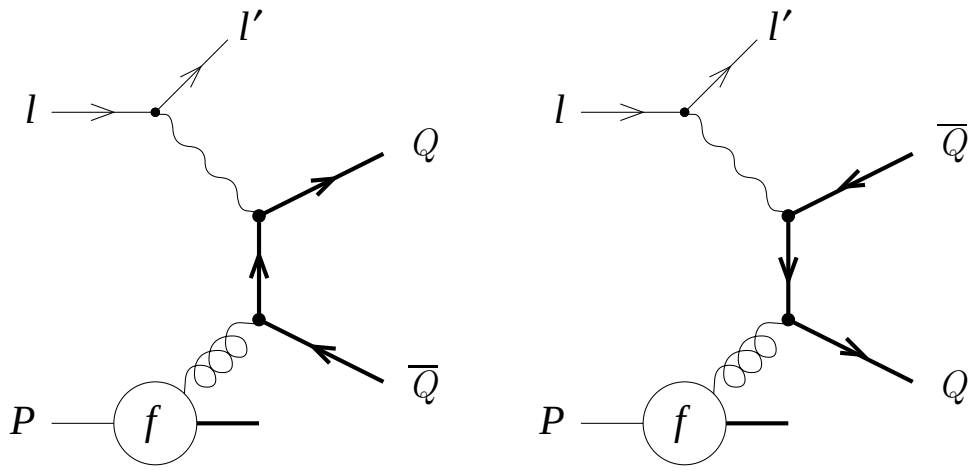


Figure 29: *Feynman diagrams corresponding to the process $\gamma^* g \to Q\overline{Q}$ in leading order.*

## 6.2 Implementation of the Cross Section Formula

The cross section is implemented in a FORTRAN program that allows us to determine arbitrary distributions in the variables describing the produced heavy quark and the scattered lepton by means of a Monte Carlo integration[36]. Depending on the particular process at hand (i.e. Born

[36] The implementation has been cross-checked by a comparison to PROJET [112] for non-vanishing $p_T$ and by an explicit analytical integration for the phase-space regions of vanishing $p_T$, for the special case of $D(x) = \delta(1-x)$. Moreover, the invariance with respect to shifts of finite contributions between regular and singular terms $D^r$ and $D^s$ of the fragmentation functions, according to the decomposition of Eq. (131), has been verified.

terms or next-to-leading-order contributions in the current and target fragmentation regions), the program generates the corresponding kinematical variables and calls a user-defined function that has to supply the value of the observable to be averaged. In a similar way, the matrix element weights of arbitrary observables may be summed up in histogram bins. The adaptive Monte Carlo integration is based on the multidimensional integration routine VEGAS [113, 114].

In the case of next-to-leading-order contributions, the user-defined subroutine is typically called several times for every event, with different momenta of the external particles, due to the necessary subtractions, as is described in Appendix C.2. In the case of heavy-quark production, where the heavy-quark fragmentation functions themselves are singular functions, the final expression for the cross section is a triple convolution (in the variables $u$, $\rho$ and $z$), where all integrals are possibly related to subtractions. The cross sections derived in this paper, integrated over physically well motivated regions to be defined later, have to be finite and positive if they are to be physical. In the current and target fragmentation regions at small transverse momenta, cancellations of tree-level terms and finite "redefinition" terms will occur. It is therefore to be expected that the numerical results will only be meaningful if the corresponding integration region is sufficiently large. This phenomenon will be studied in more detail numerically in Section 6.5.

### 6.3 Parameters and Variables

We define the kinematical parameters for a case study of heavy-quark production at HERA[37] (charm and bottom quarks), E665 (charm quarks) and NA47 (charm quarks) as follows:.

- HERA: $E_{CM} = 296\,\mathrm{GeV}$, $10^{-3} < x_B < 1$, $W > 20\,\mathrm{GeV}$. For bottom-quark production, we use $20\,\mathrm{GeV} < Q < 100\,\mathrm{GeV}$, and for charm-quark production $5\,\mathrm{GeV} < Q < 10\,\mathrm{GeV}$. We moreover require that the observed heavy quark carries at least 10% of the proton's momentum, and assume that 5 quark flavours may be produced in the photon–gluon fusion process. The integrated luminosity can be assumed to be $\int \mathcal{L}\,\mathrm{d}t = 250\,\mathrm{pb}^{-1}$.
- E665: $E_{CM} = 31\,\mathrm{GeV}$, $0.05 < y < 0.95$, $2\,\mathrm{GeV} < Q < 5\,\mathrm{GeV}$, $W > 13\,\mathrm{GeV}$. We require that the observed heavy quark carries at least 20% of the proton's momentum, and assume that 4 quark flavours may be produced in the photon–gluon fusion process.
- NA47 (SMC, HMC): $E_{CM} = 17.3\,\mathrm{GeV}$, $3 \times 10^{-3} < x_B < 0.7$, $2\,\mathrm{GeV} < Q < 7.7\,\mathrm{GeV}$, $W > 8\,\mathrm{GeV}$. As in the case of E665, we require that the observed heavy quark carries at least 20% of the proton's momentum, and assume that 4 quark flavours may be produced in the photon–gluon fusion process. The integrated luminosity for SMC is approximately $\int \mathcal{L}\,\mathrm{d}t = 300\,\mathrm{pb}^{-1}$ per year. It is expected to be larger by a factor of 5 for the HMC experiment [11, 12].

The parton-density parametrizations were taken from the packages PAKPDF [115] and PDFLIB [116]. We use the leading-order GRV distribution [105], with the heavy-quark content modified[32] according to the distribution from Ref. [106]. The running strong coupling constant $\alpha_s(\mu_r^2)$ with flavour thresholds at the single quark masses[38] is evaluated using the standard one-loop formula

[37] Please note that a measurement of the heavy-quark content of the target fragments is, at present, realistic only in fixed-target experiments, although, for instance, special-purpose detector components may permit the tagging of for example charm quarks in the target fragmentation region of the HERA experiments. In any case, it is interesting to have a comparison to an actual experimental situation at energies larger than those achievable in present fixed-target experiments.

[38] See Ref. [117] and also Ref. [118].

with $\Lambda_{\rm QCD} = 200\,{\rm MeV}$. The factorization scales $\mu_f$, $\mu_D$ and $\mu_M$ and the renormalization scale $\mu_r$ are set to $Q$, unless otherwise stated[39]. For the heavy-quark fragmentation functions, we use the leading order expressions, with the perturbative input defined at $\mu_{D,0} = m$. The perturbative heavy-quark target fragmentation functions are defined to be zero at $\mu_{M,0} = m$.

We will study distributions in the angular variable $v$, in the momentum $P_Q$ of the heavy quark in the hadronic centre-of-mass frame given by

$$P_Q = \frac{Q}{2}\sqrt{\frac{1-x_B}{x_B}}\,z, \tag{66}$$

in the transverse momentum $p_T$ in the hadronic centre-of-mass frame given by

$$p_T = \frac{Q}{2}\sqrt{\frac{1-x_B}{x_B}}\,z_T, \tag{67}$$

where $z_T \in [0,1]$ is defined by

$$z_T \doteq 2\,z\,\sqrt{v(1-v)}, \tag{68}$$

and in the Feynman variable $x_F$ [126] given by

$$x_F \doteq \frac{h_L}{W/2} = z(1-2v), \tag{69}$$

where $h_L$ is the longitudinal momentum of the heavy quark in the hadronic centre-of-mass frame. The variable $x_F$ can be used to disentangle the current ($x_F \geq 0$) and target ($x_F < 0$) fragmentation regions. We will study distributions in $p_T$ separately in these regions, and denote the corresponding variables by $p_T^c$ and $p_T^t$, respectively. We also consider the variable $z_\parallel$, as defined in Ref. [127] by

$$z_\parallel \doteq \frac{h_L^{\rm Breit}}{Q/2} = z\left(1-\frac{v}{x_B}\right), \tag{70}$$

where $h_L^{\rm Breit}$ is the longitudinal momentum in the Breit frame[40]. It is easy to see that

$$-\frac{1-x_B}{x_B} \leq z_\parallel \leq 1. \tag{71}$$

### 6.4 Cross Sections

As a first step, we give an overview of the partial cross sections for various phase-space regions in Table 2. The total cross sections $\sigma_{\rm tot}$, corresponding to arbitrary hadronic final states in deeply inelastic scattering, are calculated in leading {1}[41] and next-to-leading {2} order by means of PROJET [112]. The $\mathcal{O}(\alpha_s)$ contributions are small, of the order of 10–20%. The leading-order cross section for heavy-quark production $\sigma_{fD}$ {3} is a fraction of the order of 1–10% of $\sigma_{\rm tot}$, depending on the experiment. The leading-order contribution $\sigma_M$ {8} is much smaller than $\sigma_{fD}$

[39] For our purposes, namely to give an overview of cross sections, $Q$ is sufficient as a scale. It is of course possible to apply specific principles in order to improve the theoretical prediction, such as the principle of *Fastest Apparent Convergence* (FAC) [119, 120], the *Principle of Minimum Sensitivity* (PMS) [121–124], and the method of *Automatic Scale Fixing* (BLM) [125]. As can be seen from Figs. 41 and 42, the scale dependence is drastically reduced in next-to-leading order, so that the issue of scale choices can be postponed to a later study.

[40] The Breit frame is defined as the reference frame where the energy of the exchanged virtual photon is zero and where the incident nucleon and the virtual photon are back-to-back. Again, we define the $z$-axis to be in the current direction.

[41] The numbers in braces { } refer to the rows in the tables.

{3} in leading order. The contributions $\mathcal{O}(\alpha_s)$ are given separately for the current and target fragmentation regions. In the current fragmentation region, the size of the QCD corrections {4} varies considerably and may be as large as about 40% of the leading-order term {3}, because the photon–gluon fusion process contributes significantly. In the target fragmentation region, the contribution from $\sigma_{fD}$ {5} is roughly of the same order of magnitude as the leading-order terms in $\sigma_M$ {8}. The QCD corrections to $\sigma_M$ {9} are negative and about –5 to –10%.

Summing up leading and next-to-leading orders, we arrive at the following results. The overall next-to-leading-order correction is in the range of –5 to +40% {10, 11}, where the current fragmentation region dominates {12, 13}. A comparison of {12} with {14} and of {13} with {15} shows that a considerable fraction of heavy quarks is produced with a $p_T$ smaller than $p_{T,\min}$, where $p_{T,\min} \doteq 9\,\text{GeV}$ and $3\,\text{GeV}$ for bottom- and charm-quark production, respectively.

The results from the fragmentation function approach can be compared with those from the $\gamma^* g \to Q\overline{Q}$ matrix element, shown in rows {16–21} in the table. Comparing {6} with {18} and {7} with {19}, one sees that the cross sections for $p_T > p_{T,\min}$ agree well. We will see later in Section 6.5 that there are considerable differences for small $p_T$. In the target fragmentation region, comparing {15} and {21}, the excess in the fragmentation function approach can be attributed to the evolution of the perturbative target fragmentation functions.

The contribution from intrinsic heavy quarks in the current fragmentation region {22} is small, less than 1% of the non-intrinsic contribution {10}, except for NA47, where it reaches about 8%. The situation is very different in the target fragmentation region {25}, where the intrinsic heavy-quark component is comparable to the non-intrinsic heavy-quark component {13}, or even dominant.

The flavour decomposition of the cross sections is shown in Table 3. The heavy-quark- and gluon-initiated contributions of the total cross section are shown in rows {1–3}. Tagging a heavy quark in the current {4, 5} and target {6, 7} fragmentation regions considerably increases the fraction of processes initiated by the heavy quark and antiquark, respectively, the absolute cross sections, however, being much smaller. The fractions in leading order are fairly large {4–7}, and they are reduced in next-to-leading order {8, 9, 11, 12}, due to the inclusion of gluon-initiated processes {10, 13}. This clearly shows that the tagging of particles in the target fragments permits to bias the flavour content of the hard scattering process.

Differential distributions in $x_B$ and in the total hadronic final state energy $W$ are shown in Figs. 30 and 31, respectively. For charm-quark production at HERA, the dominant contributions come from the region of small $x_B$. Figure 31 shows that the values of the hadronic final state energy $W$ in the fragmentation function approach, compared with the $\gamma^* g \to Q\overline{Q}$ matrix element, extend to slightly smaller values.

| | | | | Bottom | Charm | | |
|---|---|---|---|---|---|---|---|
| Process | | | | HERA | HERA | E665 | NA47 |
| 1 | LO | $\sigma_{\rm tot}$ | | 864 | 23861 | 27434 | 21620 |
| 2 | NLO | | | 809 | 21451 | 22743 | 18707 |
| 3 | $\mathcal{O}(\alpha_s^0)$ | $\sigma_{fD}$ | | 10.2 | 2307 | 1007 | 433 |
| 4 | $\mathcal{O}(\alpha_s)$ | $\sigma_{fD}$ | $x_F \geq 0$ | –1.29 | 1001 | 344 | 20.8 |
| 5 | | | $x_F < 0$ | 0.144 | 14.4 | 20.2 | 19.2 |
| 6 | | | $x_F \geq 0$, $p_T > p_{T,\rm min}$ | 2.46 | 776 | 53.0 | 5.52 |
| 7 | | | $x_F < 0$, $p_T > p_{T,\rm min}$ | 0.131 | 11.8 | 4.36 | 0.623 |
| 8 | $\mathcal{O}(\alpha_s^0)$ | $\sigma_M$ | | 0.456 | 40.1 | 11.6 | 11.7 |
| 9 | $\mathcal{O}(\alpha_s)$ | | | –0.0297 | –1.99 | –1.01 | –0.922 |
| 10 | LO | $\sigma$ | | 10.6 | 2347 | 1018 | 444 |
| 11 | NLO | | | 9.48 | 3360 | 1381 | 483 |
| 12 | NLO | $\sigma$ | $x_F \geq 0$ | 8.91 | 3308 | 1351 | 453 |
| 13 | | | $x_F < 0$ | 0.570 | 52.5 | 30.7 | 29.9 |
| 14 | | | $x_F \geq 0$, $p_T \leq p_{T,\rm min}$ | 6.45 | 2532 | 1298 | 447 |
| 15 | | | $x_F < 0$, $p_T \leq p_{T,\rm min}$ | 0.439 | 40.7 | 26.3 | 29.2 |
| 16 | $\mathcal{O}(\alpha_s)$ | $\sigma_{Q\overline{Q}}$ | $x_F \geq 0$ | 8.13 | 3427 | 930 | 260 |
| 17 | | | $x_F < 0$ | 0.233 | 30.5 | 18.2 | 10.1 |
| 18 | | | $x_F \geq 0$, $p_T > p_{T,\rm min}$ | 2.40 | 939 | 50.8 | 4.57 |
| 19 | | | $x_F < 0$, $p_T > p_{T,\rm min}$ | 0.101 | 14.1 | 3.96 | 0.487 |
| 20 | | | $x_F \geq 0$, $p_T \leq p_{T,\rm min}$ | 5.73 | 2488 | 879 | 255 |
| 21 | | | $x_F < 0$, $p_T \leq p_{T,\rm min}$ | 0.132 | 16.4 | 14.2 | 9.61 |
| 22 | $\mathcal{O}(\alpha_s^0)$ | $\sigma_{fD}^{(\rm IHQ)}$ | | $0.599\times10^{-1}$ | 9.17 | 8.61 | 34.3 |
| 23 | $\mathcal{O}(\alpha_s)$ | $\sigma_{fD}^{(\rm IHQ)}$ | $x_F \geq 0$ | $0.232\times10^{-3}$ | 2.65 | 4.01 | -0.430 |
| 24 | | | $x_F < 0$ | $0.451\times10^{-3}$ | 0.212 | 0.381 | 0.613 |
| 25 | $\mathcal{O}(\alpha_s^0)$ | $\sigma_M^{(\rm IHQ)}$ | | 0.499 | 60.9 | 72.1 | 124 |
| 26 | $\mathcal{O}(\alpha_s)$ | | | $-0.170\times10^{-1}$ | –2.11 | –1.61 | –10.8 |

Table 2: *Cross sections in [pb] for the various experiments and subprocesses. The $\mathcal{O}(\alpha_s)$ contributions do not include the corresponding $\mathcal{O}(\alpha_s^0)$ term. Terms denoted by NLO are the sums of $\mathcal{O}(\alpha_s^0)$ and $\mathcal{O}(\alpha_s)$ contributions for the corresponding phase-space region. The contributions labelled by $\sigma_{fD}$ and $\sigma_M$ correspond to the terms in Eqs. (4) and (5), whereas $\sigma$ stands for the sum of these two terms. "IHQ" stands for intrinsic heavy-quark contributions. The cross section for massive heavy quarks in the $\gamma^* g \to Q\overline{Q}$ matrix element is denoted by $\sigma_{Q\overline{Q}}$, and the total cross section, including all hadronic final states, by $\sigma_{\rm tot}$.*

| Process | | | | $i$ | Bottom | Charm | | |
|---|---|---|---|---|---|---|---|---|
| | | | | | HERA | HERA | E665 | NA47 |
| 1 | LO | $\sigma_{\rm tot}$ | | $Q$, $\overline{Q}$ | 0.8 | 9.4 | 3.7 | 2.0 |
| 2 | NLO | $\sigma_{\rm tot}$ | | $Q$, $\overline{Q}$ | 0.8 | 10.3 | 4.2 | 2.2 |
| 3 | NLO | $\sigma_{\rm tot}$ | | $g$ | $-5.4$ | $-9.7$ | 14.9 | 10.0 |
| 4 | $\mathcal{O}(\alpha_s^0)$ | $\sigma_{fD}$ | | $Q$ | 69.2 | 94.7 | 98.2 | 96.7 |
| 5 | $\mathcal{O}(\alpha_s^0)$ | $\sigma_{fD}$ | | $\overline{Q}$ | 0.2 | 0.5 | 0.0 | 0.0 |
| 6 | $\mathcal{O}(\alpha_s^0)$ | $\sigma_M$ | | $Q$ | 0.3 | 2.3 | 0.0 | 0.0 |
| 7 | $\mathcal{O}(\alpha_s^0)$ | $\sigma_M$ | | $\overline{Q}$ | 59.1 | 80.5 | 98.2 | 96.5 |
| 8 | NLO | $\sigma$ | $x_F \geq 0$ | $Q$ | 79.9 | 66.5 | 74.7 | 95.1 |
| 9 | NLO | $\sigma$ | $x_F \geq 0$ | $\overline{Q}$ | 0.0 | 0.0 | 0.0 | $-0.1$ |
| 10 | NLO | $\sigma$ | $x_F \geq 0$ | $g$ | 13.3 | 32.7 | 26.3 | 7.3 |
| 11 | NLO | $\sigma$ | $x_F < 0$ | $Q$ | 0.5 | 2.0 | 0.4 | 5.0 |
| 12 | NLO | $\sigma$ | $x_F < 0$ | $\overline{Q}$ | 46.2 | 60.0 | 34.3 | 35.0 |
| 13 | NLO | $\sigma$ | $x_F < 0$ | $g$ | 10.7 | 21.7 | 60.5 | 58.0 |

Table 3: *The same as Table 2, but now shown according to the partial cross sections in per cent, for various partons i incident in the hard scattering process. Partons i not included in the table add up to* 100%. *Entries below* 0.05% *are marked as* 0.0.

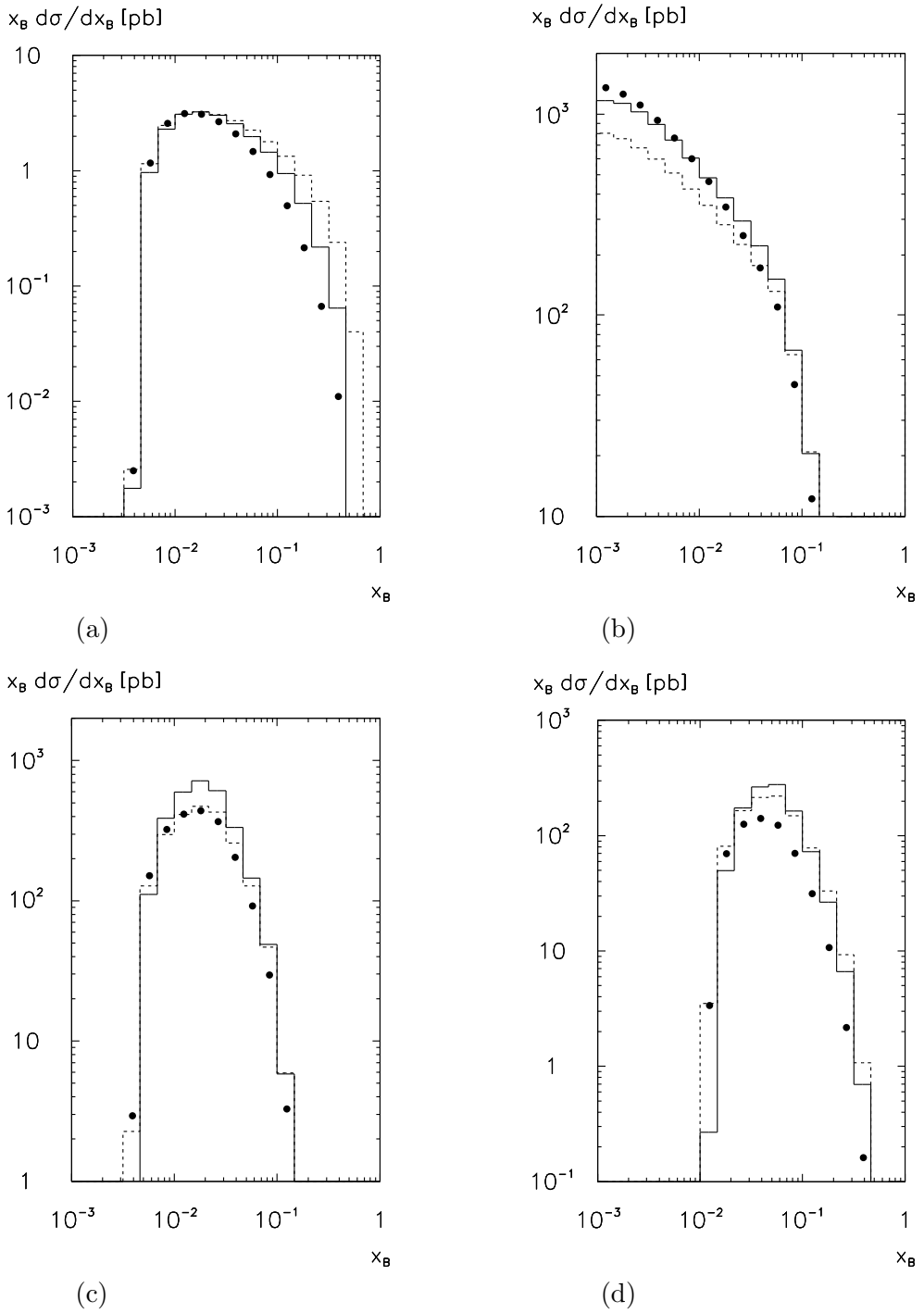


Figure 30: *Distributions in $x_B$ for bottom (a) and charm (b) quark production at HERA and for charm-quark production at E665 (c) and NA47 (d), in leading order (– – –) and in next-to-leading order (——). Also shown is the distribution from the matrix element $\gamma^* g \to Q\overline{Q}$ (•).*

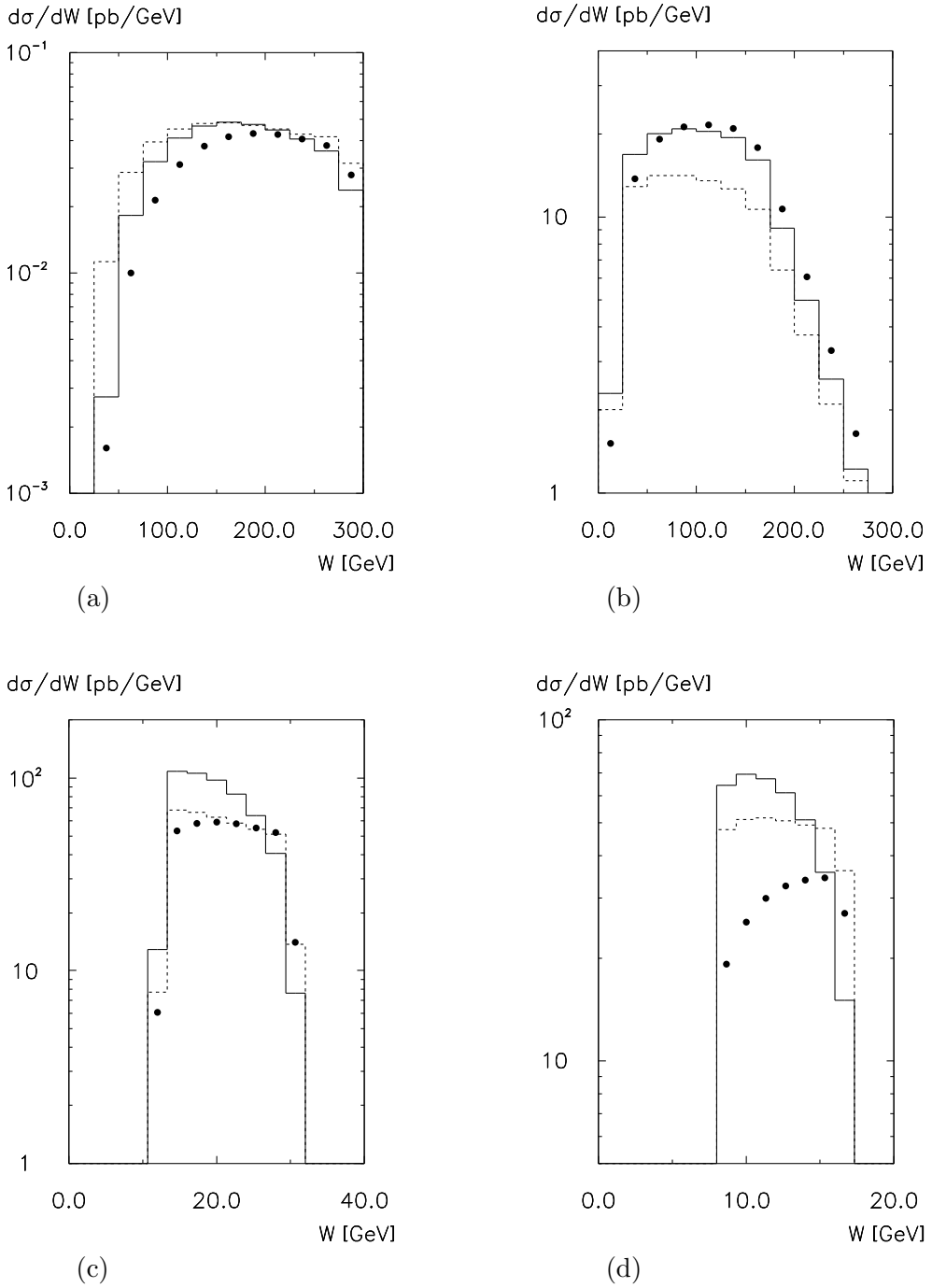


Figure 31: *Distributions in W for bottom (a) and charm (b) quark production at HERA and for charm-quark production at E665 (c) and NA47 (d), in leading order (– – –) and in next-to-leading order (——). Also shown is the distribution from the matrix element* $\gamma^* g \to Q\overline{Q}$ *(•).*

### 6.5 Distributions in $p_T$ and Collinear Subtractions

Considering the transverse momentum distributions in Figs. 32 and 33, we demonstrate that the mechanism to cancel collinear singularities in the target fragmentation region actually works in practice. The cross section, differential in $p_T$, is of the form $g(p_T)\,(1/p_T)_+$, where $g(p_T)$ is an integrable function and $(1/p_T)_+$ is the function $1/p_T$ with a subtraction at $p_T = 0$. As already mentioned in Section 6.2, the expected mechanism at work for finite cross sections is that large contributions from collinear singularities at small $p_T$ cancel against subtraction terms of opposite sign at $p_T = 0$. For too small a bin size at $p_T = 0$, this mechanism does not work, since the positive contributions will not be large enough. This is demonstrated in Figs. 32a, c and 33a, c for the case of the current fragmentation region. The differential cross section is defined by the cross section corresponding to a certain bin divided by the bin size, which makes sense, despite the subtractions, for the bin containing $p_T = 0$ as well. The cross section is strongly rising for $p_T^c \to 0$. For a small bin size, Figs. 32a and 33a, the entry in the first bin, containing $p_T^c = 0$, is negative, representing the subtraction in the current fragmentation region. For a sufficiently large bin size, Figs. 32c and 33c, the entry in the first bin is positive, showing that the perturbative result is well-defined in this case. This result is expected from the factorization theorems of perturbative QCD, applied to the absorption of singularities in the case of fragmentation functions[42].

An important result of this section, illustrated in Figs. 32b, d and 33b, d, is that a similar result can be obtained for the target fragmentation region. Again, the cross section is strongly rising for $p_T^t \to 0$, Figs. 32b and 33b. For a small bin size, the entry in the first bin, containing $p_T^t = 0$, is negative, again representing a subtraction, in this case in the target fragmentation region. For a sufficiently large bin size, Figs. 32d and 33d, the entry in the first bin is positive. This behaviour is close to the one of jet cross sections, which are meaningless unless the "jet cut", being effectively an external mass scale, is large enough.

In Figs. 32 and 33 we have also included the distributions from the corresponding $\gamma^* g \to Q\overline{Q}$ matrix element. We have a fairly good agreement for $p_T \gtrsim 2m$. For small $p_T$, the distributions for small bin sizes look very different, and the results from the fragmentation function approach overshoot those from the $\gamma^* g \to Q\overline{Q}$ matrix element considerably. For a larger bin size, the results in the charm quark cases are compatible, owing to the subtractions at $p_T = 0$. The differences remain however for bottom-quark production in the target fragmentation region at small transverse momenta.

It is also instructive to have a look at the momentum and angular distributions in the variables $P_Q$ (Fig. 34) and $v$ (Fig. 35), respectively. For $p_T > p_{T,\min}$, the momentum distributions for the fragmentation function approach and for the $\gamma^* g \to Q\overline{Q}$ matrix element agree well, as is expected. They are very different for $p_T \leq p_{T,\min}$: the fragmentation function approach yields larger cross sections for small $P_Q$, but, for E665 and NA47, it falls off more rapidly at large $P_Q$. The distribution in $v$, being directly related to the distribution in pseudorapidity

$$\eta = \frac{1}{2} \ln \frac{1-v}{v}, \tag{72}$$

is everywhere finite, albeit strongly peaked in the current fragmentation region ($v \to 0$) and, for HERA, in the target fragmentation region ($v \to 1$) as well.

[42] Please note that $p_T^c = 0$ stands for the parton configuration where the observed heavy quark is produced in the current direction, with a second parton collinear to the observed heavy quark, possibly emitted from the heavy quark's parent parton.

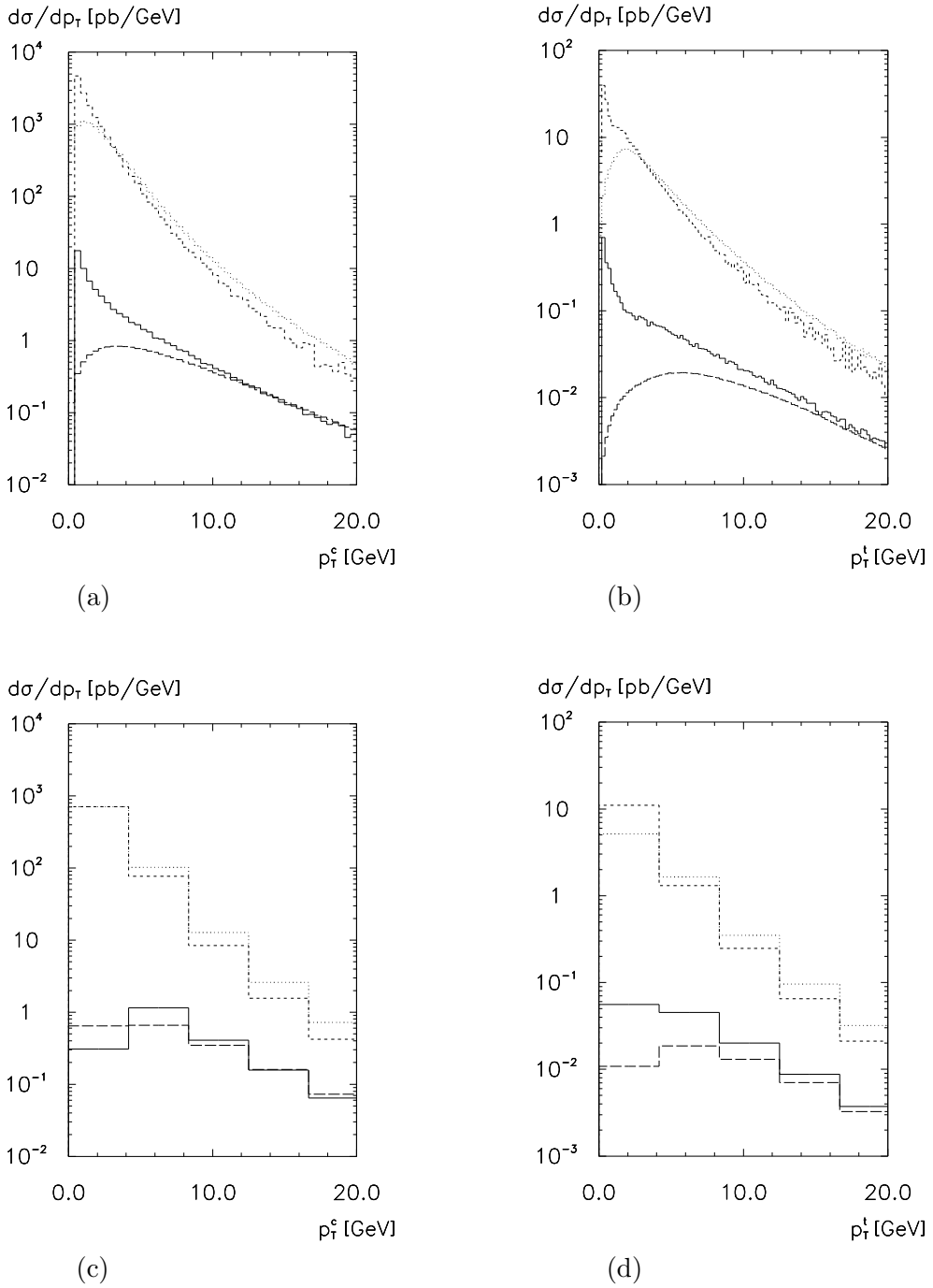


Figure 32: *Distributions in the transverse momentum $p_T$ in the current (a), (c) and target (b), (d) fragmentation regions for bottom (——) and charm (– – –) quark production at HERA for two different bin widths. Also shown are the distributions from the matrix element $\gamma^* g \to Q\overline{Q}$: bottom (— —) and charm (· · ·).*

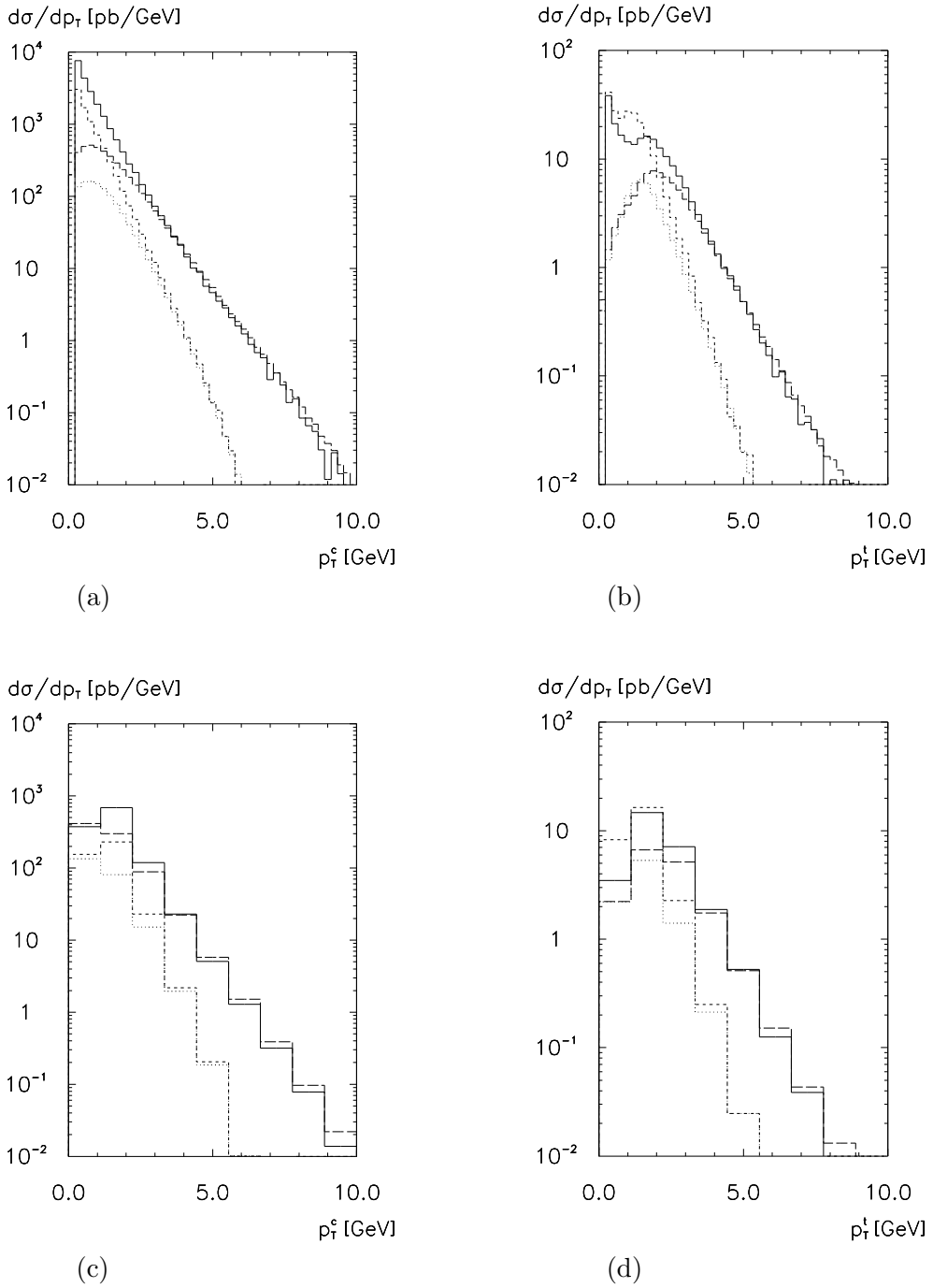


Figure 33: *Distributions in the transverse momentum $p_T$ in the current (a), (c) and target (b), (d) fragmentation regions for charm-quark production at E665 (——) and NA47 (– – –) for two different bin widths. Also shown are the distributions from the matrix element $\gamma^* g \to c\bar{c}$: E665 (— —), NA47 (· · ·).*

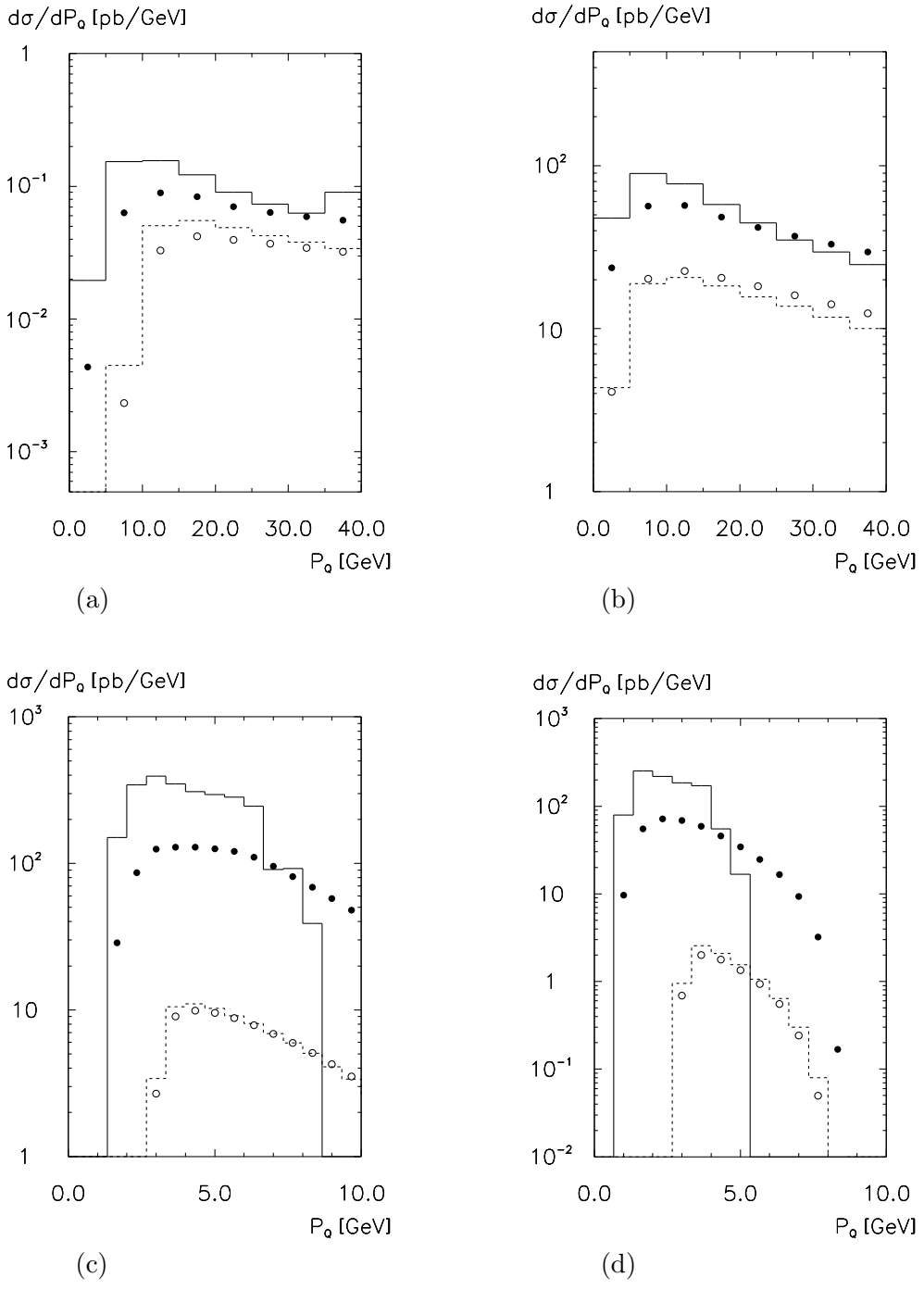


Figure 34: *Distributions in the momentum $P_Q$ of the heavy quark for bottom (a) and charm (b) quark production at HERA and for charm-quark production at E665 (c) and NA47 (d) up to $\mathcal{O}(\alpha_s)$, for $p_T \leq p_{T,\min}$ ( —— ) and $p_T > p_{T,\min}$ ( - - - ). Also shown is the distribution from the matrix element $\gamma^* g \to Q\overline{Q}$ for $p_T \leq p_{T,\min}$ ( • ) and $p_T > p_{T,\min}$ ( ∘ ). The definition of $p_{T,\min}$ is given in Section 6.4.*

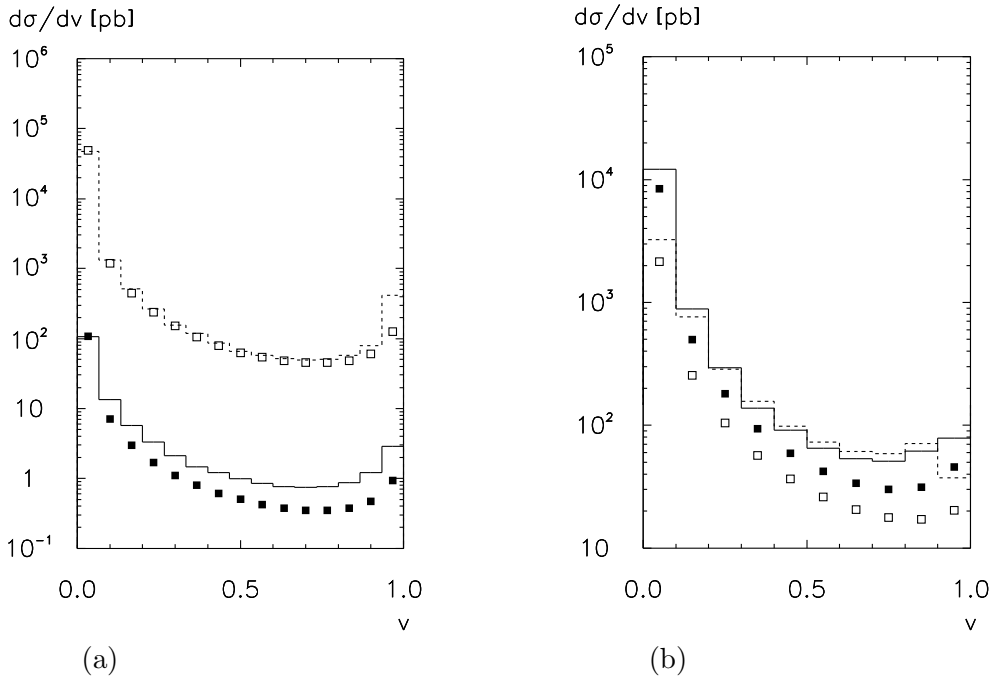


Figure 35: *Distributions in the angular variable $v$ of the heavy quark for bottom ( —— ) and charm ( – – – ) quark production at HERA (a) and for charm-quark production at E665 ( —— ) and NA47 ( – – – ) (b) in next-to-leading order. The distributions from the $\mathcal{O}(\alpha_s)$ matrix element $\gamma^* g \to Q\overline{Q}$ are: bottom ( ■ ) and charm ( □ ) quark production at HERA (a) and charm-quark production at E665 ( ■ ) and NA47 ( □ ) (b).*

### 6.6 Distributions in $x_F$ and $z_\parallel$

Differential distributions in leading and next-to-leading order for the variable $x_F$ are shown in Fig. 36. In the leading-order case, the distributions may have a dip at small values of $|x_F|$, due to the lower cut-off on the energy fraction of the observed particle. This dip disappears in next-to-leading order, where it is filled by events where the heavy quark is produced at large transverse momentum with only a small longitudinal momentum component. The shape of the distribution changes drastically for $x_F > 0$ when going from leading to next-to-leading order, in the cases where the QCD corrections are large. This effect has its origin in the fact that heavy quarks are produced copiously via photon–gluon fusion, which in our notation is next-to-leading order. Since the event topology is completely different from that in leading order, it is expected that the distributions look different[43]. Also shown in Fig. 36 is the distribution for the $\gamma^* g \to Q\overline{Q}$ matrix element. Qualitatively, it is closer to the result from the fragmentation function approach in next-to-leading order than to the one in leading order. Quantitatively, mainly in the current fragmentation region, there are however large differences. A comparison for the regions of small and large transverse momenta is shown in Fig. 37. We note that the shapes of the distributions in the target fragmentation region are comparable for $x_F \lesssim 0.2$. For $p_T > p_{T,\min}$, the results from the fragmentation function approach and from the $\gamma^* g \to Q\overline{Q}$ matrix element agree very well.

The distributions for the variable $z_\parallel$ are shown in Figs. 38 and 39 for $z_\parallel \geq 0$ and $z_\parallel < 0$, respectively, and split according to $p_T \leq p_{T,\min}$ and $p_T > p_{T,\min}$. The pattern follows the one already encountered in the case of the $x_F$-distributions. For $p_T > p_{T,\min}$, there is reasonable agreement between the fragmentation function approach and the $\gamma^* g \to Q\overline{Q}$ matrix element. For $p_T \leq p_{T,\min}$, in the region $z_\parallel < 0$, the shapes corresponding to the two approaches are comparable, although the fragmentation function approach leads to considerably larger cross sections. For $p_T \leq p_{T,\min}$ and $z_\parallel \geq 0$ neither the shapes nor the absolute sizes compare well. We wish to remark that the dip in the $z_\parallel$-distribution for $p_T \leq p_{T,\min}$ for bottom-quark production at HERA comes from the requirement that the observed heavy quark has to carry a minimum momentum fraction.

We now turn to the case of intrinsic heavy quarks. In Section 5.3 we have introduced a model for the non-perturbative piece of the target fragmentation functions based on the hypothesis of intrinsic heavy quarks in the proton. We set the parton densities to $f = f^{(\mathrm{GRV})} + f^{(\mathrm{IHQ})}$, where $f = f^{(\mathrm{GRV})}$ is the parton density parametrization by Glück, Reya and Vogt[44], and the target fragmentation functions to $M = M^{(P)} + M^{(\mathrm{IHQ})}$. In principle, the parton densities $f^{(\mathrm{IHQ})}$ contribute also to the perturbative heavy-quark target fragmentation functions $M^{(P)}$. We neglect this contribution here.

Figure 40 shows a comparison of the $x_F$-distribution of the produced heavy quark in next-to-leading order without and with intrinsic heavy quarks. As is expected from the hardness of the corresponding heavy-quark target fragmentation functions in the momentum-fraction variable of the observed heavy quarks, the distributions including intrinsic heavy quarks extend to larger negative values of $x_F$ than those without intrinsic heavy quarks. For $x_F < 0.2$ they are, in the cases studied here, always dominant. These results should, however, be interpreted carefully. First of all, the distribution that we used as input in the scale evolution is only a rough approximation, where mass effects have been neglected. Moreover, intrinsic heavy quarks

[43] We note that for E665 and NA47 the entry in the bin containing $x_F = 1$ is negative. This is due to the collinear subtraction, and could in principle be controlled by adjusting the bin size accordingly. Since we are mainly interested in the target fragmentation region, this problem shall not concern us here.

[44] In principle, the sum violates various sum rules, taken into account as constraints in the GRV fit. Since the intrinsic heavy-quark content is small, this violation may be safely neglected here.

are a non-perturbative phenomenon, and it is not clear how they fragment if the proton is hit by a high-$Q^2$ probe when neither the heavy quark nor the heavy antiquark participate in the hard scattering process. It is possible that the $Q\overline{Q}$-pair, being a quantum fluctuation of the $|uud\rangle$ state, simply recombines, in the cases where a light quark or a gluon initiates the hard scattering process. The results shown here are based on the naive assumption that every intrinsic heavy quark in the proton Fock state $|uudQ\overline{Q}\rangle$ is seen in the final state. It is beyond the scope of the present study to consider this complicated non-perturbative problem. It would, however, be very interesting to analyse this aspect of experimental data, in order to see whether there is any excess with respect to the perturbative contribution.

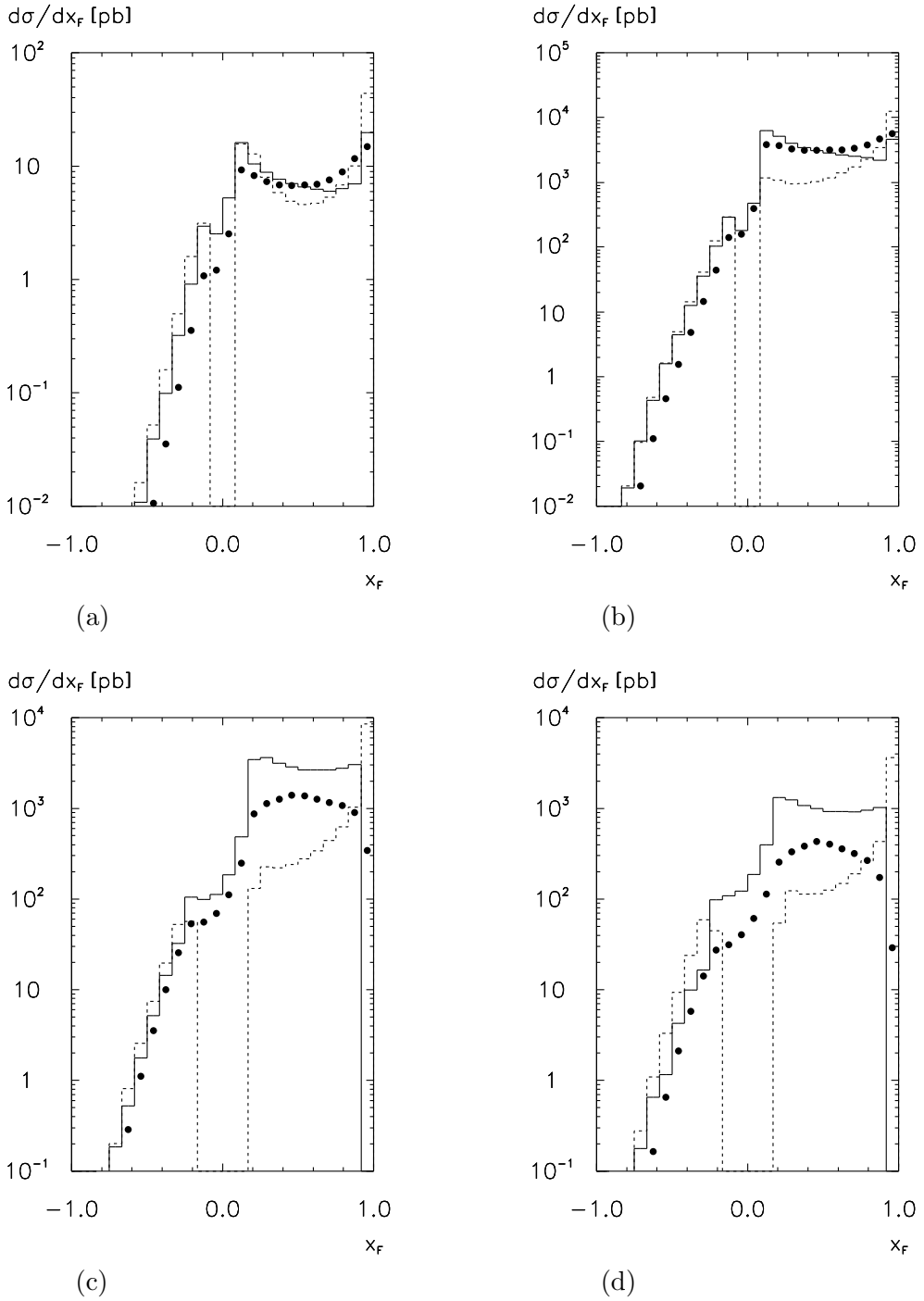


Figure 36: *Distributions in $x_F$ for bottom (a) and charm (b) quark production at HERA and for charm-quark production at E665 (c) and NA47 (d), in leading order (– – –) and in next-to-leading order (——). Also shown is the distribution from the matrix element $\gamma^* g \to Q\overline{Q}$ (•).*

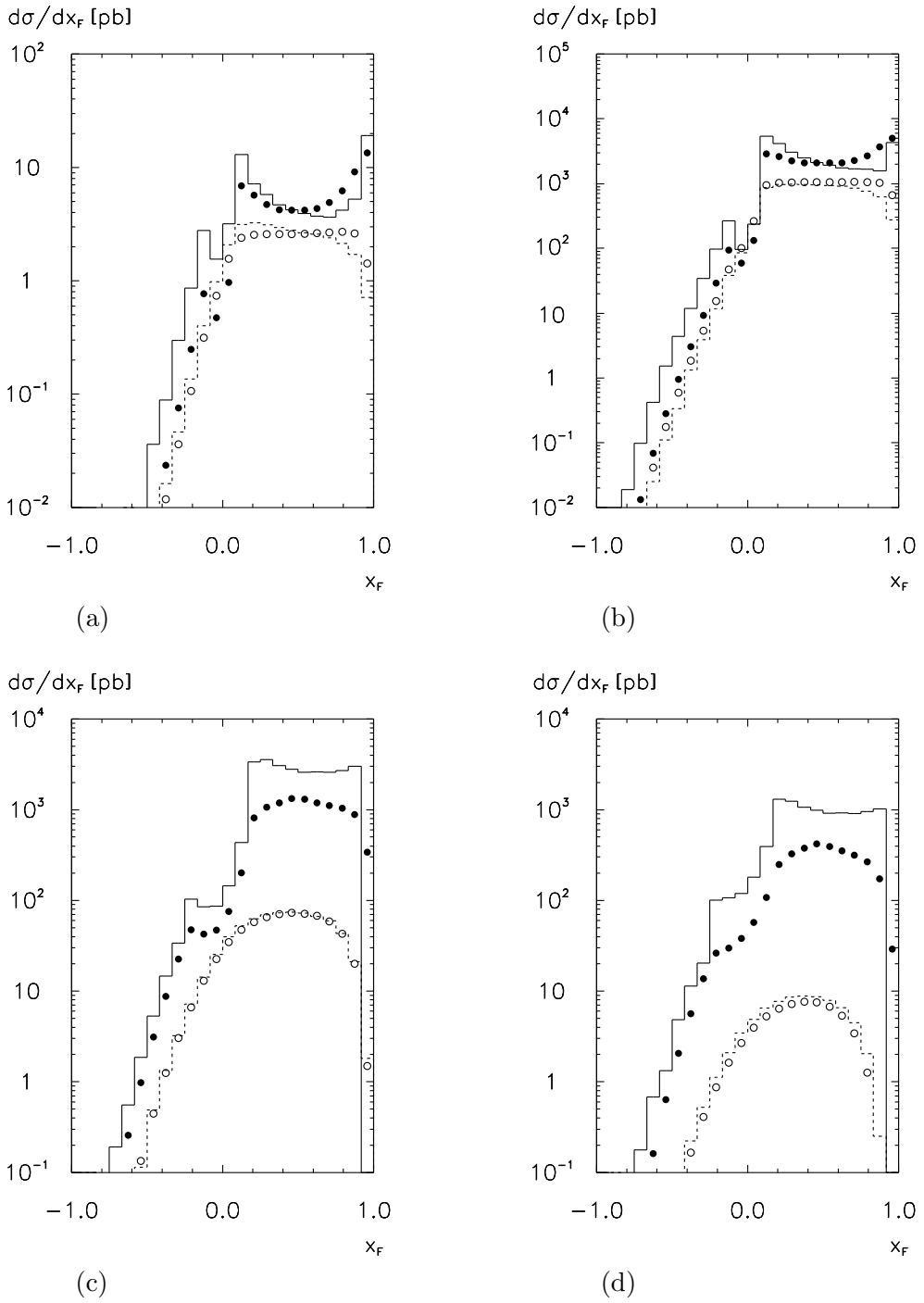


Figure 37: *Distributions in $x_F$ for bottom (a) and charm (b) quark production at HERA and for charm-quark production at E665 (c) and NA47 (d) up to $\mathcal{O}(\alpha_s)$, for $p_T \leq p_{T,\min}$ ( —— ) and $p_T > p_{T,\min}$ ( – – – ). Also shown is the distribution from the matrix element $\gamma^* g \to Q\overline{Q}$ for $p_T \leq p_{T,\min}$ ( • ) and $p_T > p_{T,\min}$ ( ∘ ). The definition of $p_{T,\min}$ is given in Section 6.4.*

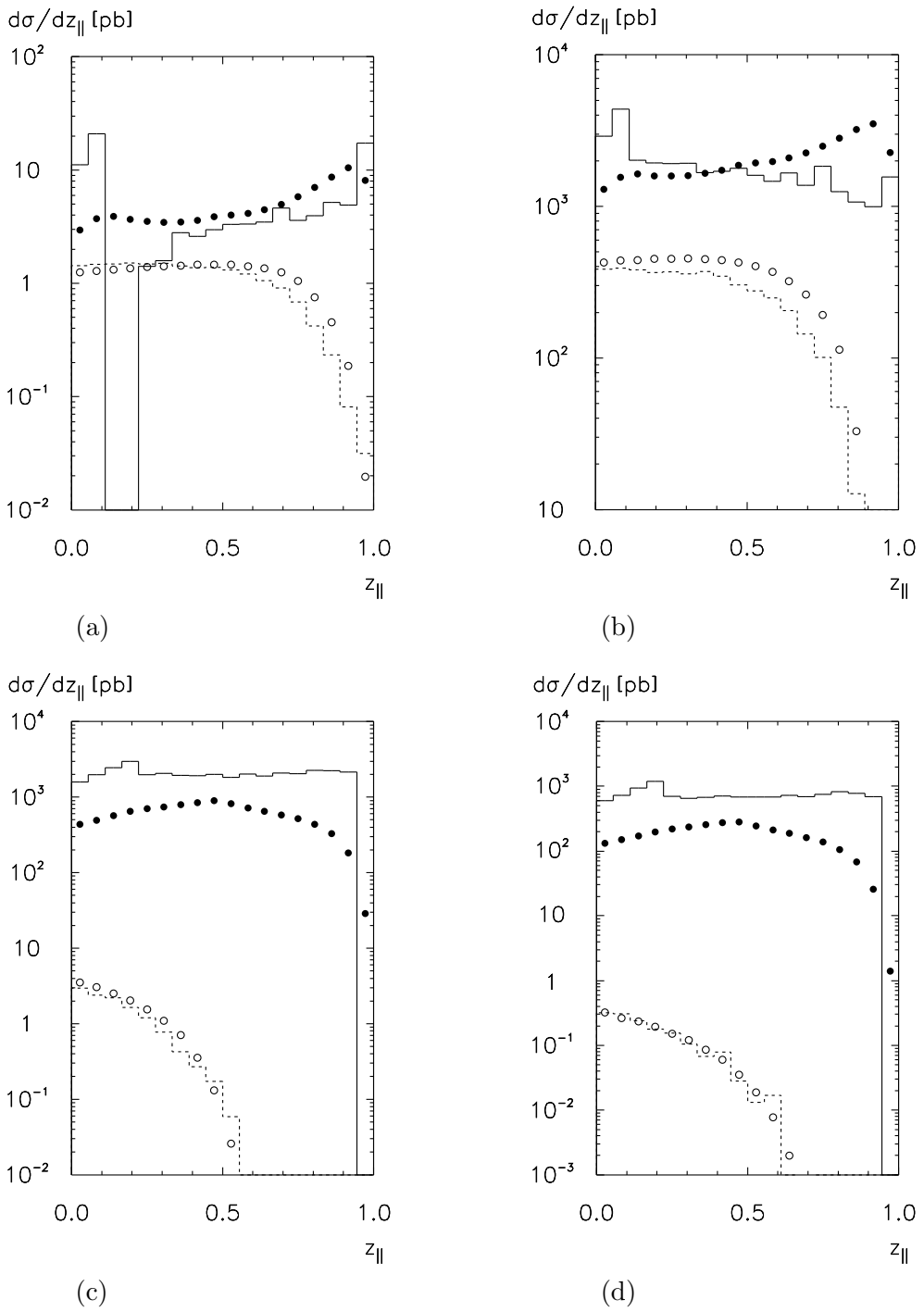


Figure 38: *Distributions in $z_\parallel$ for bottom (a) and charm (b) quark production at HERA and for charm-quark production at E665 (c) and NA47 (d) for $z_\parallel \geq 0$ up to $\mathcal{O}(\alpha_s)$, for $p_T \leq p_{T,\min}$ ( —— ) and $p_T > p_{T,\min}$ ( – – – ). Also shown is the distribution from the matrix element $\gamma^* g \to Q\overline{Q}$ for $p_T \leq p_{T,\min}$ ( • ) and $p_T > p_{T,\min}$ ( ∘ ). The definition of $p_{T,\min}$ is given in Section 6.4.*

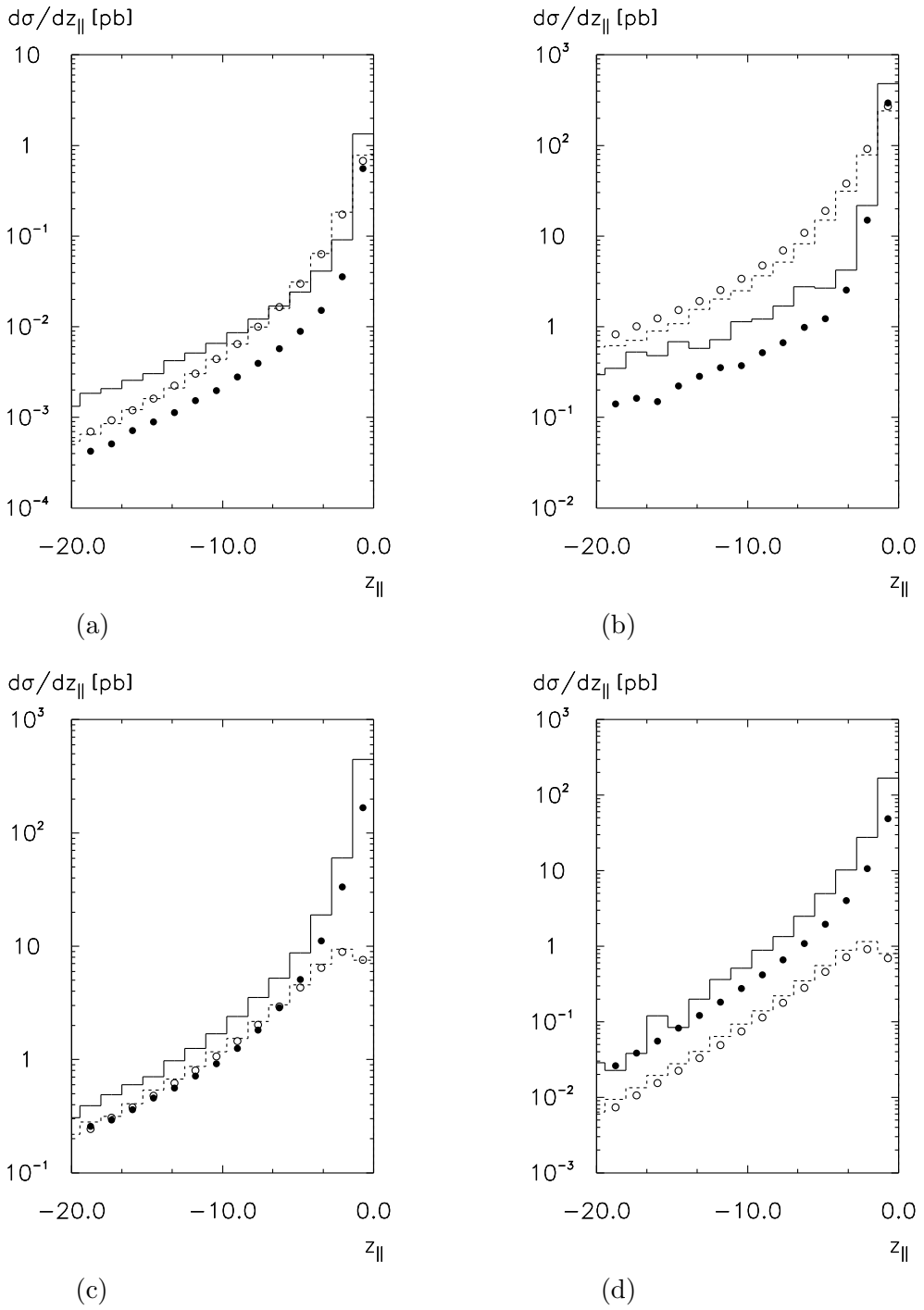


Figure 39: *Distributions in $z_\parallel$ for bottom (a) and charm (b) quark production at HERA and for charm-quark production at E665 (c) and NA47 (d) for $z_\parallel < 0$ up to $\mathcal{O}(\alpha_s)$, for $p_T \le p_{T,\min}$ (——) and $p_T > p_{T,\min}$ (– – –). Also shown is the distribution from the matrix element $\gamma^* g \to Q\overline{Q}$ for $p_T \le p_{T,\min}$ ( • ) and $p_T > p_{T,\min}$ ( ∘ ). The definition of $p_{T,\min}$ is given in Section 6.4.*

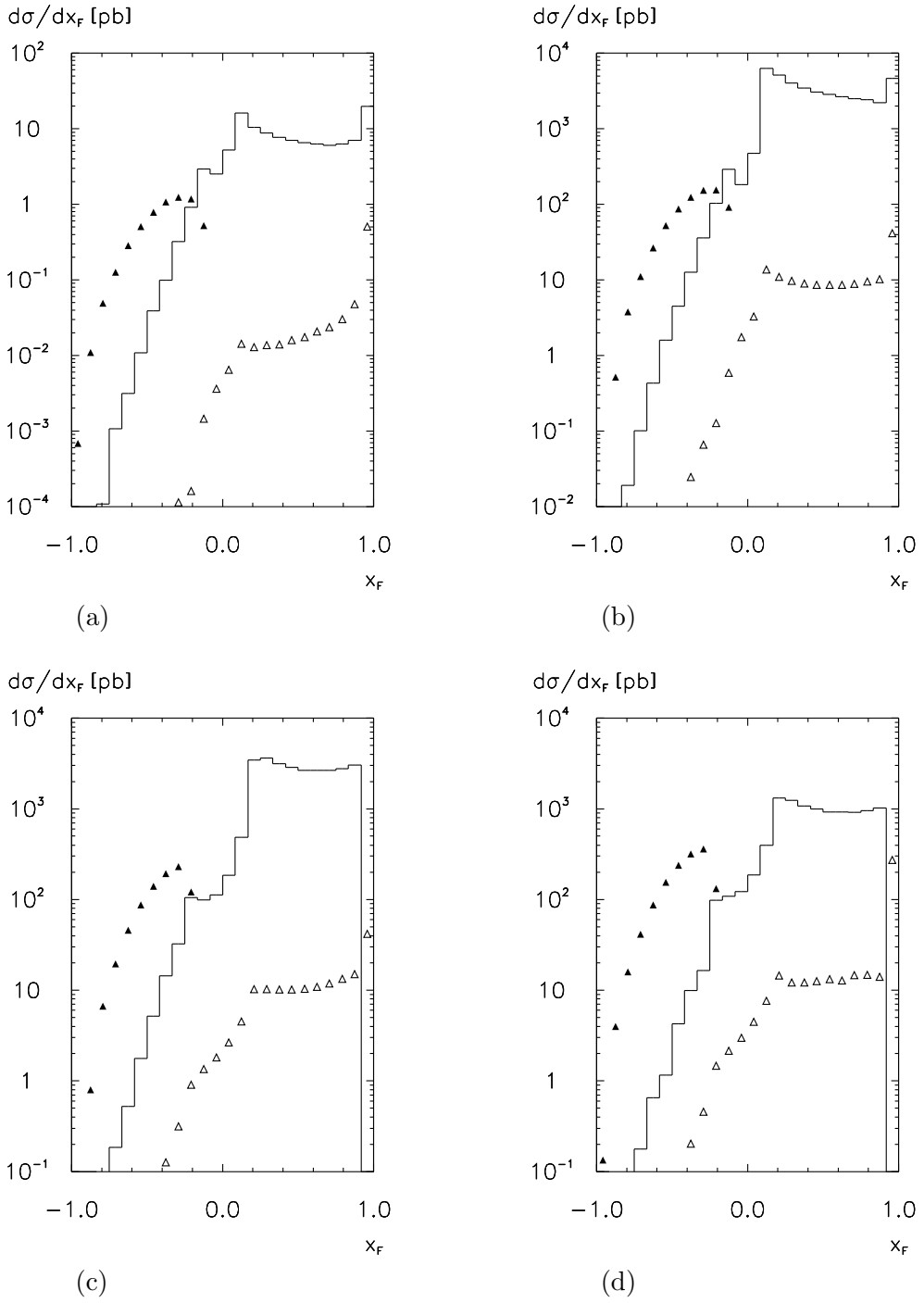


Figure 40: *Distributions in $x_F$ for bottom (a) and charm (b) quark production at HERA and for charm-quark production at E665 (c) and NA47 (d) in next-to-leading order. Contributions without ( —— ) and with intrinsic heavy quarks from $\sigma_M^{(\mathrm{IHQ})}$ ( ▲ ) and $\sigma_{fD}^{(\mathrm{IHQ})}$ ( △ ). The three histograms have to be added up to give the total differential production cross section.*

## 6.7 Factorization- and Renormalization-Scale Dependence

In this section we study the factorization and renormalization-scale dependence of the cross sections. In general, leading-order cross sections strongly depend on the factorization and renormalization scales, because the distribution functions and coupling constants are themselves scale-dependent, whereas the lowest-order parton-level scattering cross sections, excluding the coupling constants, are scale-independent. This situation is improved in higher orders, where compensating terms arise in the mass-factorized and renormalized parton-level scattering cross sections, giving an overall reduction of the sensitivity to scale variations.

In our case, the leading-order cross section is of $\mathcal{O}(\alpha_s^0)$, and thus independent of the strong coupling constant, and therefore renormalization-scale independent. To compensate for the renormalization-scale dependence of the next-to-leading order, contributions of the next-to-next-to-leading order would have to be incorporated, which we have not done.

Regarding the factorization scales, the situation looks better. We have three factorization scales, namely $\mu_f$, $\mu_D$ and $\mu_M$, for parton densities, fragmentation functions and target fragmentation functions, respectively. A look at the explicit expressions for the cross sections in Appendix C.1 shows that compensating terms in the form of a product of the Born cross section, a splitting function and a logarithm of the factorization scale are present; a variation in the leading-order cross section from a scale variation of the distribution functions is thus compensated to first order in the coupling constant. The remaining scale variation is due to higher-order variations of the distribution functions, i.e. their resummation, and due to the genuine scale variation of the next-to-leading-order cross section, excluding the compensating terms.

We now study the various scale dependences for the production of bottom and charm quarks at HERA, E665 and NA47 numerically, by varying the factorization scales $\mu_f$, $\mu_D$, $\mu_M$ and the renormalization scale $\mu_r$ as $\rho Q$, where $\rho$ is a parameter between 0.5 and 2[45]. In order to stay away from very small scales, we moreover require the scales to be larger than 1.5 GeV. The choice of $p_T$ as a factorization scale is not possible in the case under study, as we are interested in particular in the limit $p_T \to 0$. We discuss the case of bottom-quark production at HERA in detail, cf. Figs. 41a and b, by studying the scale dependence separately in the current and target fragmentation regions.

In the current fragmentation region, the dependence on $\mu_f$ and $\mu_D$ is large in leading order, and is reduced substantially in next-to-leading order. Please note that the renormalization-scale dependence is fairly small, although it is not compensated from a higher order term. This is due to the fact that the $\mu_r$-dependent matrix element itself is of $\mathcal{O}(\alpha_s)$, and the cross section is dominated by the renormalization-scale independent $\mathcal{O}(\alpha_s^0)$-term.

In the target fragmentation region, the leading-order term depends only on $\mu_f$, and varies by about a factor of two in the range of $\rho$ under consideration. This situation is considerably improved in next-to-leading order, where the cross-section variation due to a variation of $\mu_M$ is only about $\pm 5\%$. The dependence on $\mu_f$, $\mu_D$ and $\mu_r$ in the target fragmentation region is not compensated in next-to-leading order, because the leading order does not depend on any of these scales. Again, the dependence on these scales is small, because the next-to-leading-order correction is small, cf. Table 2. We have also studied the case when either $\sigma_M$ or $\sigma_{fD}$ in $\mathcal{O}(\alpha_s)$ is not included. We then obtain a large variation when varying $\mu_M$. This shows that both terms, corresponding to the homogeneous and inhomogeneous evolution contributions, are equally important to partially cancel the $\mu_M$-dependence.

[45] (This is a footnote, not an exponent.) The curves do not always cross at $\rho = 1$ due to small shifts from the interpolation and smoothing of the Monte Carlo results.

The scale dependence for charm-quark production at HERA, E665 and NA47 is shown in Figs. 41c, d and Fig. 42. We do not repeat the detailed discussion just given for bottom-quark production, and simply note that the results follow a similar pattern. We want to mention, however, that the scale compensation in the case of charm-quark production apparently does not work for the scale $\mu_D$ in the current fragmentation region. This is however due to the fact that the scale variation in leading order is particularly small. We have checked that the variation in next-to-leading order is much smaller if only the compensating terms, i.e. those consisting of a product of the leading-order cross section, a splitting function and a logarithm containing $\mu_D$, are included.

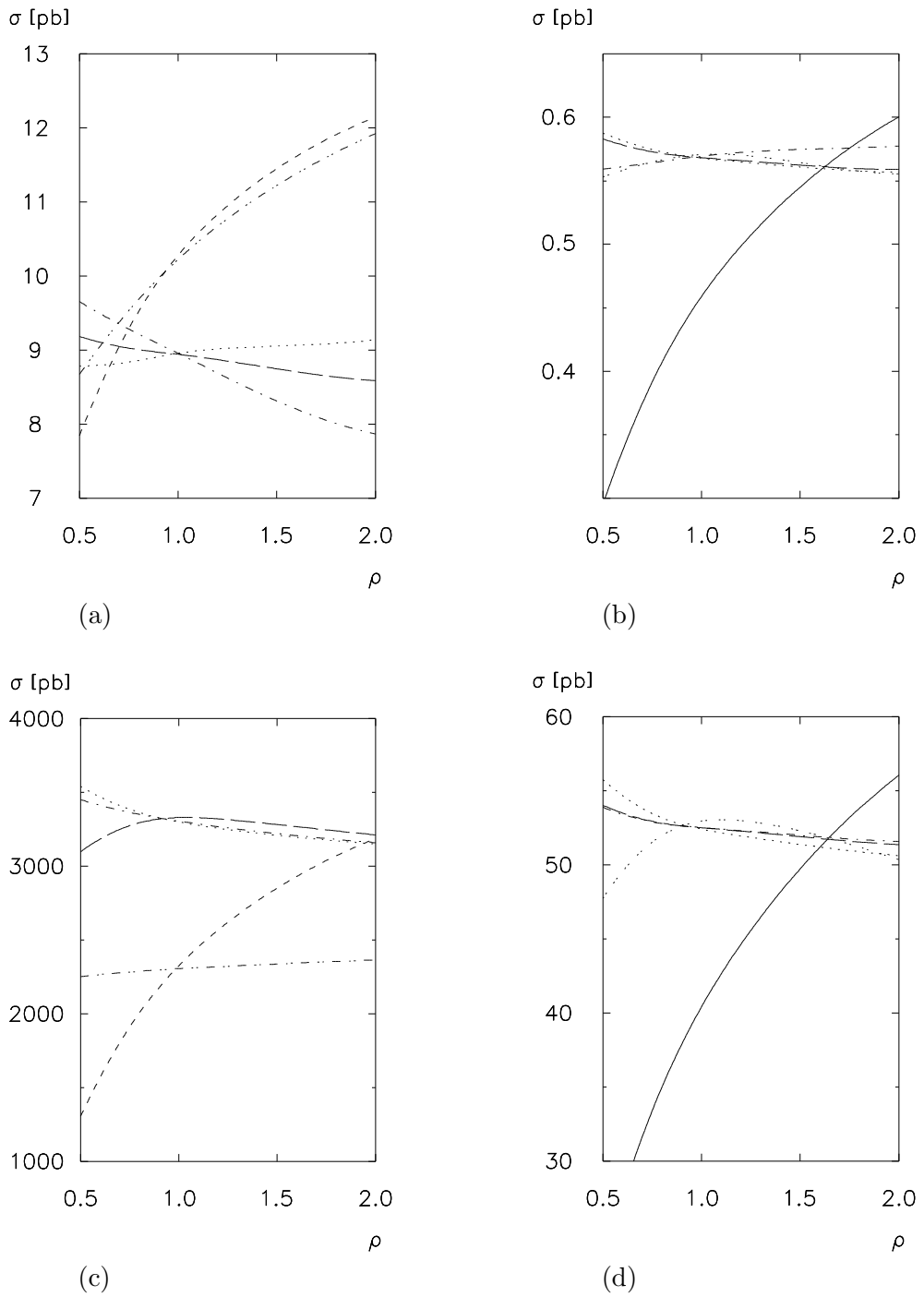


Figure 41: *Scale dependence for bottom (a), (b) and charm (c), (d) quark production at HERA in the current (a), (c) and target (b), (d) fragmentation regions. The particular scale set to $\rho Q$ is given by $\mu_f$ (– – –), $\mu_D$ (– ··), $\mu_M$ (——) in leading order and $\mu_r$ (· · ·), $\mu_f$ (— —), $\mu_D$ (– · –), $\mu_M$ (·· ··) in next-to-leading order; the other scales are fixed to be equal to $Q$.*

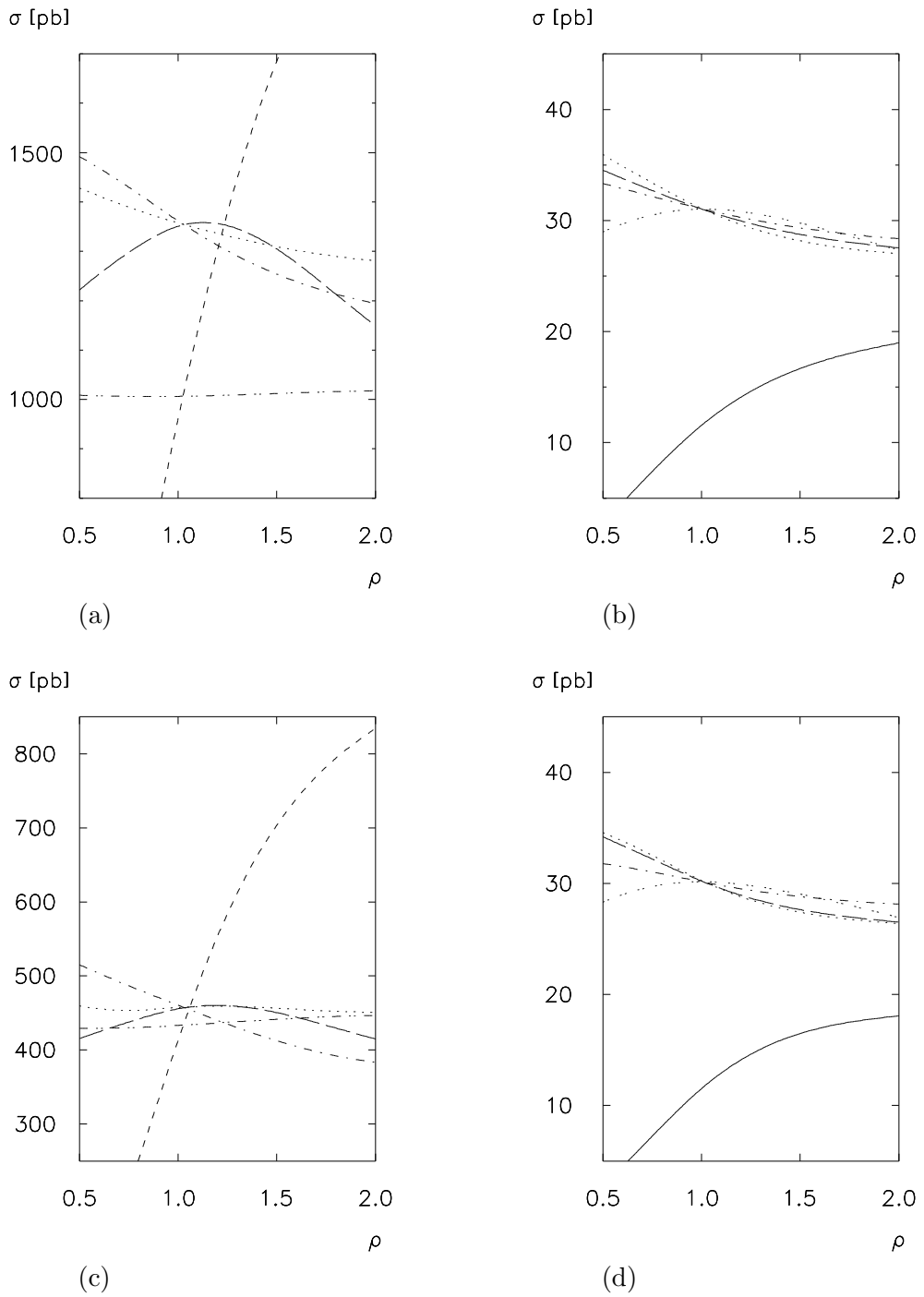


Figure 42: *Scale dependence for charm-quark production at E665 (a), (b) and NA47 (c), (d) in the current (a), (c) and target (b), (d) fragmentation regions. The particular scale set to $\rho Q$ is given by $\mu_f$ (– – –), $\mu_D$ (– ··), $\mu_M$ (——) in leading order and $\mu_r$ (· · ·), $\mu_f$ (— —), $\mu_D$ (– · –), $\mu_M$ (·· ··) in next-to-leading order; the other scales are fixed to be equal to $Q$.*

# 7 Summary, Open Problems and Conclusions

## 7.1 Summary

We have presented a formalism to describe the production of particles in the target fragmentation region of deeply inelastic lepton–nucleon scattering in the framework of perturbative QCD. An explicit one-loop calculation shows the necessity to introduce new phenomenological distribution functions, the target fragmentation functions or "fracture functions" [77]. Their renormalization group equation is inhomogeneous owing to a source term that describes the "perturbative production" of particles in the backward direction. It is shown that, to one-loop, all collinear singularities can be consistently absorbed into renormalized distribution functions. This is also true of a new singularity, which does not appear in the case when the observed particle is produced strictly in the current fragmentation region or, at finite $p_T$, in the target fragmentation region. It is conjectured that this mechanism works to all orders in perturbation theory. The finite cross section is a convolution of a mass-factorized parton-level scattering cross section with parton densities, fragmentation functions and target fragmentation functions.

The formalism has been applied in the case of the production of heavy quarks. The renormalization group equations for heavy-quark fragmentation functions, perturbative heavy-quark target fragmentation functions and target fragmentation functions for an intrinsic heavy-quark content of the proton have been solved numerically. In a case study of deeply inelastic lepton–nucleon scattering, we have investigated in detail the production of bottom and charm quarks at HERA, E665 and NA47. Cross sections have been presented for various phase-space regions of the produced heavy quark. Restricting the phase space to the target fragmentation region, it has been shown that the perturbative piece from the evolution of the target fragmentation functions contributes significantly.

Using the example of $p_T$-distributions, we have demonstrated how the subtraction process in the singular phase-space regions works in practice. From a theoretical point of view, the calculated cross sections are finite; all divergences are being absorbed into renormalized parton densities, fragmentation functions and target fragmentation functions. The finite differential cross section in $p_T$ is, however, a distribution (in the mathematical sense), with a singularity at $p_T = 0$. Therefore it has to be integrated over a certain region around $p_T = 0$ in order to give rise to a well-defined numerical prediction. For realistic parameters, reasonable numerical results for heavy-quark production cross sections in the target fragmentation region can be obtained. It should be stressed that the results discussed here only include the perturbative part of the target fragmentation functions, obtained by the corresponding inhomogeneous renormalization group equation with a specific boundary condition at a small input scale, and a non-perturbative part based on a model assumption assuming intrinsic heavy quarks in the proton. The true non-perturbative piece of these functions, which are in principle process-independent, must be obtained from experiment.

The shape of the $x_F$-distributions in the current fragmentation region is modified considerably if next-to-leading-order contributions are included, whereas the shape in the target fragmentation region is stable. In particular in the case of charm-quark production, the next-to-leading-order corrections for $x_F \geq 0$ are large.

We have also studied $x_F$-distributions for a model based on the hypothesis of intrinsic heavy quarks in the proton. According to Refs. [38, 39], the heavy quarks $Q$, $\overline{Q}$ from a Fock space component $|uudQ\overline{Q}\rangle$ of the proton should carry a large momentum fraction. If the proton is hit by a large-$Q^2$ probe, these heavy quarks may fragment in the target fragmentation region, even if they themselves do not participate in the hard scattering subprocess. As expected, the $x_F$-distribution in the target fragmentation region is much more pronounced and extends to larger

negative values of $x_F$ if the intrinsic component is included, compared with the case where the heavy quark is produced via the hard matrix element or by evolution of the perturbative target fragmentation function.

The factorization-scale dependence follows the expected pattern, namely that compensating terms lead to a smaller overall scale dependence in next-to-leading order. The dependence on the factorization scales $\mu_f$ and $\mu_D$ in the current fragmentation region and on $\mu_M$ in the target fragmentation region is reduced in next-to-leading order, as expected, with the exception of the $\mu_D$-dependence in the cases of E665 and NA47, due to a very small $\mu_D$-dependence in leading order. Since in leading order the process under consideration does not depend on the strong coupling constant, the renormalization-scale dependence arises first in next-to-leading order, and would be compensated only by contributions in next-to-next-to-leading order.

We add a short remark on the possibility to observe the heavy quarks in the target fragmentation region of an actual experiment. In Ref. [11] it is assumed that the acceptance for a $D^0$ meson is about 0.4. Assuming that about half of all produced charm quarks fragment into a $D^0$, and using the branching ratio of about 4% of the decay $D^0 \to K^-\pi^+$, we arrive at an overall probability of 0.8% that a produced charm quark will be detected. Assuming the same value in the target fragmentation region[46] as well, the total number of reconstructed charm-quark events in the target fragmentation region of the HMC experiment, based on an integrated luminosity of 1500 pb$^{-1}$, will be 360. This is probably not enough to attempt a fit of target fragmentation functions, but it shows that a similar study in photoproduction[47], where the expected charm-quark production cross section would be expected to be much higher, may well be feasible.

In order to study the mechanism for particle production in the target fragmentation region, as discussed in this paper, the production of mesons not containing heavy valence quarks, such as $\pi^+$, $\pi^-$ and $\pi^0$, could also be considered; there, the cross sections are expected to be larger. In this case, the perturbative piece of the target fragmentation function can be obtained by using experimentally determined pion fragmentation functions, as recently given, for instance, in Ref. [134].

## 7.2 Restrictions of the Approach

For the case of regular fragmentation functions, the finite cross section is a distribution in the angular variable $v$. If the fragmentation functions themselves are singular, as in the case of heavy-quark fragmentation functions, then there is an additional subtraction related to the energy-fraction variable $z$. In any case, in next-to-leading order, there are subtractions at small transverse momenta $p_T$, which means that a meaningful prediction can be made only for the integral of the differential cross section $\mathrm{d}\sigma/\mathrm{d}p_T$ over $p_T$ from 0 to some $p_{T,\max}$, where $p_{T,\max}$ is not allowed to be small. This certainly limits the range of applicability of the presented results. This particular restriction is, however, already present in the standard formulation for the current fragmentation region.

The approach is formulated in terms of fragmentation functions and therefore incorporates leading twist effects only. Similarly, it cannot be expected that non-perturbative leading-particle effects can be described.

[46] In the target fragmentation region, leading particle effects are expected, and the fragmentation of, for example, a charm quark into a $D^0$ meson will take place with a different probability from that in the current fragmentation region. See also Ref. [128].

[47] Up to now, experimental studies in photoproduction are available in the current fragmentation region only, see for instance Refs. [129–133]. We note that, for the resolved contribution in the current fragmentation region, the target fragmentation functions for real photons have to be introduced.

The case study for heavy-quark production in deeply inelastic scattering had to be restricted to the perturbative contributions and to a model for intrinsic heavy quarks in the proton, because the non-perturbative piece $M^{(NP)}$ of the heavy-quark target fragmentation functions is not yet known. A limitation of the numerical investigation is that we have used the target fragmentation functions in the leading-logarithmic approximation only. To have a consistent renormalization-group-improved next-to-leading-order prediction, the target fragmentation functions should be evolved with next-to-leading-logarithmic accuracy.

## 7.3 Open Problems

The question of extended factorization of the form conjectured in Eq. (55) is a central issue related to the problem of universality of target fragmentation functions. In Ref. [135] it is shown in the framework of an explicit toy model for the case of *diffractive* hadron–hadron scattering that factorization breaks down when there are *two* strongly interacting particles in the initial state, due to the exchange of soft gluons in the final state. This cannot happen for the case of deeply inelastic lepton–nucleon scattering. The process considered in Ref. [135] is diffractive, so the target is essentially untouched. The toy model makes no prediction of what happens if the target nucleon fragments, as is required, for example, in the case of heavy-quark or meson production in the target fragmentation region.

The formalism developed in this paper may be applied to other processes as well, such as the photoproduction[48] of hadrons or heavy quarks in lepton–nucleon scattering, or one-particle-inclusive Drell–Yan-like processes, i.e. $pp \to \mu^+\mu^- hX$. Lepton–nucleon scattering is very interesting because it permits the direct measurement of the non-perturbative part $M^{(NP)}$ of the target fragmentation functions. Photoproduction is particularly attractive because of the large cross sections, but it introduces a large uncertainty due to the poorly constrained gluon content of the photon structure function.

We have considered the problem of the production of heavy quarks in the target fragmentation region, but we have not touched the problem of how these quarks eventually fragment into hadrons. The fragmentation into mesons containing a heavy quark may be treated by adding a convolution of the fragmentation function of a heavy quark into a meson [35] with the cross section for heavy-quark production as determined in this paper. However, it is to be expected that, in particular in the target fragmentation region, leading particle effects may play a rôle[49], although they should be of higher twist. The experimental study of the production of mesons containing heavy quarks in this region of phase space may shed some light on this issue.

As has been stressed in Section 7.2, the cross section, being a distribution in the phase-space variables of the observed heavy quark, is only well-defined if integrated over a certain phase-space region. This problem is related to a similar and familiar phenomenon in jet physics. There, only sufficiently inclusive infrared-safe quantities are physically meaningful, and the limit of small jet cuts leads to meaningless results. It is interesting, however, that in the present case of one-particle-inclusive processes the subtractions have to be done in terms of in principle *measurable* quantities such as the transverse momentum of the observed hadron, contrary to the case of jet physics, where the subtractions are done in terms of unobservable parton momenta. This problem deserves further study.

Two formulations of the theory of one-particle-inclusive processes go back to A.H. Mueller; one based on an analysis of Regge poles [137, 138][50], the other one related to the formalism of

[48] In diffractive photoproduction, the situation is different due to the hadronic component of the incident real photon, and the factorization assumption might not apply.

[49] See for example Ref. [136].

[50] For a review, see Ref. [139].

cut vertices [140–143]. The approach mentioned first is based on the crossing of the observed particle into the initial state with a subsequent application of the optical theorem and Regge phenomenology. The second approach can be formulated within perturbative QCD. There should be a possibility to relate the concept of target fragmentation functions to expectation values of operators corresponding to cut vertices.

For a complete next-to-leading-logarithmic calculation, the scale evolution equation (42) should be known in next-to-leading order. This would require the calculation of the splitting functions related to the inhomogeneous term on the two-loop level, in analogy to the corresponding calculation for parton densities and fragmentation functions [91, 144]. As long as the scales $\mu_e$, where target fragmentation functions are extracted from experimental data, and $\mu_p$, where they are used for predictions, are not too different, i.e. as long as $\alpha_s \ln(\mu_e^2/\mu_p^2)$ is small, the leading-order evolution equation should be sufficient.

## 7.4 Outlook

A measurement of the non-perturbative part $M^{(NP)}$ of the target fragmentation functions would be a new interesting test of QCD, since QCD predicts the scale evolution according to Eq. (42). Fixed-target experiments allow in principle a detector with a solid-angle coverage of $4\pi$ because of the strong forward boost and therefore permit measurements in the target fragmentation region; for a recent proposal, see Ref. [11, 12]. Because of their clean experimental signature, the tagging of charmed and strange mesons is particularly attractive.

Target fragmentation functions may also be applied in hard diffractive processes, e.g. in diffractive deeply inelastic electron–proton scattering, where the proton, either essentially untouched or excited, is the observed particle. In the Ingelman–Schlein picture [145, 146], the exchanged object with vacuum quantum numbers initiates the hard scattering process, and fragments. From experimental determinations of the structure functions of the exchanged object, it is possible to obtain explicit parametrizations for diffractive target fragmentation functions, cf. Ref. [147]. A similar concept has been developed in Ref. [148].

As mentioned in the introduction, an interesting possibility is that the tagging of certain particles in the target fragmentation region may reveal additional information about the hard scattering process. The tagging of, for example, a proton in the backward direction is expected to enhance the event sample of gluon-initiated events. Similar conclusions are possible for other tagged particles, see Ref. [77]. The possibility to constrain the hard scattering process may be helpful to measure the part of the spin of the proton that is carried by gluons and strange quarks [19]. For this application, however, the present study has to be generalized to the case of strange quarks in the polarized case. Since the strange-quark mass is too small to permit the calculation of perturbative heavy-quark fragmentation functions, one would have to go back to measured fragmentation functions of strange hadrons to obtain the perturbative target fragmentation functions.

## 7.5 Conclusions

It is possible to describe particle production in the current and target fragmentation regions in a unified way by an extension of the standard QCD formalism involving parton densities and fragmentation functions, as developed in this paper. From the theoretical side, the extended factorization conjecture remains to be proved, and the extension of the formalism to a true next-to-leading-logarithmic framework is to be done. Experimentally, in particular in the case of heavy-quark production, a rich phenomenology is waiting to be explored. It will be interesting to confront the theoretical ideas presented in this paper with actual experimental data.

## Acknowledgements

I wish to thank

— L. Trentadue and G. Veneziano, who invented the beautiful concept of target fragmentation functions, for numerous discussions,

— H. Joos, G. Kramer and P.M. Zerwas for helpful conversations,

— G. Altarelli for a discussion on Ref. [70],

— W. Buchmüller for a discussion about diffractive scattering,

— H. Heßling for some remarks related to the experimental aspects of the backward direction at HERA,

— E. Laenen for a discussion about heavy-quark production,

— O. Nachtmann for drawing my attention to Refs. [73, 74, 76],

— P. Nason for a discussion about heavy-quark fragmentation functions,

— D. Soper for a discussion about factorization in QCD,

— A. Vogt for some remarks regarding the heavy-quark content of the proton,

— the Theory Divisions of the Argonne National Laboratory, the Lawrence Berkeley National Laboratory and the Stanford Linear Accelerator Center for the warm hospitality extended to me during visits in the autumn of 1995, and E.L. Berger, S.J. Brodsky, M. Derrick, D. Geesaman, I. Hinchliffe, R. Vogt and A. White for valuable discussions about target fragmentation functions, heavy-quark production and diffractive physics,

— E. Gianolio, L. Lönnblad and R. Sommer for support related to UNIX, work stations and computing,

— the CERN computer centre, in particular E. McIntosh, B. Panzer–Steindel and H. Renshall, for technical support.

I am grateful to S.J. Brodsky, G. Kramer, H. Spiesberger, L. Trentadue and G. Veneziano for comments on the manuscript. The numerical calculations for this paper were done on the CERNSP and on the CERN CS2 cluster of the GPMIMD–2 ESPRIT project financed by the European Union. This work was supported in part by a Habilitandenstipendium from the Deutsche Forschungsgemeinschaft.

# A Distributions

In this section, the distributions used in the text are defined and some of their properties are exhibited. Attention is paid in particular to convolution formulae of distributions involving the "+" prescriptions and to expressions involving a variable transformation useful for the solution of the renormalization group equations.

## A.1 Definition of Singular Functions

Apart from the familiar $\delta$-function[51] defined by

$$\delta_c[\varphi] \doteq \int \mathrm{d}x\, \delta(x-c)\, \varphi(x) \doteq \varphi(c), \tag{73}$$

singular functions with "+" prescriptions appear frequently. They arise in Laurent expansions of the form

$$x^{-1-\epsilon} = \frac{\Gamma^2(1-\epsilon)}{\Gamma(1-2\epsilon)} \left[ -\frac{1}{\epsilon}\,\delta(x) + \left(\frac{1}{x}\right)_{+x[0,\underline{1}]} + \epsilon \left( -\left(\frac{\ln x}{x}\right)_{+x[0,\underline{1}]} - \frac{\pi^2}{6}\,\delta(x) \right) \right] + \mathcal{O}(\epsilon^2) \tag{74}$$

for $x \in [0,1]$, and they are defined by a subtraction via [149]

$$D_{+[a,b]c}[\varphi] \doteq \int_a^b \mathrm{d}x\, D(x)\, \left(\varphi(x) - \varphi(c)\right). \tag{75}$$

This subtraction is sufficient as long as the singularity of $D$ at $c$ is not worse than $\sim 1/x^{1+\rho}$, $\rho < 1$. For $\rho \geq 1$, higher orders in the Taylor expansion of $\varphi$ have to be subtracted:

$$D_{+[a,b]c,n}[\varphi] \doteq \int_a^b \mathrm{d}x\, D(x)\, \left(\varphi(x) - \varphi^{[n]}(c,x)\right), \tag{76}$$

where

$$\varphi^{[n]}(c,x) = \sum_{k=0}^{n} \frac{1}{k!}\, \partial^k \varphi(c) (x-c)^k \tag{77}$$

is the $n$-jet of $\varphi$ at $c$. For the rest of this section, we need only the case $n = 0$; however, in Appendix F.3 we will briefly discuss a situation with $n > 1$. For subtractions at the boundaries of the integration region we use the short-hand notation

$$\begin{aligned} D_{+[\underline{a},b]}[\varphi] &\doteq \int_a^b \mathrm{d}x\, D(x)\, \left(\varphi(x) - \varphi(a)\right), \\ D_{+[a,\underline{b}]}[\varphi] &\doteq \int_a^b \mathrm{d}x\, D(x)\, \left(\varphi(x) - \varphi(b)\right). \end{aligned} \tag{78}$$

If a function depends on several variables or is given in an explicit form, we include the variable relevant to the subtraction in the subscript as in $(1/x)_{+x[0,\underline{1}]}$.

The singular functions $D_+$ can be rewritten for a changed domain of their definition. To this end, we define the characteristic function $\chi_A$ for a set $A$ by

$$\chi_A(x) \doteq \begin{cases} 1, & \text{if} \quad x \in A \\ 0, & \text{else} \end{cases}. \tag{79}$$

[51] All relations discussed in this section may also be derived in a more rigorous mathematical framework, cf. Ref. [149].

Then, for $d \in [a,b]$,

$$\begin{aligned} D_{+[\underline{a},b]} &= D_{+[\underline{a},d]} + \chi_{[d,b]}\, D - \int_d^b \mathrm{d}x\, D(x)\, \delta_a, \\ D_{+[a,\underline{b}]} &= D_{+[d,\underline{b}]} + \chi_{[a,d]}\, D - \int_a^d \mathrm{d}x\, D(x)\, \delta_b. \end{aligned} \tag{80}$$

This leads for instance to the expressions

$$\begin{aligned} \left(\frac{1}{1-x}\right)_{+x[0,\underline{1}]} &= \left(\frac{1}{1-x}\right)_{+x[d,\underline{1}]} + \chi_{[0,d]}(x)\frac{1}{1-x} + \delta(1-x)\ln(1-d), \\ \left(\frac{\ln(1-x)}{1-x}\right)_{+x[0,\underline{1}]} &= \left(\frac{\ln(1-x)}{1-x}\right)_{+x[d,\underline{1}]} + \chi_{[0,d]}(x)\frac{\ln(1-x)}{1-x} \\ &\quad + \delta(1-x)\frac{1}{2}\ln^2(1-d). \end{aligned} \tag{81}$$

Similarly, a regular function $f$ can be written as a "+" distribution as

$$\begin{aligned} f(x)\,\chi_{[a,b]}(x) &= f_{+[\underline{a},b]}(x) + \delta(x-a)\int_a^b \mathrm{d}v\, f(v), \\ f(x)\,\chi_{[a,b]}(x) &= f_{+[a,\underline{b}]}(x) + \delta(b-x)\int_a^b \mathrm{d}v\, f(v). \end{aligned} \tag{82}$$

It turns out to be useful to perform a variable transformation $y = \ln(1/x)$ in order to express the scale evolution equation for fragmentation functions in terms of convolutions of Laguerre polynomials. This transformation has also advantages for the numerical evaluation of convolutions. More precisely, define the function $y \mapsto \tilde{f}(y)$ for a function $x \mapsto f(x)$ by

$$\tilde{f}(y) \doteq x f(x), \quad y = \ln\frac{1}{x}, \quad x = \mathrm{e}^{-y}. \tag{83}$$

If $x \in [0,1]$, then $y \in [0,\infty]$. We have to give a meaningful definition of the quantity $\tilde{D}$ in the case where $D$ is a distribution. In order to do so, we consider the convolution of the distributions $D$ and $\tilde{D}$ with the test functions $\varphi$ and $\tilde{\varphi}$, respectively, where $\tilde{\varphi}$ is defined by Eq. (83). The definition of the convolution "$\otimes$" is given in Appendix A.2, Eqs. (86) and (89). $(D \otimes \varphi)(x)$ and $\left(\tilde{D} \otimes \tilde{\varphi}\right)(y)$ are regular functions of $x$ and $y$, $(D \otimes \varphi)^{\sim}$ is well defined by Eq. (83), and we may require that

$$(D \otimes \varphi)^{\sim} = \tilde{D} \otimes \tilde{\varphi} \tag{84}$$

for any test function $\varphi$. An explicit calculation then shows that

$$\begin{aligned} \tilde{\delta}_1 &= \delta_0, \\ \left(D_{+[\xi,\underline{1}]}\right)^{\sim} &= \tilde{D}_{+[\underline{0},\ln(1/\xi)]}. \end{aligned} \tag{85}$$

## A.2 Convolution of Distributions

The convolution of two functions $f$, $g$ defined on $[0,1]$ is given by

$$(f \otimes g)(x) \doteq \int_x^1 \frac{\mathrm{d}u}{u}\, f(u)\, g\left(\frac{x}{u}\right). \tag{86}$$

This definition is also applicable in the case when $f$ is a distribution on $[0,1]$, by writing

$$\begin{aligned}(f\otimes g)(x) &= \int_0^1 \frac{\mathrm{d}u}{u}\, f(u)\,\chi_{[x,1]}(u)\, g\left(\frac{x}{u}\right)\\ &= f\left[u\mapsto \frac{1}{u}\,\chi_{[x,1]}(u)\, g\left(\frac{x}{u}\right)\right],\end{aligned} \tag{87}$$

and by interpreting the latter expression in terms of an application of a distribution to a test function. This simple prescription fails in the case of two distributions $f$ and $g$. It is, however, possible to give a well-defined meaning to $f\otimes g$ by applying it to a test function $\varphi$:

$$\begin{aligned}(f\otimes g)[\varphi] &= \int_0^1 \mathrm{d}x \int_x^1 \frac{\mathrm{d}u}{u}\, f(u)\, g\left(\frac{x}{u}\right)\,\varphi(x)\\ &= \int_0^1 \mathrm{d}u\, f(u) \int_0^1 \mathrm{d}w\, g(w)\,\varphi(uw).\end{aligned} \tag{88}$$

Now $f\otimes g$ is rewritten in terms of a twofold application of distributions to a test function, which is a well-defined procedure. From Eq. (88), it follows that $f\otimes g = g\otimes f$.

Convolutions for functions $\tilde{f}$, $\tilde{g}$ (cf. Eq. (83)) can be defined by[52]

$$\left(\tilde{f}\otimes\tilde{g}\right)(y) = \int_0^y \mathrm{d}z\,\tilde{f}(z)\,\tilde{g}(y-z). \tag{89}$$

Again, this expression is well defined for a distribution $\tilde{f}$ by

$$\begin{aligned}\left(\tilde{f}\otimes\tilde{g}\right)(y) &= \int_0^\infty \mathrm{d}z\,\tilde{f}(z)\,\chi_{[0,y]}(z)\,\tilde{g}(y-z)\\ &= \tilde{f}\left[z\mapsto \chi_{[0,y]}(z)\,\tilde{g}(y-z)\right].\end{aligned} \tag{90}$$

If $\tilde{f}$ and $\tilde{g}$ are distributions, then

$$\begin{aligned}\left(\tilde{f}\otimes\tilde{g}\right)[\varphi] &= \int_0^\infty \mathrm{d}y \int_0^y \mathrm{d}z\,\tilde{f}(z)\,\tilde{g}(y-z)\,\varphi(y)\\ &= \int_0^\infty \mathrm{d}z\,\tilde{f}(z) \int_0^\infty \mathrm{d}v\,\tilde{g}(v)\,\varphi(z+v).\end{aligned} \tag{91}$$

We wish to derive explicit expressions for the cases where $\tilde{f}$, $\tilde{g}$ are of the forms $\delta_0$ or $\tilde{D}_{+[\underline{0},M]}$. The case of $\delta$-functions is straightforward, and one easily obtains $\delta_0\otimes\tilde{h}=\tilde{h}$ for any regular or singular function $\tilde{h}$. The case of distributions $\tilde{D}_{+[\underline{0},M]}$ is slightly more complicated. By defining

$$\begin{aligned}\tilde{D}^{M1}(y) &\doteq \int_y^M \mathrm{d}z\,\tilde{D}(z),\\ \left(\tilde{D}\ltimes\tilde{g}\right)(y) &\doteq \left(\tilde{D}_{+[\underline{0},y]}\otimes\tilde{g}\right)(y) = \int_0^y \mathrm{d}z\tilde{D}(z)\,\left[\tilde{g}(y-z)-\tilde{g}(y)\right],\end{aligned} \tag{92}$$

we obtain for a regular function $\tilde{g}$ and for $y<M$

$$\begin{aligned}\left(\tilde{D}_{+[\underline{0},M]}\otimes\tilde{g}\right)(y) &= \int_0^M \mathrm{d}z\,\tilde{D}_{+[\underline{0},M]}(z)\,\chi_{[0,y]}(z)\,\tilde{g}(y-z)\\ &= \int_0^M \mathrm{d}z\,\tilde{D}(z)\,\left[\chi_{[0,y]}(z)\,\tilde{g}(y-z)-\chi_{[0,y]}(0)\,\tilde{g}(y)\right]\\ &= \int_0^y \mathrm{d}z\,\tilde{D}(z)\,\left[\tilde{g}(y-z)-\tilde{g}(y)\right]-\int_y^M \mathrm{d}z\,\tilde{D}(z)\,\tilde{g}(y)\\ &= \left(\tilde{D}\ltimes\tilde{g}\right)(y)-\tilde{D}^{M1}(y)\,\tilde{g}(y).\end{aligned} \tag{93}$$

[52] We use the same symbol as in Eq. (86). The meaning of "$\otimes$" will be clear from the context.

Note that $\tilde{D}^{M1}(M-z) = \mathcal{O}(z)$. In order to state the result for $\tilde{E}_{+[\underline{0},M]} \otimes \tilde{F}_{+[\underline{0},M]}$, we introduce the following notation:

$$\begin{aligned}
\left(\tilde{E} \wedge \tilde{F}\right)(y) &\doteq \int_0^y \mathrm{d}z \, \left(\tilde{E}(z)\tilde{F}(y-z) - \tilde{E}(y)\tilde{F}(y-z) - \tilde{E}(z)\tilde{F}(y)\right), \\
c^M_{\tilde{E}\tilde{F}} &\doteq \int_0^M \mathrm{d}z \, \tilde{E}(z) \int_{M-z}^M \mathrm{d}w \, \tilde{F}(w) \\
&= \int_0^M \mathrm{d}z \, \tilde{E}(z) \, \tilde{F}^{M1}(M-z) = \left(\tilde{E} \otimes \tilde{F}^{M1}\right)(M). \qquad (94)
\end{aligned}$$

The quantity $c^M_{\tilde{E}\tilde{F}}$ is symmetric in $\tilde{E}$ and $\tilde{F}$. A lengthy calculation then yields, after performing suitable subtractions,

$$\tilde{E}_{+[\underline{0},M]} \otimes \tilde{F}_{+[\underline{0},M]} = \left(\tilde{E} \wedge \tilde{F} - \tilde{E}\tilde{F}^{M1} - \tilde{E}^{M1}\tilde{F}\right)_{+[\underline{0},M]} - c^M_{\tilde{E}\tilde{F}}\delta_0. \qquad (95)$$

The final result for the convolution of two arbitrary linear combinations

$$\begin{aligned}
\tilde{K} &= \tilde{K}^\delta\delta_0 + \tilde{K}^s_{+[\underline{0},M]} + \tilde{K}^r, \\
\tilde{L} &= \tilde{L}^\delta\delta_0 + \tilde{L}^s_{+[\underline{0},M]} + \tilde{L}^r \qquad (96)
\end{aligned}$$

is

$$\begin{aligned}
\tilde{K} \otimes \tilde{L} = {} & \left(\tilde{K}^\delta\tilde{L}^\delta - c^M_{\tilde{K}^s\tilde{L}^s}\right)\delta_0 \\
& + \left(\tilde{K}^\delta\tilde{L}^s + \tilde{K}^s\tilde{L}^\delta + \tilde{K}^s \wedge \tilde{L}^s - \tilde{K}^s\tilde{L}^{sM1} - \tilde{K}^{sM1}\tilde{L}^s\right)_{+[\underline{0},M]} \\
& + \left(\tilde{K}^\delta - \tilde{K}^{sM1}\right)\tilde{L}^r + \left(\tilde{L}^\delta - \tilde{L}^{sM1}\right)\tilde{K}^r + \tilde{K}^r \otimes \tilde{L}^r \\
& + \tilde{K}^s \ltimes \tilde{L}^r + \tilde{L}^s \ltimes \tilde{K}^r. \qquad (97)
\end{aligned}$$

This is again a linear combination of a term proportional to $\delta_0$, a term with a "+" prescription of the form $D_{+[\underline{0},M]}$, and a regular term. The decomposition in Eq. (96) is therefore stable under convolutions. Consequently, heavy-quark fragmentation functions can be parametrized in this way, stable under scale evolution by means of the renormalization group equation.

# B Phase-Space Parametrizations

The $d$-dimensional phase-space element $\mathrm{dPS}^{(N)}(\underline{p},\underline{m})$ for $N$ outgoing particles with momenta $\underline{p}=(p_1,\ldots,p_N)$ and masses $\underline{m}=(m_1,\ldots,m_N)$ is defined by

$$\mathrm{dPS}^{(N)}(\underline{p},\underline{m}) = (2\pi)^d\,\delta\left(\sum_{\alpha=1}^{N} p_\alpha - w\right)\prod_{\alpha=1}^{N}\frac{\mathrm{d}p_\alpha\,\delta(p_\alpha^2-m_\alpha^2)}{(2\pi)^{d-1}}, \tag{98}$$

where $w$ is the sum of all outgoing momenta. We use the short-hand notation $\mathrm{dPS}^{(N)}(\underline{p})$ if all masses are zero.

## B.1 Massless Partons

The one-particle phase space for a massless parton is

$$\int \mathrm{dPS}^{(1)}(p_1) = 2\pi\,\frac{x_B}{Q^2}\,\delta(\xi-x_B) = 2\pi\,\frac{1}{Q^2}\,\delta(1-u), \tag{99}$$

where $u=x_B/\xi$, the variables being defined as in Section 2.2. The energy of $p_1$ is given by $E_1=P_0(1-x_B)$.

Now we give three different parametrizations of the phase space $\mathrm{dPS}^{(2)}(p_1,p_2)$ of two massless partons with momenta $p_1$ and $p_2$. In the following, energies and angles are defined in the hadronic centre-of-mass frame, cf. the remarks in Section 2.2. The azimuthal angle has been integrated out.

- *Parametrization A (cf. Fig. 9):*
  The integration variable $\rho$ is the energy $E_1$ of the parton with momentum $p_1$, scaled by a multiple of the proton momentum:

  $$\rho \doteq \frac{E_1}{P_0(1-x_B)}. \tag{100}$$

  This parametrization is used for those contributions where a collinear singularity has to be absorbed into a fragmentation function $D$; its explicit form is

  $$\begin{aligned}\int \mathrm{dPS}^{(2)}(p_1,p_2) &= \int \frac{1}{8\pi}\,\frac{(4\pi)^\epsilon}{\Gamma(1-\epsilon)}\left(Q^2\right)^{-\epsilon}\,\frac{u(1-x_B)}{u-x_B}\\ &\quad\cdot(1-x_B)^{-2\epsilon}\,u^{-\epsilon}\,(1-u)^{-\epsilon}\,(u-x_B)^{2\epsilon}\,(\rho-a(u))^{-\epsilon}\,(1-\rho)^{-\epsilon}\,\mathrm{d}\rho.\end{aligned} \tag{101}$$

  Here

  $$a(u) \doteq \frac{x_B}{1-x_B}\,\frac{1-u}{u}. \tag{102}$$

  The inverse function of $u\mapsto a(u)$ is denoted by $\rho\mapsto u_0(\rho)$ and is given by

  $$u_0(\rho) = \frac{x_B}{x_B+(1-x_B)\rho}. \tag{103}$$

  The energies and invariants are given by

  $$\begin{aligned} E_1 &= P_0(1-x_B)\rho,\\ E_2 &= P_0(1-x_B)(1-\rho+a(u)),\\ s_{12} &= Q^2\frac{1-u}{u},\\ s_{i1} &= Q^2\frac{1-x_B}{u-x_B}(\rho-a(u)),\\ s_{i2} &= Q^2\frac{1-x_B}{u-x_B}(1-\rho).\end{aligned} \tag{104}$$

The angular variable $v_1 = (1 - \cos\vartheta_1)/2$ is

$$v_1 = v(\rho, u) = \frac{x_B(1-u)}{u - x_B}\frac{1-\rho}{\rho}. \tag{105}$$

The range of integration is restricted to $\rho \in [a(u), 1]$; however, in order to ensure that the energy of the parent parton is larger than that of the observed hadron itself, the additional condition $\rho \geq z$ must be satisfied, for the case that the parent parton's momentum is $p_1$.

- *Parametrization B:*
  The integration variable $w$ is related to an angular variable in the centre-of-mass system of the virtual photon and the incoming parton. Its relation to $\rho$ is

$$w \doteq \frac{1-\rho}{1-a(u)}. \tag{106}$$

This parametrization is used for the contributions that involve a target fragmentation function; it is given by

$$\int \mathrm{dPS}^{(2)}(p_1, p_2) \;=\; \int \frac{1}{8\pi}\,\frac{(4\pi)^\epsilon}{\Gamma(1-\epsilon)}\,\left(Q^2\right)^{-\epsilon}\,(1-u)^{-\epsilon}\,u^\epsilon\,(w(1-w))^{-\epsilon}\mathrm{d}w. \tag{107}$$

The energies and invariants are

$$\begin{aligned} E_1 &= P_0(1-x_B)(1-(1-a(u))w), \\ E_2 &= P_0(1-x_B)(a(u)+(1-a(u))w), \\ s_{12} &= Q^2\frac{1-u}{u}, \\ s_{i1} &= Q^2\frac{1}{u}(1-w), \\ s_{i2} &= Q^2\frac{1}{u}w. \end{aligned} \tag{108}$$

The angular variable $v_1$ is

$$v_1 = v(w, u) = \frac{a(u)w}{1-(1-a(u))w}. \tag{109}$$

The range of integration is restricted to $w \in [0, 1]$.

- *Parametrization C:*
  This parametrization is convenient for the contributions where the observed hadron originates from a parton that is collinear to the incoming parton. A variable $u'$ is introduced by

$$u' = 1 - \frac{1-x_B}{x_B}\,\rho\,u. \tag{110}$$

The parametrization is given by

$$\begin{aligned} \int \mathrm{dPS}^{(2)}(p_1, p_2) \;=\; & \int \frac{1}{8\pi}\,\frac{(4\pi)^\epsilon}{\Gamma(1-\epsilon)}\,\left(Q^2\right)^{-\epsilon}\,\frac{x_B}{u-x_B}\,(u-u')^{-\epsilon}\,(1-u)^{-\epsilon} \\ & \cdot\left(1-\frac{x_B}{1-x_B}\,\frac{1-u'}{u}\right)^{-\epsilon}\,(u-x_B)^{2\epsilon}\,{x_B}^{-\epsilon}\,(1-x_B)^{-\epsilon}\,\mathrm{d}u'. \end{aligned} \tag{111}$$

[53] Please note that the remark in footnote 20 does not apply in this case.

The energies and invariants are

$$\begin{aligned} E_1 &= P_0\, x_B \frac{1-u'}{u}, \\ E_2 &= P_0(1-x_B)\left(1-\frac{x_B}{1-x_B}\frac{u-u'}{u}\right), \\ s_{12} &= Q^2\frac{1-u}{u}, \\ s_{i1} &= Q^2\frac{x_B}{u-x_B}\frac{u-u'}{u}, \\ s_{i2} &= Q^2\frac{1-x_B}{u-x_B}\left(1-\frac{x_B}{1-x_B}\frac{1-u'}{u}\right). \end{aligned} \tag{112}$$

The angular variable $v_1$ is

$$v_1 = v(u',u) = \frac{1-u}{u-x_B}\frac{(1-x_B)u - x_B(1-u')}{1-u'}. \tag{113}$$

The range of integration is restricted to $u' \in [1-u(1-x_B)/x_B, u]$. It has to be further restricted by

$$u' \le 1 - \frac{1-x_B}{x_B}\, z\, u \tag{114}$$

in order to avoid that the outgoing hadron has an energy larger than its parent parton's.

## B.2 Massive Partons

The two-particle phase space for massive partons of mass $m$ in $d = 4$ space-time dimensions can be written as

$$\int \mathrm{dPS}^{(2)}(p_1,p_2,m,m) = \int \frac{1}{8\pi}\sqrt{1-\frac{4m^2}{w^2}}\,\mathrm{d}r. \tag{115}$$

Here $w = p_1 + p_2$, and $r = (1-\cos\chi)/2$, where $\chi$ is a polar angle of $p_1$ in the centre-of-mass frame of $p_1$ and $p_2$. The azimuthal angle is already integrated out. The range of $r$ is $[0,1]$. We briefly summarize some expressions for the energies in the centre-of-mass frame of $p_1$ and $p_2$ in the case of $w = \xi P + q$:

$$\begin{aligned} E_w &= Q\sqrt{\frac{\xi - x_B}{x_B}}, \\ E_P &= \frac{Q}{2}\frac{1}{\sqrt{x_B(\xi-x_B)}}, \\ E_1 &= E_w/2, \\ E_2 &= E_w/2. \end{aligned} \tag{116}$$

The expressions for the invariants $s_{AB}$ follow easily. We have the following phase-space restrictions on $Q^2$ and $\xi$:

$$\begin{aligned} Q^2 &\ge 4m^2\frac{x_B}{1-x_B}, \\ \xi &\ge x_B\left(1+\frac{4m^2}{Q^2}\right). \end{aligned} \tag{117}$$

# C Finite Contributions of the Real Corrections

## C.1 Explicit Expressions

This appendix contains the explicit results of the finite contributions from the real corrections[54]. We have dropped terms that vanish for $\epsilon \to 0$. The results are given by

$$
\begin{aligned}
\mathcal{A}^f_{B_1^M} &= Y^M \sum_{i=q,\overline{q}} c_i \frac{\alpha_s}{2\pi} \int_{x_B}^{x_B/(x_B+(1-x_B)z)} \frac{\mathrm{d}u}{u} \int_{a(u)}^1 \frac{\mathrm{d}\rho}{\rho} A(v(\rho,u)) \\
&\cdot \Bigg[ f^r_{i/P}\left(\frac{x_B}{u},\mu_f^2\right) D^r_{h/i}\left(\frac{z}{\rho},\mu_D^2\right) \left\{ -\ln\frac{\mu_f^2}{Q^2} P_{q\leftarrow q}(u)\,\delta(1-\rho) + C_F\,\Phi^M_{1qq} \right\} \\
&+ f^r_{i/P}\left(\frac{x_B}{u},\mu_f^2\right) D^r_{h/g}\left(\frac{z}{\rho},\mu_D^2\right) \left\{ -\ln\frac{\mu_M^2}{Q^2} \hat{P}_{gq\leftarrow q}(u)\,\delta(\rho-a(u)) + C_F\,\Phi^M_{1qg} \right\} \\
&+ f^r_{g/P}\left(\frac{x_B}{u},\mu_f^2\right) D^r_{h/i}\left(\frac{z}{\rho},\mu_D^2\right) \\
&\cdot \left\{ -\ln\frac{\mu_M^2}{Q^2} \hat{P}_{\overline{q}q\leftarrow g}(u)\,\delta(\rho-a(u)) - \ln\frac{\mu_f^2}{Q^2} P_{q\leftarrow g}(u)\,\delta(1-\rho) + T_f\,\Phi^M_{1gq} \right\} \Bigg], \\
\mathcal{A}^f_{B_2^M} &= Y^M \sum_{i=q,\overline{q}} c_i \frac{\alpha_s}{2\pi} \int_{x_B/(x_B+(1-x_B)z)}^1 \frac{\mathrm{d}u}{u} \int_z^1 \frac{\mathrm{d}\rho}{\rho} A(v(\rho,u)) \\
&\cdot \Bigg[ f^r_{i/P}\left(\frac{x_B}{u},\mu_f^2\right) D^r_{h/i}\left(\frac{z}{\rho},\mu_D^2\right) \\
&\cdot \left\{ -\ln\frac{\mu_f^2}{Q^2} P_{q\leftarrow q}(u)\,\delta(1-\rho) - \ln\frac{\mu_D^2}{Q^2} P_{q\leftarrow q}(\rho)\,\delta(1-u) + C_F\,\Phi^M_{2qq} \right\} \\
&+ f^r_{i/P}\left(\frac{x_B}{u},\mu_f^2\right) D^r_{h/g}\left(\frac{z}{\rho},\mu_D^2\right) \left\{ -\ln\frac{\mu_D^2}{Q^2} P_{g\leftarrow q}(\rho)\,\delta(1-u) + C_F\,\Phi^M_{2qg} \right\} \\
&+ f^r_{g/P}\left(\frac{x_B}{u},\mu_f^2\right) D^r_{h/i}\left(\frac{z}{\rho},\mu_D^2\right) \left\{ -\ln\frac{\mu_f^2}{Q^2} P_{q\leftarrow g}(u)\,\delta(1-\rho) + T_f\,\Phi^M_{2gq} \right\} \Bigg], \\
\mathcal{A}^f_{C^M} &= Y^M \sum_{i=q,\overline{q}} c_i \frac{\alpha_s}{2\pi} \int_{x_B/(1-(1-x_B)z)}^1 \frac{\mathrm{d}u}{u} A(1) \\
&\cdot \Bigg[ M^r_{i,h/P}\left(\frac{x_B}{u},(1-x_B)z,\mu_M^2\right) \left\{ -\ln\frac{\mu_M^2}{Q^2} P_{q\leftarrow q}(u)\,(1-x_B) + C_F\,\Phi^M_q \right\} \\
&+ M^r_{g,h/P}\left(\frac{x_B}{u},(1-x_B)z,\mu_M^2\right) \left\{ -\ln\frac{\mu_M^2}{Q^2} P_{q\leftarrow g}(u)\,(1-x_B) + T_f\,\Phi^M_g \right\} \Bigg], \\
\mathcal{A}^f_{B_1^L} &= Y^L \sum_{i=q,\overline{q}} c_i \frac{\alpha_s}{2\pi} \int_{x_B}^{x_B/(x_B+(1-x_B)z)} \frac{\mathrm{d}u}{u} \int_{a(u)}^1 \frac{\mathrm{d}\rho}{\rho} A(v(\rho,u)) \\
&\cdot \Bigg[ f^r_{i/P}\left(\frac{x_B}{u},\mu_f^2\right) D^r_{h/i}\left(\frac{z}{\rho},\mu_D^2\right) C_F\,\Phi^L_{1qq} \\
&+ f^r_{i/P}\left(\frac{x_B}{u},\mu_f^2\right) D^r_{h/g}\left(\frac{z}{\rho},\mu_D^2\right) C_F\,\Phi^L_{1qg} \\
&+ f^r_{g/P}\left(\frac{x_B}{u},\mu_f^2\right) D^r_{h/i}\left(\frac{z}{\rho},\mu_D^2\right) T_f\,\Phi^L_{1gq} \Bigg],
\end{aligned}
$$

[54] The calculations have been done with the help of the algebraic manipulation programs "Maple" [150], "Mathematica" [151] and "REDUCE" [152], and by using the package "Tracer" [153] for trace calculations of $\gamma$-matrices.

$$
\begin{aligned}
\mathcal{A}^f_{B_2^L} &= Y^L \sum_{i=q,\overline{q}} c_i \frac{\alpha_s}{2\pi} \int_{x_B/(x_B+(1-x_B)z)}^1 \frac{\mathrm{d}u}{u} \int_z^1 \frac{\mathrm{d}\rho}{\rho} A(v(\rho,u)) \\
&\cdot\Bigg[ f^r_{i/P}\left(\frac{x_B}{u},\mu_f^2\right) D^r_{h/i}\left(\frac{z}{\rho},\mu_D^2\right) C_F\, \Phi^L_{2qq} \\
&+ f^r_{i/P}\left(\frac{x_B}{u},\mu_f^2\right) D^r_{h/g}\left(\frac{z}{\rho},\mu_D^2\right) C_F\, \Phi^L_{2qg} \\
&+ f^r_{g/P}\left(\frac{x_B}{u},\mu_f^2\right) D^r_{h/i}\left(\frac{z}{\rho},\mu_D^2\right) T_f\, \Phi^L_{2gq}\Bigg], \\
\mathcal{A}^f_{C^L} &= Y^L \sum_{i=q,\overline{q}} c_i \frac{\alpha_s}{2\pi} \int_{x_B/(1-(1-x_B)z)}^1 \frac{\mathrm{d}u}{u} A(1) \\
&\cdot\Bigg[ M^r_{i,h/P}\left(\frac{x_B}{u},(1-x_B)z,\mu_M^2\right) C_F\, \Phi^L_q \\
&+ M^r_{g,h/P}\left(\frac{x_B}{u},(1-x_B)z,\mu_M^2\right) T_f\, \Phi^L_g\Bigg],
\end{aligned}
\tag{118}
$$

where the functions $\Phi$ are given by

$$
\begin{aligned}
\Phi^M_{1qq} &= \delta(1-\rho)\left[2\frac{\ln(1-u)}{1-u} + 1 - u - (1+u)\ln(1-u) - \frac{1+u^2}{1-u}\ln\frac{u-x_B}{1-x_B}\right] \\
&+ 2\left(\frac{1}{1-\rho}\right)_{+\rho[0,\underline{1}]} \frac{1}{1-u} - \frac{1}{1-u}(1+\rho) - \left(\frac{1}{1-\rho}\right)_{+\rho[0,\underline{1}]} (1+u) \\
&+ (1-\rho)\frac{x_B}{u-x_B}\left(1+\frac{u(1-x_B)}{u-x_B}\right) - 2\frac{ux_B}{u-x_B} + 2, \\
\Phi^M_{1qg} &= \delta(\rho-a(u))\left[1-u+\frac{1+u^2}{1-u}\ln\frac{1-u}{u}\right] + \left(\frac{1}{\rho-a(u)}\right)_{+\rho[\underline{a(u)},1]} \frac{1+u^2}{1-u} \\
&+ \frac{(1-x_B)^2}{(u-x_B)^2}\frac{u^2}{1-u}\rho - \frac{x_B(1-x_B)}{(u-x_B)^2}u - 2\frac{1-x_B}{u-x_B}\frac{u^2}{1-u}, \\
\Phi^M_{1gq} &= \delta(\rho-a(u))\left[2u(1-u) + (1-2u+2u^2)\ln\frac{1-u}{u}\right] \\
&+ \delta(1-\rho)\left[2u(1-u) + (1-2u+2u^2)\ln\frac{(1-u)(1-x_B)}{u-x_B}\right] \\
&+ \left(\frac{1}{\rho-a(u)}\right)_{+\rho[\underline{a(u)},1]} (1-2u+2u^2) \\
&+ \left(\frac{1}{1-\rho}\right)_{+\rho[0,\underline{1}]} (1-2u+2u^2) - 2\frac{1-x_B}{u-x_B}u, \\
\Phi^M_{2qq} &= \delta(1-u)\,\delta(1-\rho)\,\frac{\pi^2}{3} \\
&+ \delta(1-\rho)\left[2\left(\frac{\ln(1-u)}{1-u}\right)_{+u[0,\underline{1}]} + 1 - u - (1+u)\ln(1-u) - \frac{1+u^2}{1-u}\ln\frac{u-x_B}{1-x_B}\right]
\end{aligned}
$$

$$
\begin{aligned}
&+\delta(1-u)\left[2\left(\frac{\ln(1-\rho)}{1-\rho}\right)_{+\rho[0,\underline{1}]}+1-\rho-(1+\rho)\ln(1-\rho)+\frac{1+\rho^2}{1-\rho}\ln\rho\right]\\
&+2\left(\frac{1}{1-\rho}\right)_{+\rho[0,\underline{1}]}\left(\frac{1}{1-u}\right)_{+u[0,\underline{1}]}-\left(\frac{1}{1-u}\right)_{+u[0,\underline{1}]}(1+\rho)-\left(\frac{1}{1-\rho}\right)_{+\rho[0,\underline{1}]}(1+u)\\
&+(1-\rho)\frac{x_B}{u-x_B}\left(1+\frac{u(1-x_B)}{u-x_B}\right)-2\frac{ux_B}{u-x_B}+2,
\end{aligned}
$$

$$
\begin{aligned}
\Phi^M_{2qg} &= \delta(1-u)\left[\rho+(\ln\rho+\ln(1-\rho))\left(\rho+\frac{2}{\rho}-2\right)\right]\\
&+\left(\frac{1}{1-u}\right)_{+u[0,\underline{1}]}\left(\rho+\frac{2}{\rho}-2\right)\\
&+2-2\frac{x_Bu}{u-x_B}+\frac{x_B}{u-x_B}\rho-\frac{x_B(1-x_B)u}{(u-x_B)^2}(1-\rho)+\frac{1}{\rho-a(u)}\frac{1+u^2}{1-u}-2\frac{1}{\rho}\frac{1}{1-u},
\end{aligned}
$$

$$
\begin{aligned}
\Phi^M_{2gq} &= \delta(1-\rho)\left[2u(1-u)+(1-2u+2u^2)\ln\frac{(1-u)(1-x_B)}{u-x_B}\right]\\
&+\frac{1}{\rho-a(u)}(1-2u+2u^2)+\left(\frac{1}{1-\rho}\right)_{+\rho[0,\underline{1}]}(1-2u+2u^2)-2\frac{1-x_B}{u-x_B}u,
\end{aligned}
$$

$$
\begin{aligned}
\Phi^M_{q} &= (1-x_B)\left[\frac{7}{2}\,\delta(1-u)-\frac{3}{2}\left(\frac{1}{1-u}\right)_{+u[0,\underline{1}]}+2\left(\frac{\ln(1-u)}{1-u}\right)_{+u[0,\underline{1}]}\right.\\
&\qquad\left.+3-u-(1+u)\ln(1-u)-\frac{1+u^2}{1-u}\ln u\right],
\end{aligned}
$$

$$
\Phi^M_{g} = (1-x_B)\left(\ln\frac{1-u}{u}-1\right)(1-2u+2u^2),
$$

$$
\Phi^L_{1qq} = 2\frac{(1-x_B)^2}{(u-x_B)^2}u^3\rho-2\frac{x_B(1-x_B)}{(u-x_B)^2}u^2(1-u),
$$

$$
\Phi^L_{1qg} = 2\frac{(1-x_B)^2}{(u-x_B)^2}u^3(1-\rho),
$$

$$
\Phi^L_{1gq} = 4\frac{1-x_B}{u-x_B}u^2(1-u),
$$

$$
\Phi^L_{2qq} = \Phi^L_{1qq},
$$

$$
\Phi^L_{2qg} = \Phi^L_{1qg},
$$

$$
\Phi^L_{2gq} = \Phi^L_{1gq},
$$

$$
\Phi^L_{q} = (1-x_B)\,u,
$$

$$
\Phi^L_{g} = (1-x_B)\,2u(1-u). \tag{119}
$$

## C.2 The Case of Singular Fragmentation Functions

The expressions given in the previous section can be applied directly in a numerical evaluation in the case where the fragmentation functions are regular functions. In the application that we have in mind, the production of heavy quarks, the fragmentation functions $D_{Q/i}(z/\rho)$ are singular for $\rho \to z$. A direct application of the given formulae by means of the convolution formula in Eq. (97) fails for the contributions from the separate phase-space regions $R_1$ and $R_2$, due to a logarithmic divergence at $\rho = z$ after having performed the $u$-integration. It turns out that these dangerous terms cancel out, as they should, if the contributions from the phase space regions $R_1$ and $R_2$ (see Fig. 9) are added. In order to see this explicitly, the distributions $\delta(\rho - a(u))$ and $1/(\rho - a(u))_{+\rho[a(u),\underline{1}]}$ have to be expressed in terms of distributions in the variable $u$. The corresponding relations are given by

$$\begin{aligned}
\delta(\rho - a(u)) &= \frac{1-x_B}{x_B}(u_0(\rho))^2\ \delta(u - u_0(\rho)), \\
\left(\frac{1}{\rho - a(u)}\right)_{+\rho[\underline{a(u)},1]} &= \frac{1-x_B}{x_B}(u_0(\rho))^2 \left[\left(\frac{1}{u - u_0(\rho)}\right)_{+u[\underline{u_0(\rho)},1]} + \frac{1}{u_0(\rho)}\right. \\
&\qquad \left. -\delta(u - u_0(\rho)) \ln\left(\frac{1-\rho}{\rho} u_0(\rho)\right)\right].
\end{aligned} \tag{120}$$

The expressions for the cross sections are integrated in $\rho$ from $z$ to 1 and in $u$ from $u_0(\rho)$ to 1. The subtractions in the variable $u$ are performed first, leaving a regular expression depending on the variable $\rho$. Then the subtractions in $\rho$ are performed. In cases where a "+" prescription in $z/\rho$ from the heavy-quark fragmentation functions is multiplied by a "+" prescription in $\rho$ from the matrix element, the convolution formula from Eq. (95) has to be applied. The resulting expression is singular in the variable $z$. An integration over $z$ involving an observable therefore contains an additional subtraction. The explicit expressions which are needed for this procedure are given in the following. We consider the integrals

$$I(d,s) \doteq \int_{z_0}^1 \frac{\mathrm{d}z}{z} \int_z^1 \frac{\mathrm{d}\sigma}{\sigma}\, d(\sigma)\, s\left(\frac{z}{\sigma}\right)\, C\left(\frac{z}{\sigma}, z\right), \tag{121}$$

where $\sigma \mapsto d(\sigma)$ and $\rho \mapsto s(\rho)$ are distributions with possible singularities at $\sigma = 1$ and $\rho = 1$, and $C$ is a test function standing for the product of the remaining regular terms of the matrix elements, the parton densities and the observable under consideration. In order to achieve a compact notation, we introduce the following short-hand notation:

$$M \doteq \ln\frac{1}{z_0}, \quad \zeta \doteq \ln\frac{1}{z}, \quad \mu \doteq \frac{1}{\zeta}\ln\frac{1}{\sigma}, \quad \lambda \doteq \frac{\zeta}{M}, \quad \rho \doteq \frac{z}{\sigma}. \tag{122}$$

We obtain

$$\begin{aligned}
d(\sigma) &= \delta(1-\sigma), \quad s(\rho) = \delta(1-\rho): \\
I(d,s) &= \int_0^1 \mathrm{d}\lambda \int_0^1 \mathrm{d}\mu\ C(1,1);
\end{aligned}$$

$$\begin{aligned}
d(\sigma) &= \delta(1-\sigma), \quad s(\rho) = S(\rho): \\
I(d,s) &= \int_0^1 \mathrm{d}\lambda \int_0^1 \mathrm{d}\mu\ M\, S(z)\, C(z,z);
\end{aligned}$$

$$
\begin{aligned}
d(\sigma) &= \delta(1-\sigma), \quad s(\rho) = S_{+[z_0,\underline{1}]}(\rho): \\
I(d,s) &= \int_0^1 \mathrm{d}\lambda \int_0^1 \mathrm{d}\mu \; M\, S(z) \Big[ C(z,z) - zC(1,1) \Big];
\end{aligned}
$$

$$
\begin{aligned}
d(\sigma) &= D(\sigma), \quad s(\rho) = \delta(1-\rho): \\
I(d,s) &= \int_0^1 \mathrm{d}\lambda \int_0^1 \mathrm{d}\mu \; M\, D(z)\, C(1,z);
\end{aligned}
$$

$$
\begin{aligned}
d(\sigma) &= D(\sigma), \quad s(\rho) = S(\rho): \\
I(d,s) &= \int_0^1 \mathrm{d}\lambda \int_0^1 \mathrm{d}\mu \; M\zeta\, D(\sigma)\, S(\rho)\, C(\rho,z);
\end{aligned}
$$

$$
\begin{aligned}
d(\sigma) &= D(\sigma), \quad s(\rho) = S_{+[z_0,\underline{1}]}(\rho): \\
I(d,s) &= \int_0^1 \mathrm{d}\lambda \int_0^1 \mathrm{d}\mu \; \Big\{ M\zeta\, D(\sigma)\, S(\rho) \Big[ C(\rho,z) - C(1,z) \Big] \\
&\qquad + M\zeta \Big[ D(\sigma) - \rho D(z) \Big] S(\rho)\, C(1,z) \\
&\qquad - M D(z) S^i_{z_0}(z)\, C(1,z) \Big\};
\end{aligned}
$$

$$
\begin{aligned}
d(\sigma) &= D_{+[z_0,\underline{1}]}(\sigma), \quad s(\rho) = \delta(1-\rho): \\
I(d,s) &= \int_0^1 \mathrm{d}\lambda \int_0^1 \mathrm{d}\mu \; M\, D(z) \Big[ C(1,z) - zC(1,1) \Big];
\end{aligned}
$$

$$
\begin{aligned}
d(\sigma) &= D_{+[z_0,\underline{1}]}(\sigma), \quad s(\rho) = S(\rho): \\
I(d,s) &= \int_0^1 \mathrm{d}\lambda \int_0^1 \mathrm{d}\mu \; \Big\{ M\zeta\, D(\sigma) \Big[ S(\rho)\, C(\rho,z) - \sigma S(z)\, C(z,z) \Big] \\
&\qquad - M\, D^i_{z_0}(z)\, S(z)\, C(z,z) \Big\};
\end{aligned}
$$

$$
\begin{aligned}
d(\sigma) &= D_{+[z_0,\underline{1}]}(\sigma), \quad s(\rho) = S_{+[z_0,\underline{1}]}(\rho): \\
I(d,s) &= \int_0^1 \mathrm{d}\lambda \int_0^1 \mathrm{d}\mu \; \Big\{ \Big[ M\zeta \Big( D(\sigma)\, S(\rho) - \rho D(z)\, S(\rho) - \sigma D(\sigma)\, S(z) \Big) \\
&\qquad - M \Big( D(z) S^i_{z_0}(z) + D^i_{z_0}(z)\, S(z) \Big) \Big] \cdot \Big[ C(1,z) - zC(1,1) \Big] \\
&\qquad - M\, zD(z)\, S^i_{z_0} \left( \frac{z_0}{z} \right) C(1,1) \\
&\qquad + M\zeta\, D(\sigma) \Big[ S(\rho) \Big( C(\rho,z) - C(1,z) \Big) - \sigma S(z) \Big( C(z,z) - C(1,z) \Big) \Big] \\
&\qquad - M\, D^i_{z_0}(z)\, S(z) \Big[ C(z,z) - C(1,z) \Big] \Big\}. \qquad (123)
\end{aligned}
$$

Here we have defined

$$
F^i_{x_0}(x) \doteq \int_{x_0}^{x} \mathrm{d}\xi\, F(\xi), \qquad (124)
$$

cf. Eq. (132). Similarly, the integral of the $u$-integration may be written as

$$
J(e) \doteq \int_{u_0(\rho)}^1 \frac{\mathrm{d}u}{u}\, e(u)\, F(u), \qquad (125)
$$

where $u \mapsto e(u)$ is a distribution with possible singularities at $u = u_0(\rho)$ and $u = 1$. Using the short-hand notation

$$T(\rho) \doteq \ln \frac{1}{u_0(\rho)}, \quad \nu \doteq \frac{1}{T(\rho)} \ln \frac{1}{u}, \tag{126}$$

we obtain:

$$\begin{aligned}
e(u) &= \delta(1-u): \\
J(e) &= \int_0^1 \mathrm{d}\nu\, F(1); \\
\\
e(u) &= E(u): \\
J(e) &= \int_0^1 \mathrm{d}\nu\, T(\rho)\, E(u)\, F(u); \\
\\
e(u) &= E_{+[u_0(\rho),\underline{1}]}(u): \\
J(e) &= \int_0^1 \mathrm{d}\nu\, T(\rho)\, E(u) \Big[F(u) - uF(1)\Big]; \\
\\
e(u) &= E_{+[\underline{u_0(\rho)},1]}(u): \\
J(e) &= \int_0^1 \mathrm{d}\nu\, T(\rho)\, E(u) \Big[F(u) - \frac{u}{u_0(\rho)} F(u_0(\rho))\Big].
\end{aligned} \tag{127}$$

The expressions given here are particularly useful for a numerical evaluation.

# D Splitting Functions

## D.1 Altarelli–Parisi Splitting Functions

The Altarelli–Parisi splitting functions $P_{B\leftarrow A}(u)$ are the splitting probabilities for a parton $A$ into a parton $B$, where parton $B$ carries a fraction $u$ of parton $A$'s momentum. These splitting functions are singular at $u = 1$ because a soft singularity has to be subtracted. The unsubtracted splitting functions $\hat{P}_{CB\leftarrow A}(u)$ are the splitting probabilities for a parton $A$ into partons $B$ and $C$, where, again, $B$ carries a fraction $u$ of parton $A$'s momentum. They are only applied in cases where parton $C$ is not soft, so there are no subtractions at $u = 1$. In the case considered in the present paper, a heavy-quark fragmentation function is attached to parton $C$, and therefore $C$ is not allowed to be soft, because the observed heavy-quark has to have a non-vanishing energy.

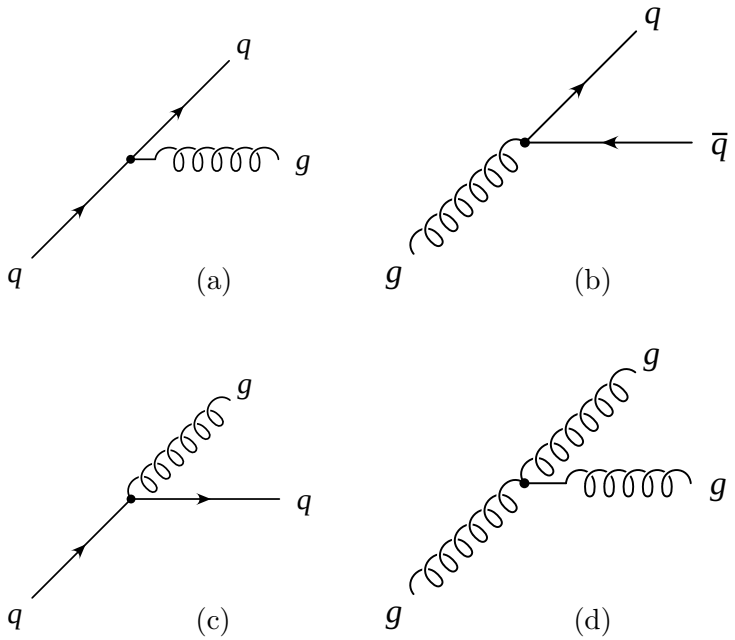


Figure 43: *Vertices corresponding to Altarelli–Parisi splitting functions: $P_{q\leftarrow q}(u)$ (a), $P_{q\leftarrow g}(u)$ (b), $P_{g\leftarrow q}(u)$ (c), $P_{g\leftarrow g}(u)$ (d).*

Explicitly, the subtracted and unsubtracted Altarelli–Parisi splitting functions corresponding to the vertices in Fig. 43 are given by[22] [45, 99]:

$$
\begin{aligned}
P_{q\leftarrow q}(u) &= C_F \left[ 2 \left( \frac{1}{1-u} \right)_{+u[0,\underline{1}]} + \frac{3}{2}\,\delta(1-u) - 1 - u \right], \\
P_{q\leftarrow g}(u) &= T_f \left[ 1 - 2u + 2u^2 \right], \\
P_{g\leftarrow q}(u) &= C_F \left[ 2\frac{1}{u} - 2 + u \right], \\
P_{g\leftarrow g}(u) &= 2C_A \left[ \left( \frac{1}{1-u} \right)_{+u[0,\underline{1}]} + \frac{1}{u} + u(1-u) - 2 \right] \\
&\quad + \left( \frac{11}{6} C_A - \frac{2}{3} T_R \right) \delta(1-u),
\end{aligned}
$$

$$
\begin{aligned}
\hat{P}_{qq\leftarrow q}(u) &= C_F \left[ 2\frac{1}{1-u} - 1 - u \right], \\
\hat{P}_{\overline{q}q\leftarrow g}(u) &= T_f \left[ 1 - 2u + 2u^2 \right], \\
\hat{P}_{qg\leftarrow q}(u) &= C_F \left[ 2\frac{1}{u} - 2 + u \right], \\
\hat{P}_{gg\leftarrow g}(u) &= 2C_A \left[ \frac{1}{1-u} + \frac{1}{u} + u(1-u) - 2 \right].
\end{aligned} \tag{128}
$$

The explicit expressions for a range of integration in $u$ from $\alpha$ to 1 are

$$
\begin{aligned}
P_{q\leftarrow q}(u) &= C_F \left[ 2\left(\frac{1}{1-u}\right)_{+u[\alpha,\underline{1}]} + \left(\frac{3}{2} + 2\ln(1-\alpha)\right)\delta(1-u) - 1 - u \right], \\
P_{g\leftarrow g}(u) &= 2C_A \left[ \left(\frac{1}{1-u}\right)_{+u[\alpha,\underline{1}]} + \frac{1}{u} + u(1-u) - 2 \right] \\
&\quad + \left( \frac{11}{6}C_A - \frac{2}{3}T_R + 2C_A \ln(1-\alpha) \right) \delta(1-u).
\end{aligned} \tag{129}
$$

## D.2 Heavy-Quark Fragmentation Functions

Heavy-quark fragmentation functions can be considered to be scale-dependent splitting functions for partons into heavy quarks, cf. Fig. 14. They have been calculated in next-to-leading order in Refs. [37, 101] and are given in the $\overline{\rm MS}$ scheme by

$$
\begin{aligned}
D_{Q/Q}(x,\mu^2) &= \delta(1-x) + C_f \frac{\alpha_s}{2\pi} \left[ \frac{1+x^2}{1-x} \left( \ln\frac{\mu^2}{m^2} - 2\ln(1-x) - 1 \right) \right]_{+x[0,\underline{1}]} + \mathcal{O}(\alpha_s^2), \\
D_{Q/q}(x,\mu^2) &= \mathcal{O}(\alpha_s^2), \\
D_{Q/g}(x,\mu^2) &= T_f \frac{\alpha_s}{2\pi} \left(x^2 + (1-x)^2\right) \ln\frac{\mu^2}{m^2} + \mathcal{O}(\alpha_s^2).
\end{aligned} \tag{130}
$$

Here $m$ is the mass of the heavy quark, and $q$ stands for any light-flavoured quark or antiquark or for the heavy antiquark $\overline{Q}$. The origin of the terms logarithmic in the scale $\mu$ can be understood by considering the renormalization group equation (11) in the case of the leading-order input distribution from Eq. (57). These expressions are valid as long as $\alpha_s \ln(\mu^2/m^2)$ is a small quantity. The heavy-quark fragmentation functions for arbitrary scales can be obtained by means of the renormalization group equation, see Section 4.2.

# E Numerical Solution of the Renormalization Group Equations

Here we describe the numerical solution of the renormalization group equations, based on the methods of Laguerre polynomials and direct discretization.

## E.1 Fragmentation Functions

For the heavy-quark fragmentation functions, we solve the renormalization group equation by two different methods. In the first method, the heavy-quark fragmentation function is written in the form[55]

$$D_{Q/i}(x,\mu^2) = D^\delta(\mu^2)\,\delta(1-x) + D^s_{+[\xi_M,1]}(x,\mu^2) + \chi_{[0,\xi_M]}(x)\,D^r(x,\mu^2). \tag{131}$$

The functions $D^s(x,\mu^2)$ and $D^r(x,\mu^2)$ represent the singular and regular part of the functional dependence and are transformed into functions $\tilde{D}^s(y,\mu^2)$ and $\tilde{D}^r(y,\mu^2)$ by means of the variable transformation $y = \ln(1/x)$, cf. Eqs. (83) and (84). For fixed $\mu$, the functional dependence in $y$ of $\tilde{D}^s(y,\mu^2)$ and $\tilde{D}^r(y,\mu^2)$ is parametrized by means of $N_{\rm spline} = 50$ equidistant support points. For the evolution, the functions are reconstructed by means of a third-order spline interpolation [154]. The evolution equation is solved in $N_{\rm int} = 500$ equidistant steps[56] in the variable $\ln\mu$ from the starting scale $\mu_0$ up to $\mu = 200\,\text{GeV}$, where the convolutions $\overline{P}\otimes D$ from Eq. (11) are performed by a numerical integration using the convolution formula in Eq. (97). The $N_{\rm spline}$ values of the parametrizations are stored for $N_{\rm scale} = 25$ values of the scale parameter $\ln\mu$. For a fast numerical evaluation in the applications, the values of the functions $\tilde{D}^s$ and $\tilde{D}^r$ are obtained by a quadratic interpolation in both variables $y$ and $\ln\mu$. The lower boundary of the integration region of the singular term $D^s$ in Eq. (131) is chosen to be $\xi_M$, being of the order of $10^{-3}$. The region of $x$ below a certain $\xi_M$ is not interesting in the applications because the heavy quark as a massive particle is not allowed to be soft. The range of integration $[\xi,1]$ in the convolution of the mass-factorized parton-level cross section and the fragmentation function is in general different from $[\xi_M,1]$. In the case of distributions, one may use Eq. (80) to rewrite everything in terms of the parametrized quantities. The integration region $[\xi_M,\xi]$ must therefore be subtracted. For this reason, $\tilde{D}^{sM1}$, defined in Eq. (92), is parametrized as well. The $\tilde{D}^{sM1}$ can be related to the integral

$$D^{s\xi_M 1}(x) = \int_{\xi_M}^x \mathrm{d}u\, D^s(u) \tag{132}$$

by $D^{s\xi_M 1}(x) = \tilde{D}^{s\ln(1/\xi_M)1}(\ln(1/x))$.

Alternatively, the heavy-quark fragmentation functions are expanded in terms of Laguerre polynomials, cf. Appendix F. The Laguerre coefficients are evolved, and the functional dependence is reconstructed. Because of the small number of Laguerre coefficients, of the order of $N_{\rm Laguerre} = 20$, and the explicit convolution equations (135) and (152), the method can be implemented very efficiently. It was employed so as to have a cross check and to make sure that the discretization in $x$ and $\mu$ used by the other method did not lead to intolerable errors. The method is, however, not very reliable to parametrize functions at values of $x$ very close to 1, because of strong oscillations of the sum of approximating polynomials. For the parametrizations employed for the numerical study, we have therefore relied on the method of direct discretization.

[55] For the conventions related to distributions see Appendix A.

[56] The CPU time needed for a complete parametrization of a fragmentation function is about 8 h on a "thin" SP2 node or 16 h on one 100 MHz HyperSparc processor.

## E.2 Target Fragmentation Functions

The renormalization group equations for the heavy-quark target fragmentation functions are solved by a discretization in the relevant variables $y = \ln(1/x)$, $\ln \mu$ and $\ln(1/\zeta)$, for $N_{\rm spline} = 50$, $N_{\rm scale} = 25$ and $N_\zeta = 25$ support points, respectively. Again, for the evolution, the interpolation in $y$ is done by means of a third-order spline interpolation routine. The evolution in $\ln \mu$ is done in $N_{\rm int} = 500$ steps[57]. It has been checked that the obtained result was stable with respect to changes in $N_{\rm spline}$ and $N_{\rm int}$. The variable $\zeta$ is a fixed parameter in Eq. (46). The final parametrization of the $N_{\rm parton} = 13$ distributions is given in terms of the values of the function $M$ on the $N_{\rm spline} \cdot N_{\rm scale} \cdot N_\zeta$ support points. For efficiency reasons, the final interpolations are done by a quadratic interpolation in the variables $y$, $\ln \mu$ and $\ln(1/\zeta)$.

[57] The CPU time needed for a complete parametrization of a target fragmentation function is about 250 h on a "thin" SP2 node or 480 h on one 100 MHz HyperSparc processor.

# F The Laguerre Method for the Solution of Integro-Differential Equations

In this section we describe the Laguerre method for the solution of homogeneous integro-differential equations. We use this method for cross checks of the direct method based on the discretization in the scaling and scale variables $x$ and $\mu$, respectively, for the evolution of the heavy-quark fragmentation functions. Because these particular fragmentation functions are distributions, the explicit convolution formula in Eq. (97) is quite complicated, and thus the accuracy of the discretized direct method has to be checked. We first give some basic properties of Laguerre polynomials, then describe the method, and finally discuss the prescription on how the singular functions can be reconstructed from the Laguerre coefficients.

## F.1 Laguerre Polynomials

In this section we define Laguerre polynomials and state some of their properties. Moreover, we give explicit expressions for the Laguerre coefficients of various regular and singular functions. For more details and for the omitted proofs, see Refs. [155–157].

The Laguerre polynomials $L_n(y)$ are orthogonal polynomials on $[0,\infty]$ with respect to the measure $\mathrm{d}y\,\exp(-y)$. They satisfy

$$\int_0^\infty \mathrm{d}y\,\mathrm{e}^{-y}\,L_m(y)\,L_n(y) \;=\; \delta_{mn}. \tag{133}$$

The indices $n, m$ run through the integers $\mathbb{N}$ including 0. An explicit expression is given by

$$L_n(y) \;=\; \mathrm{e}^y\,\frac{1}{n!}\,\partial_y^n\,\left(\mathrm{e}^{-y}\,y^n\right). \tag{134}$$

Here $\partial_y^n$ is the $n^{\text{th}}$ derivative with respect to $y$. In order to evaluate convolutions of series in Laguerre polynomials of the type of Eq. (89), the following identity is needed [157]:

$$\int_0^y \mathrm{d}t\,L_m(t)\,L_n(y-t) = L_{m+n}(y) - L_{m+n+1}(y). \tag{135}$$

Expressions for Laguerre polynomials $L_n(y)$ multiplied by powers of $y$ are calculated in the following way. We define the coefficients $s_{nk}^{(\alpha)}$ for $\alpha > 0$ by[58]

$$y^\alpha\,L_n(y) \;=\; \sum_{k=0}^{n+\alpha} s_{nk}^{(\alpha)}\,L_k(y). \tag{136}$$

The $s_{nk}^{(\alpha)}$ can be expressed in terms of a function $p_r^{(\alpha)}(n)$ by $s_{nk}^{(\alpha)} = p_{k-n}^{(\alpha)}(n)$. The $p_r^{(\alpha)}(n)$ satisfy the recursion relation

$$\begin{aligned}
p_0^{(0)}(n) \quad &= \quad 1, \\
p_r^{(\alpha)}(n) \quad &= \quad 0, \quad \text{if} \quad |r| > \alpha, \\
p_r^{(\alpha+1)}(n) \quad &= \quad -(n+r)\,p_{r-1}^{(\alpha)}(n) \;+\; (2(n+r)+1)\;p_r^{(\alpha)}(n) \\
&\qquad -(n+r+1)\,p_{r+1}^{(\alpha)}(n).
\end{aligned} \tag{137}$$

[58] The $s_{nk}^{(\alpha)}$ are implicitly assumed to be zero for values of the indices outside the explicit domain of definition.

The Laguerre polynomials, being orthogonal polynomials on $[0,\infty]$, cf. Eq. (133), can be used as a basis for a series expansion

$$F(y) \;=\; \sum_{n=0}^{\infty} F_n \, L_n(y) \tag{138}$$

of sufficiently regular[59] functions $F$. The Laguerre coefficients $F_n$ are given by

$$F_n \;=\; \int_0^\infty \mathrm{d}y \, \mathrm{e}^{-y} \, L_n(y) \, F(y). \tag{139}$$

A generating function for the Laguerre coefficients of a function $g$ can be obtained from the Mellin moments[60]

$$\hat{g}(s) = \int_0^1 \mathrm{d}x \, x^s \, g(x) = \int_0^\infty \mathrm{d}y \, \mathrm{e}^{-ys} \, \tilde{g}(y) \tag{140}$$

of this function by the formula [158]

$$\frac{1}{1-z} \, \hat{g}\left(\frac{1}{1-z}\right) = \sum_{n=0}^{\infty} \tilde{g}_n \, z^n, \tag{141}$$

where

$$\tilde{g}(y) \;=\; \sum_{n=0}^{\infty} \tilde{g}_n \, L_n(y). \tag{142}$$

We need the Laguerre coefficients of the following functions:

$$\begin{aligned}
F^{(a)}(y) &= \left(x \mapsto x^\beta\right)^\sim (y) \;: \\
F_n^{(a)} &= \frac{(\beta+1)^n}{(\beta+2)^{n+1}}, \\
\\
F^{(b)}(y) &= \left(x \mapsto x^\alpha \ln(1-x)\right)^\sim (y) \;: \\
F_n^{(b)} &= \sum_{k=0}^{n} \binom{n}{k} (-1)^k (-1) \frac{1}{(\alpha+2)^k} \\
&\quad \cdot \left\{ \sum_{i=1}^{k+1} (\alpha+2)^{i-2} \zeta_i(\alpha+2) - \sum_{i=2}^{k+1} (\alpha+2)^{i-2} \zeta(i) \right\}.
\end{aligned} \tag{143}$$

The Riemann $\zeta$-function and the function $\zeta_k(r)$ are defined by

$$\zeta(s) = \sum_{k=1}^{\infty} \frac{1}{k^s}, \quad \zeta_k(r) = \sum_{i=1}^{r} \frac{1}{i^k}. \tag{144}$$

As for functions, Laguerre coefficients may be defined for distributions as well, by interpreting Eq. (139) as the application of a distribution to the test function $\exp(-y) \, L_n(y)$. This is trivial for the $\delta$-function:

$$\begin{aligned}
T^{(a)}(y) &= \left(x \mapsto \delta(1-x)\right)^\sim (y) : \\
T_n^{(a)} &= 1.
\end{aligned} \tag{145}$$

[59] For the precise properties required, see Ref. [155]; basically, $F(y)$ must be integrable in a neighbourhood of zero and of at most polynomial growth for $y \to \infty$.

[60] For the definition of the "$\sim$" operation, see Appendix A.1.

In the case when $F$ is given by a "+" prescription, i.e. $F = D_+$, Eq. (139) is defined only if the function $D$ is integrable on $[\rho, \infty]$ for some $\rho > 0$. This condition is fulfilled for the following functions, owing to the fact that the "$\sim$" operation multiplies functions $f(x)$ by $x$:

$$\begin{aligned} T^{(b)}(y) &= \left( x \mapsto \left( \frac{1}{1-x} \right)_{+x[0,\underline{1}]} \right)^{\sim} (y) : \\ T_n^{(b)} &= \sum_{l=1}^{n} \binom{n}{l} (-1)^l \, \zeta(l+1) - \delta_{n0}, \\ T^{(c)}(y) &= \left( x \mapsto \left( \frac{\ln(1-x)}{1-x} \right)_{+x[0,\underline{1}]} \right)^{\sim} (y) : \\ T_n^{(c)} &= \sum_{r=0}^{n} \binom{n}{r} (-1)^r \cdot \begin{cases} \zeta(r+2) - \zeta_{r+1}^{[1]} + r + 1 - \sum_{s=2}^{r+1} \zeta(s), & \text{if } r > 0 \\ 1, & \text{if } r = 0 \end{cases}. \end{aligned} \tag{146}$$

Here $\delta_{ij}$ is the Kronecker symbol and $\zeta_k^{[1]}$, being defined by

$$\zeta_k^{[1]} = -\frac{1}{(k-1)!} \int_0^1 \mathrm{d}t \, \frac{\ln^{k-1} \frac{1}{t}}{1-t} \, \ln(1-t) + \zeta(k+1), \tag{147}$$

can be shown to be[61]

$$\zeta_k^{[1]} = \left( 1 + \frac{1}{2} k \right) \zeta(k+1) - \frac{1}{k-1} \sum_{i=1}^{k-2} i \, \zeta(i+1) \, \zeta(k-i). \tag{148}$$

The integral in Eq. (147) can be evaluated explicitly [159, 160] by using the expression

$$\partial_x^k \, \partial_y^l \, B(x,y) = \int_0^1 \mathrm{d}t \, \ln^k t \, \ln^l(1-t) \, t^{x-1} \, (1-t)^{y-1} \tag{149}$$

and by the recursive evaluation in $k$ of the expression $\partial_x^{k-1}\Big|_{x=1} \partial_y \Big|_{y=0} B(x,y)$ involving the Euler beta function.

## F.2 The Evolution Equation

The Laguerre method [158, 161] allows for the quick numerical solution of equations of the type

$$\partial_t F(x,t) = \int_x^1 \frac{\mathrm{d}u}{u} \, K(u,t) \, F\left( \frac{x}{u}, t \right), \tag{150}$$

where $K$ is the convolution kernel and $F$ the function or distribution to be evolved. As a first step, the equation is rewritten in terms of the functions (or distributions) $\tilde{K}$ and $\tilde{F}$ via the transformation in Eqs. (83) and (84), yielding

$$\partial_t \tilde{F}(y,t) = \int_0^y \mathrm{d}z \, \tilde{K}(z,t) \, \tilde{F}\left( y - z, t \right). \tag{151}$$

$\tilde{K}$ and $\tilde{F}$ are then expanded in Laguerre series as in Eq. (138) with coefficients $\tilde{K}_m(t)$ and $\tilde{F}_n(t)$. In the case when $F$ is a singular function, the corresponding expansion has to be understood as

[61] $\zeta_k^{[1]}$ as given in Ref. [158] contains a misprint.

a formal series, with coefficients defined by Eq. (139). The Laguerre coefficients of $\partial_t \tilde{F}(y,t)$ can be obtained by means of Eq. (135), and they read

$$\partial_t \tilde{F}_n(t) = \sum_{k=0}^{n} K_k(t)\ [F_{n-k}(t) - F_{n-k-1}(t)] = \sum_{k=0}^{n} F_k(t)\ [K_{n-k}(t) - K_{n-k-1}(t)]\,, \tag{152}$$

where $K_{-1}(t) \doteq 0$ and $F_{-1}(t) \doteq 0$. In practice, the series for $\tilde{K}(z,t)$ and $\tilde{F}(z,t)$ are truncated after a finite number of $N$ terms. As can be seen from Eq. (152), this allows for the calculation of $\partial_t \tilde{F}_n(t)$ for $n \leq N$. It can be shown that in the case of the Altarelli–Parisi scale evolution [97], Eq. (152) may be solved explicitly [158, 161], i.e. the evolution kernel $E_{kl}(t,t_0)$ of

$$\tilde{F}_k(t) = \sum_l E_{kl}(t,t_0)\, \tilde{F}_l(t_0) \tag{153}$$

can be written down in closed form. Since we are interested in a cross check at all intermediate scales, this explicit solution would not be an advantage, so the integro-differential equation is solved by a discretization in $t$, iterating the expression in Eq. (152) for very small $\Delta t$.

### F.3 Reconstruction of the Functional Dependence

The Laguerre method has been applied in the case of parton distribution functions [162–164]. These functions are regular, and therefore they can be obtained directly from the Laguerre coefficients by means of the Laguerre series in Eq. (138). In the case of scale-evolved singular functions $F(x,t)$, the situation is different. As has already been stressed, in this case the series expansion has to be considered to be a formal one. For example, if $F(x) = (1/(1-x))_{+x[0,\underline{1}]}$, then inserting the corresponding $\tilde{F}_n$ into Eq. (138) would lead to a rapidly oscillating function, since a function with a singular behaviour $\sim (1/y)$ cannot be expanded in terms of polynomials. Instead, it is possible to extract the singular term as a multiplicative factor and express the remainder in terms of the Laguerre coefficients.

Consider the general case of a function $G$ defined on $[0,\infty]$, which is singular at the origin like $\sim 1/y^{\beta+\rho}$, $\rho < 1$. Define the function $g$ by $g(y) = y^\alpha G(y)$, where $\alpha > \beta$. The Laguerre coefficients of $g$ are given by

$$g_n \;=\; \sum_{k=0}^{n+\alpha} s_{nk}^{(\alpha)} \left(G_{+[0,\infty]0,\beta}\right)_n, \tag{154}$$

cf. Eqs. (76) and (136). The function $G$ is then given by

$$G(y) = \frac{1}{y^\alpha} \sum_{n=0}^{\infty} g_n\, L_n(y). \tag{155}$$

It should be noted that for truncated series the Laguerre coefficients of $G_{+[0,\infty]0,\beta}$ have to be known up to the order of $N+\alpha$ if $g$ is to be determined up to order $N$.

In our particular case, the singularities of the fragmentation functions $D_{Q/i}(x)$ are of the form $(\ln^m(1-x)/(1-x))_{+x[0,\underline{1}]}$. For $\tilde{D}_{Q/i}(y)$, this singular behaviour translates into $(\ln^m y/y)_{+y[\underline{0},\infty]}$, and so $\alpha = 1$ can be used. A possible term $\sim \delta(1-x)$ translates into a term $\sim \delta(y)$, and drops out after the multiplication by $y^\alpha$ for $\alpha > 0$ in Eq. (154).

## References


[1] **V. Ammosov et al.:** *Properties of $K^0$ and $\Lambda$ Inclusive Production in Charged-Current Antineutrino–Nucleon Interactions,* Nucl. Phys. B162 (1980) 205.

[2] **D. Allasia et al.:** *Production of Neutral Strange Particles in $\overline{\nu}_\mu d_2$ and $\nu_\mu d_2$ Charged Current Interactions,* Nucl. Phys. B224 (1983) 1.

[3] **G.T. Jones et al.:** *Polarization of $\Lambda$ Hyperons Produced Inclusively in $\nu p$ and $\overline{\nu} p$ Charged Current Interactions,* Z. Phys. C28 (1985) 23.

[4] **S. Willocq et al.:** *Neutral Strange Particle Production in Antineutrino–Neon Charged Current Interactions,* Z. Phys. C53 (1992) 207.

[5] **J.A. Appel:** *Hadroproduction of Charm Particles,* Annu. Rev. Part. Sci. 42 (1992) 367.

[6] **M. Aguilar-Benitez et al.:** *Inclusive Properties of D Mesons Produced in 360 GeV $\pi^- p$ Interactions,* Phys. Lett. 161B (1985) 400.

[7] **M. Aguilar-Benitez et al.:** *Charm Hadron Properties in 360 GeV/c $\pi^- p$-Interactions,* Z. Phys. C31 (1986) 491.

[8] **M. Aguilar-Benitez et al.:** *Charm Hadron Properties in 400 GeV/c pp Interactions,* Z. Phys. C40 (1988) 321.

[9] **S. Barlag et al.:** *Production Properties of $D^0$, $D^+$, $D^{*+}$ and $D_s^+$ in 230 GeV/c $\pi^-$ and $K^-$–Cu Interactions,* Z. Phys. C49 (1991) 555.

[10] **G.A. Alves et al.:** *Feynman-x and Transverse Momentum Dependence of $D^\pm$ and $D^0$, $\overline{D^0}$ Production in 250 GeV $\pi^-$–Nucleon Interactions,* Phys. Rev. Lett. 69 (1992) 3147.

[11] **K.G. Mallot et al.:** *Letter of Intent: Semi-Inclusive Muon Scattering from a Polarized Target,* CERN/SPSLC 95–27 (March 1995).

[12] **G. Baum et al.:** *A Proposal for a Common Muon and Proton Apparatus for Structure and Spectroscopy,* CERN/SPSLC 96–14 (March 1996).

[13] **A. Bartl, H. Fraas, W. Majerotto:** *Quark and Diquark Fragmentation into Mesons and Baryons,* Phys. Rev. D26 (1982) 1061.

[14] **B. Andersson, G. Gustafson, G. Ingelman, T. Sjöstrand:** *Parton Fragmentation and String Dynamics,* Phys. Rep. 97 (1983) 31.

[15] **B. Webber:** *A QCD Model for Jet Fragmentation Including Soft Gluon Interference,* Nucl. Phys. B238 (1984) 492.

[16] **B. Andersson, G. Gustafson, L. Lönnblad, U. Pettersson:** *Coherence Effects in Deep Inelastic Scattering,* Z. Phys. C43 (1989) 625.

[17] **G. Ingelman:** *LEPTO Version 6.1: The Lund Monte Carlo for Deep Inelastic Lepton–Nucleon Scattering,* in: Proceedings of the HERA Workshop 1991, eds. W. Buchmüller, G. Ingelman (Hamburg 1991).

[18] **M. Seymour:** *HERWIG: A Monte Carlo Event Generator for Simulating Hadron Emission Reactions With Interfering Gluons. Version 5.1,* Comput. Phys. Commun. 67 (1992) 465.

[19] **J. Ellis, D. Kharzeev, A. Kotzinian:** *The Proton Spin Puzzle and $\Lambda$ Polarization in Deep-Inelastic Scattering,* preprint CERN–TH/95–135 (June 1995).

[20] **S. Frixione, M.L. Mangano, P. Nason, G. Ridolfi:** *On the Determination of the Gluon Density of the Proton from Heavy-Flavour Production at HERA,* preprint CERN–TH.6864/93 (April 1993).

[21] **S. Frixione, M.L. Mangano, P. Nason, G. Ridolfi:** *Charm and Bottom Production: Theoretical Results versus Experimental Data,* preprint CERN–TH.7292/94 (June 1994).

[22] **S. Frixione, M.L. Mangano, P. Nason, G. Ridolfi:** *Total Cross Sections for Heavy Flavour Production at HERA,* preprint CERN–TH.7527/94 (December 1994).

[23] **M. Cacciari, M. Greco:** *Charm Photoproduction via Fragmentation,* preprint DESY 95–103 (May 1995).

[24] **S. Frixione, P. Nason, G. Ridolfi:** *Differential Distributions for Heavy Flavour Production at HERA,* preprint CERN–TH/95–143 (May 1995).

[25] **B.A. Kniehl, M. Krämer, G. Kramer, M. Spira:** *Cross Sections for Charm Production in ep Collisions: Massive versus Massless Scheme,* preprint DESY 95–098 (May 1995).

[26] **E. Laenen, S. Riemersma, J. Smith, W.L. van Neerven:** *$\mathcal{O}(\alpha_s)$ Corrections to Heavy-Flavour Inclusive Distributions in Electroproduction,* Nucl. Phys. B392 (1993) 229.

[27] **E. Laenen, S. Riemersma, J. Smith, W.L. van Neerven:** *Complete $\mathcal{O}(\alpha_s)$ Corrections to Heavy-Flavour Structure Functions in Electroproduction,* Nucl. Phys. B392 (1993) 162.

[28] **M.A.G. Aivazis, F.I. Olness, Wu-Ki Tung:** *Leptoproduction of Heavy Quarks I: General Formalism and Kinematics of Charged Current and Neutral Current Production Processes,* Phys. Rev. D50 (1994) 3085.

[29] **M.A.G. Aivazis, J.C. Collins, F.I. Olness, Wu-Ki Tung:** *Leptoproduction of Heavy Quarks II: A Unified QCD Formulation of Charged and Neutral Current Processes from Fixed-Target to Collider Energies,* Phys. Rev. D50 (1994) 3102.

[30] **M. Glück, E. Reya, M. Stratmann:** *Heavy Quarks at High Energy Colliders,* Nucl. Phys. B422 (1994) 37.

[31] **P. Agrawal, F.I. Olness, S.T. Riemersma, Wu-Ki Tung:** *Leptoproduction of Heavy Quarks,* Southern Methodist Univ. preprint SMU–HEP/95–04 (May 1995).

[32] **B.W. Harris, J. Smith:** *Heavy-Quark Correlations in Deep-Inelastic Electroproduction,* State Univ. of New York at Stony Brook preprint ITP–SB–95–08 (March 1995).

[33] **G. Kramer, B. Lampe, H. Spiesberger:** *Scheme and Scale Dependence of Charm Production in Neutrino Scattering,* preprint DESY 95–201 (November 1995).

[34] **S.J. Brodsky, P. Hoyer, W.K. Tang:** *Systematics of Heavy Quark Production at HERA,* Phys. Rev. D52 (1995) 6285.

[35] **C. Peterson, D. Schlatter, I. Schmitt, P.M. Zerwas:** *Scaling Violations in Inclusive $e^+e^-$ Annihilation Spectra,* Phys. Rev. D27 (1983) 105.

[36] **R. Odorico:** *Hadronic Production of Charm Flavour Excitation,* Nucl. Phys. B209 (1982) 77.

[37] **B. Mele, P. Nason:** *The Fragmentation Function for Heavy Quarks in QCD,* Nucl. Phys. B361 (1991) 626.

[38] **S.J. Brodsky, P. Hoyer, C. Peterson, N. Sakai:** *The Intrinsic Charm of the Proton,* Phys. Lett. 93B (1980) 451.

[39] **S.J. Brodsky, C. Peterson, N. Sakai:** *Intrinsic Heavy-Quark States,* Phys. Rev. D23 (1981) 2745.

[40] **F. Bloch, A. Nordsieck:** *Note on the Radiation Field of the Electron,* Phys. Rev. 52 (1937) 54.

[41] **D.R. Yennie, S.C. Frautschi, H. Suura:** *The Infrared Divergence Phenomena and High-Energy Processes,* Ann. Phys. 13 (1961) 379.

[42] **T. Kinoshita:** *Mass Singularities of Feynman Amplitudes,* J. Math. Phys. 3 (1962) 650.

[43] **T.D. Lee, M. Nauenberg:** *Degenerate Systems and Mass Singularities,* Phys. Rev. 133 (1964) 1549.

[44] **G. Altarelli, R.K. Ellis, G. Martinelli:** *Leptoproduction and Drell–Yan Processes Beyond the Leading Approximation in Chromodynamics,* Nucl. Phys. B143 (1978) 521, Erratum Nucl. Phys. B146 (1978) 544.

[45] **G. Altarelli, R.K. Ellis, G. Martinelli:** *Large Perturbative Corrections to the Drell–Yan Process in QCD,* Nucl. Phys. B157 (1979) 461.

[46] **R. Baier, K. Fey:** *Finite Corrections to Quark Fragmentation Functions in Perturbative QCD,* Z. Phys. C2 (1979) 339.

[47] **H.D. Politzer:** *Reliable Perturbative Results for Strong Interactions?,* Phys. Rev. Lett. 30 (1973) 1346.

[48] **D.J. Gross, F. Wilczek:** *Ultraviolet Behaviour of Nonabelian Gauge Theories,* Phys. Rev. Lett. 30 (1973) 1343.

[49] **D.J. Gross, F. Wilczek:** *Asymptotically Free Gauge Theories I,* Phys. Rev. D8 (1973) 3633.

[50] **D.J. Gross, F. Wilczek:** *Asymptotically Free Gauge Theories II,* Phys. Rev. D9 (1974) 980.

[51] **K.G. Wilson:** *On Products of Quantum Field Operators at Short Distances,* Cornell report (1964).

[52] **K.G. Wilson:** *Non-Lagrangian Models of Current Algebra,* Phys. Rev. 179 (1969) 1499.

[53] **R.A. Brandt, G. Preparata:** *Operator Product Expansions near the Light Cone,* Nucl. Phys. B27 (1971) 541.

[54] **K.G. Wilson, W. Zimmermann:** *Operator Product Expansions and Composite Field Operators in the General Framework of Quantum Field Theory,* Commun. Math. Phys. 24 (1972) 87.

[55] **W. Zimmermann:** *Normal Products and the Short Distance Expansion in the Perturbation Theory of Renormalizable Interactions,* Ann. Phys. 77 (1973) 570.

[56] **N. Christ, B. Hasslacher, A.H. Mueller:** *Light-Cone Behaviour of Perturbation Theory,* Phys. Rev. D6 (1972) 3543.

[57] **A. Buras:** *Asymptotic Freedom in Deep Inelastic Processes in the Leading Order and Beyond,* Rev. Mod. Phys. 52 (1980) 199.

[58] **E. Reya:** *Perturbative Quantum Chromodynamics,* Phys. Rep. 69 (1981) 195.

[59] **G. Altarelli:** *Partons in Quantum Chromodynamics,* Phys. Rep. 81 (1982) 1.

[60] **R.P. Feynman:** *Photon Hadron Interactions,* W.A. Benjamin, Inc. (Reading, Mass., 1972).

[61] **H.D. Politzer:** *QCD off the Light Cone and the Demise of the Transverse Momentum Cut-Off,* Phys. Lett. 70B (1977) 430.

[62] **D. Amati, R. Petronzio, G. Veneziano:** *Relating Hard QCD Processes Through Universality of Mass Singularities,* Nucl. Phys. B140 (1978) 54.

[63] **D. Amati, R. Petronzio, G. Veneziano:** *Relating Hard QCD Processes Through Universality of Mass Singularities (II),* Nucl. Phys. B146 (1978) 29.

[64] **R.K. Ellis, H. Georgi, M. Machacek, H.D. Politzer, G.G. Ross:** *Factorization and the Parton Model in QCD,* Phys. Lett. 78B (1978) 281.

[65] **R.K. Ellis, H. Georgi, M. Machacek, H.D. Politzer, G.G. Ross:** *Perturbation Theory and the Parton Model in QCD,* Nucl. Phys. B152 (1979) 285.

[66] **W. Furmanski, R. Petronzio:** *Lepton–Hadron Processes Beyond Leading Order in Quantum Chromodynamics,* Z. Phys. C11 (1982) 293.

[67] **J.C. Collins, D.E. Soper:** *The Theorems of Perturbative QCD,* Annu. Rev. Nucl. Part. Sci. 37 (1987) 383.

[68] **J.C. Collins, D.E. Soper, G. Sterman:** *Soft Gluons and Factorization,* Nucl. Phys. B308 (1988) 833.

[69] **J.C. Collins, D.E. Soper, G. Sterman:** *Factorization of Hard Processes in QCD,* in: Perturbative Quantum Chromodynamics, ed. A.H. Mueller, World Scientific (Singapore, 1989).

[70] **G. Altarelli, R.K. Ellis, G. Martinelli, S.Y. Pi:** *Processes Involving Fragmentation Functions Beyond the Leading Order in QCD,* Nucl. Phys. B160 (1979) 301.

[71] **N. Sakai:** *Factorization Breaking in Deep Inelastic Neutrino Hadron Production in Perturbative QCD,* Phys. Lett. 85B (1979) 67.

[72] **P. Chiappetta, J.P. Guillet:** *QCD Effects in Semiinclusive Deep Inelastic Scattering from a Polarized Target,* Z. Phys. C32 (1986) 209.

[73] **J.D. Stack:** *Generalized Scaling Laws for the Electroproduction of Hadrons,* Phys. Rev. Lett. 28 (1972) 57.

[74] **O. Nachtmann:** *Some Consequences of Light-Cone Dominance for Inclusive Electroproduction,* Phys. Rev. D6 (1972) 1718.

[75] **A.V. Kiselev, V.A. Petrov:** *Hadron Production in Hard Processes,* Sov. J. Part. & Nucl. 19 (1988) 21.

[76] **J. Ellis:** *Light-Cone Analysis of Inclusive Electromagnetic Processes,* Phys. Lett. 35B (1971) 537.

[77] **L. Trentadue, G. Veneziano:** *Fracture Functions: an Improved Description of Inclusive Hard Processes in QCD,* Phys. Lett. B323 (1994) 201.

[78] **D. Graudenz:** *One-Particle Inclusive Processes in Deeply Inelastic Lepton–Nucleon Scattering,* Nucl. Phys. B432 (1994) 351.

[79] **D. de Florian, C.A. Garcia Canal, R. Sassot:** *Factorization in Semi-Inclusive Polarized Deep Inelastic Scattering,* preprint hep-ph/9510262 (October 1995).

[80] **HERMES Collaboration:** *Technical Design Report,* DESY report (July 1993).

[81] **J.P. Ma:** *Calculating Fragmentation Functions from Definitions,* Phys. Lett. B332 (1994) 398.

[82] **E.L. Berger:** *Semi-Inclusive Inelastic Electron Scattering from Nuclei,* in: Proceedings of the NPAS Workshop 1987, Stanford.

[83] **G. Leibbrandt:** *Introduction to the Technique of Dimensional Regularization,* Rev. Mod. Phys. 47 (1975) 849.

[84] **S. Narison:** *Techniques of Dimensional Regularization and the Two-Point Function of QCD and QED,* Phys. Rep. 84 (1982) 263.

[85] **G. 't Hooft, M. Veltman:** *Regularization and Renormalization of Gauge Fields,* Nucl. Phys. B44 (1972) 189.

[86] **R. Gastmans, R. Meuldermans:** *Dimensional Regularization of the Infrared Problem,* Nucl. Phys. B63 (1973) 277.

[87] **W.J. Marciano, A. Sirlin:** *Dimensional Regularization of Infrared Divergences,* Nucl. Phys. B88 (1975) 86.

[88] **W.J. Marciano:** *Dimensional Regularization and Mass Singularities,* Phys. Rev. D12 (1975) 3861.

[89] **G. Sterman:** *Kinoshita's Theorem in Yang–Mills Theories,* Phys. Rev. D14 (1976) 2123.

[90] **J. Chýla:** *Parton Distributions Beyond the Leading Order,* Phys. Rev. D48 (1993) 4385.

[91] **G. Curci, W. Furmanski, R. Petronzio:** *Evolution of Parton Densities Beyond Leading Order,* Nucl. Phys. B175 (1980) 27.

[92] **Ch. Rumpf, G. Kramer, J. Willrodt:** *Jet Cross Sections in Leptoproduction from QCD,* Z. Phys. C7 (1981) 337.

[93] **A. Mendez:** *QCD Predictions for Semi-Inclusive and Inclusive Leptoproduction,* Nucl. Phys. B145 (1978) 199.

[94] **R.D. Peccei, R. Rückl:** *Energy Flow and Energy Correlations in Deep Inelastic Scattering,* Nucl. Phys. B162 (1980) 125.

[95] **J.G. Körner, E. Mirkes, G.A. Schuler:** *QCD Jets at HERA. I: $\mathcal{O}(\alpha_s)$ Radiative Corrections to Electroweak Cross Sections and Jet Rates,* Int. J. Mod. Phys. A4 (1989) 1781.

[96] **L. Trentadue:** *Fracture Functions,* in: Proceedings of the "QCD 94" Conference, Montpellier (July 1994).

[97] **G. Altarelli, G. Parisi:** *Asymptotic Freedom in Parton Language,* Nucl. Phys. B126 (1977) 298.

[98] **K. Konishi, A. Ukawa, G. Veneziano:** *A Simple Algorithm for QCD Jets,* Phys. Lett. 78B (1978) 243.

[99] **K. Konishi, A. Ukawa, G. Veneziano:** *Jet Calculus: A Simple Algorithm for Resolving QCD Jets,* Nucl. Phys. B157 (1979) 45.

[100] **The Particle Data Group:** *Review of Particle Properties,* Phys. Rev. 50 (1994) 1173.

[101] **B. Mele, P. Nason:** *Next-to-Leading QCD Calculation of the Heavy Quark Fragmentation Function,* Phys. Lett. B245 (1990) 635.

[102] **P. Nason:** *Heavy Quark Production,* in: Heavy Flavours, eds. A. Buras, M. Lindner, World Scientific (Singapore, 1993).

[103] **M. Cacciari, M. Greco:** *Large-$p_\perp$ Hadroproduction of Heavy Quarks,* Nucl. Phys. B421 (1994) 530.

[104] **M. Glück, E. Reya, A. Vogt:** *Parton Structure of the Photon Beyond the Leading Order,* Phys. Rev. D45 (1992) 3986.

[105] **M. Glück, E. Reya, A. Vogt:** *Dynamical Parton Distributions of the Proton and Small x Physics,* Z. Phys. C67 (1995) 433.

[106] **M. Glück, E. Reya, A. Vogt:** *Parton Distributions for High Energy Collisions,* Z. Phys. C53 (1992) 127.

[107] **CTEQ Collaboration:** *Global QCD Analysis and the CTEQ Parton Distributions,* Phys. Rev. D51 (1995) 4763.

[108] **A. Martin, R. Roberts, J. Stirling:** *Pinning Down the Glue in the Proton,* Phys. Lett. B354 (1995) 155.

[109] **B.W. Harris, J. Smith, R. Vogt:** *Reanalysis of the EMC Charm Production Data with Extrinsic and Intrinsic Charm at NLO,* State Univ. of New York at Stony Brook preprint ITP–SB–95–15 (October 1995).

[110] **S.J. Brodsky, P. Hoyer, A.H. Mueller, W.K. Tang:** *New QCD Production Mechanism for Hard Processes at Large x,* Nucl. Phys. B369 (1992) 519.

[111] **B. Lampe:** *One Loop QCD Corrections to the Inclusive Production Cross-Section for Heavy Quarks in $p\overline{p}$ Collisions at High Transverse Energies,* Fortschr. Phys. 40 (1992) 329.

[112] **D. Graudenz:** *PROJET: Jet Cross Sections in Deeply Inelastic Scattering, Version 4.1,* Comput. Phys. Commun. 92 (1995) 65.

[113] **G.P. Lepage:** *A New Algorithm for Adaptive Multidimensional Integration,* J. Comput. Phys. 27 (1978) 192.

[114] **G.P. Lepage:** *VEGAS — An Adaptive Multi-Dimensional Integration Program,* Cornell preprint CLNS-80/447 (March 1980).

[115] **K. Charchuła:** *The Package PAKPDF Version 1.1 of Parametrizations of Parton Distribution Functions in the Proton,* Comput. Phys. Commun. 69 (1992) 360.

[116] **H. Plothow-Besch:** *PDFLIB: a Library of All Available Parton Density Functions of the Nucleon, the Pion and the Photon and the Corresponding $\alpha_s$ Calculations,* Comput. Phys. Commun. 75 (1993) 396.

[117] **W.J. Marciano:** *Flavour Thresholds and $\Lambda$ in the Modified Minimal-Subtraction Scheme,* Phys. Rev. D29 (1984) 580.

[118] **W. Bernreuther:** *Decoupling of Heavy Quarks in Quantum Chromodynamics,* Ann. Phys. 151 (1983) 127.

[119] **G. Grunberg:** *Renormalization Group Improved Perturbative QCD,* Phys. Lett. 95B (1980) 70, Erratum Phys. Lett. 110B (1982) 501.

[120] **G. Grunberg:** *Renormalization Scheme Independent QCD and QED: The Method of Effective Charges,* Phys. Rev. D29 (1984) 2315.

[121] **P.M. Stevenson:** *Resolution of the Renormalization Scheme Ambiguity in Perturbative QCD,* Phys. Lett. 100B (1981) 61.

[122] **P.M. Stevenson:** *Optimized Perturbation Theory,* Phys. Rev. D23 (1981) 2916.

[123] **P.M. Stevenson:** *Sense and Nonsense in the Renormalization-Scheme-Dependence Problem,* Nucl. Phys. B203 (1982) 472.

[124] **P.M. Stevenson:** *Optimization and the Ultimate Convergence of QCD Perturbation Theory,* Nucl. Phys. B231 (1984) 65.

[125] **S.J. Brodsky, G.P. Lepage, P.B. Mackenzie:** *On the Elimination of Scale Ambiguities in Perturbative Quantum Chromodynamics,* Phys. Rev. D28 (1983) 228.

[126] **R.P. Feynman:** *Very High-Energy Collisions of Hadrons,* Phys. Rev. Lett. 23 (1969) 1415.

[127] **K.H. Streng, T.F. Walsh, P.M. Zerwas:** *Quark and Gluon Jets in the Breit Frame of Lepton–Nucleon Scattering,* Z. Phys. C2 (1979) 237.

[128] **S.J. Brodsky, J.F. Gunion, D.E. Soper:** *Physics of Heavy-Quark Production in Quantum Chromodynamics,* Phys. Rev. D36 (1987) 2710.

[129] **J.C. Anjos et al.:** *Charm Photoproduction,* Phys. Rev. Lett. 62 (1989) 513.

[130] **J.C. Anjos et al.:** *Photon–Gluon-Fusion Analysis of Charm-Photoproduction,* Phys. Rev. Lett. 65 (1990) 2503.

[131] **M.P. Alvarez et al.:** *Branching Ratios and Properties of D-Meson Decays,* Z. Phys. C50 (1991) 11.

[132] **M.P. Alvarez et al.:** *Study of Charm Photoproduction Mechanisms,* Z. Phys. C60 (1993) 53.

[133] **ZEUS Collaboration:** *Study of $D^*(2010)^{\pm}$ Production in ep collisions at HERA,* Phys. Lett. B349 (1995) 225.

[134] **J. Binnewies, B.A. Kniehl, G. Kramer:** *Next-to-Leading Order Fragmentation Functions for Pions and Kaons,* Z. Phys. C65 (1995) 471.

[135] **A. Berera, D.E. Soper:** *Diffractive Jet Production in a Simple Model with Applications to DESY HERA,* Phys. Rev. D50 (1994) 4328.

[136] **S.J. Brodsky, R. Vogt:** *QCD and Intrinsic Heavy Quark Predictions for Leading Charm and Beauty Hadroproduction,* preprint SLAC-PUB-6468 (April 1994).

[137] **A.H. Mueller:** *$O(2,1)$ Analysis of Single-Particle Spectra at High Energy,* Phys. Rev. D2 (1970) 2963.

[138] **R.N. Cahn, E.W. Colglazier:** *Unified Mueller Picture of Deep-Inelastic Inclusive Leptoproduction,* Phys. Rev. D8 (1973) 3019.

[139] **D. Horn, F. Zachariasen:** *Hadron Physics at Very High Energies,* W. Benjamin, Inc. (Reading, Mass., 1973), Chapter 6.

[140] **A.H. Mueller:** *Cut Vertices and their Renormalization: A Generalization of the Wilson Expansion,* Phys. Rev. D10 (1978) 3705.

[141] **S. Gupta, A.H. Mueller:** *High-Energy Predictions in Quantum Chromodynamics,* Phys. Rev. D20 (1979) 118.

[142] **A.H. Mueller:** *Perturbative QCD at High Energies,* Phys. Rep. 73 (1981) 237.

[143] **L. Baulieu, E.G. Floratos, C. Kounnas:** *Parton Model Interpretation of the Cut Vertex Formalism,* Nucl. Phys. B166 (1980) 321.

[144] **E.G. Floratos, D.A. Ross, C.T. Sachrajda:** *Higher Order Effects in Asymptotically Free Gauge Theories. 2. Flavor Singlet Wilson Operators and Coefficient Functions,* Nucl. Phys. B152 (1979) 493.

[145] **G. Ingelman and P.E. Schlein:** *Jet Structure in High Mass Diffractive Scattering,* Phys. Lett. 152B (1985) 256.

[146] **E.L. Berger, J.C. Collins, D.E. Soper and G. Sterman:** *Diffractive Hard Scattering,* Nucl. Phys. B286 (1987) 704.

[147] **D. Graudenz, G. Veneziano:** *Estimating Diffractive Higgs Boson Production at LHC from HERA Data,* Phys. Lett. B365 (1996) 302.

[148] **A. Berera, D.E. Soper:** *Behaviour of Diffractive Parton Distribution Functions,* Pennsylvania State Univ. preprint PSU/TH/163 (September 1995).

[149] **I.M. Gel'fand, G.E. Shilov:** *Generalized Functions, Vol. I,* Academic Press (New York, London, 1964).

[150] **B.W. Char et al.:** *Maple V Reference Manual,* Springer Verlag (Berlin, 1991).

[151] **S. Wolfram:** *Mathematica,* Addison Wesley (Reading, Mass., 1991).

[152] **A.C. Hearn:** *REDUCE User's Manual, Version 3.4.1,* ZIB Publication M 2.032.04 (July 1992).

[153] **M. Jamin, M.E. Lautenbacher:** *Tracer Version 1.1: A Mathematica Package for $\gamma$-Algebra in Arbitrary Dimensions,* Comput. Phys. Commun. 74 (1993) 265.

[154] **W.H. Press, B.P. Flannery, S.A. Teukolsky, W.T. Vetterling:** *Numerical Recipes in C,* Cambridge University Press (Cambridge 1988).

[155] **N.N. Lebedev:** *Special Functions & Their Applications,* Dover Publications, Inc. (New York, 1972).

[156] **H. Hochstadt:** *The Functions of Mathematical Physics,* Dover Publications, Inc. (New York, 1986).

[157] **M. Abramowitz, I.A. Stegun (eds.):** *Pocketbook of Mathematical Functions,* Verlag Harri Deutsch (Thun, Frankfurt/M., 1984).

[158] **W. Furmanski, R. Petronzio:** *A Method of Analyzing the Scaling Violation of Inclusive Spectra in Hard Processes,* Nucl. Phys. B195 (1982) 237.

[159] **H. Bateman:** *Higher Transcendental Functions I–III,* McGraw-Hill (1953).

[160] **I. Gradstein, I. Ryshik:** *Tables of Series, Products, and Integrals, Vols. I and II,* Verlag Harri Deutsch (Thun, Frankfurt/M., 1981).

[161] **G.P. Ramsey:** *The Laguerre Method for Solving Integro-Differential Equations,* J. Comput. Phys. 60 (1985) 97.

[162] **S. Kumano, J.T. Londergan:** *A FORTRAN Program for the Numerical Solution of the Altarelli–Parisi Equations by the Laguerre Method,* Comput. Phys. Commun. 69 (1992) 373.

[163] **R. Kobayashi, M. Konuma, S. Kumano:** *FORTRAN program for a numerical solution of the nonsinglet Altarelli–Parisi equation,* Saga University preprint SAGA-HE-63-94 (August 1994).

[164] **R. Kobayashi, M. Konuma, S. Kumano, M. Miyama:** *Numerical Solution of Altarelli–Parisi Equations,* Saga University preprint SAGA-HE-74-94 (December 1994).

## List of Figures

## List of Tables